ISSN 1948-0210 (online)

World Journal of *Stem Cells*

World J Stem Cells 2022 February 26; 14(2): 146-218

Published by Baishideng Publishing Group Inc

World Journal of Stem Cells

Contents

Monthly Volume 14 Number 2 February 26, 2022

World Journal of Stem Cells

Monthly Volume 14 Number 2 February 26, 2022

Contents

ABOUT COVER

Editorial Board Member of *World Journal of Stem Cells*, Mohammed Grawish, PhD, Professor, Department of Oral Biology, Faculty of Dentistry, Mansoura University, Mansoura 740005, Egypt. grawish2005@yahoo.com

AIMS AND SCOPE

The primary aim of *World Journal of Stem Cells* (*WJSC*, *World J Stem Cells*) is to provide scholars and readers from various fields of stem cells with a platform to publish high-quality basic and clinical research articles and communicate their research findings online. *WJSC* publishes articles reporting research results obtained in the field of stem cell biology and regenerative medicine, related to the wide range of stem cells including embryonic stem cells, germline stem cells, tissue-specific stem cells, adult stem cells, mesenchymal stromal cells, induced pluripotent stem cells, embryonal carcinoma stem cells, hemangioblasts, lymphoid progenitor cells, *etc*.

INDEXING/ABSTRACTING

The *WJSC* is now indexed in Science Citation Index Expanded (also known as SciSearch®), Journal Citation Reports/Science Edition, Biological Abstracts, BIOSIS Previews, Scopus, PubMed, and PubMed Central. The 2021 Edition of Journal Citation Reports® cites the 2020 impact factor (IF) for *WJSC* as 5.326; IF without journal self cites: 5.035; 5-year IF: 4.956; Journal Citation Indicator: 0.55; Ranking: 14 among 29 journals in cell and tissue engineering; Quartile category: Q2; Ranking: 72 among 195 journals in cell biology; and Quartile category: Q2. The *WJSC*'s CiteScore for 2020 is 3.1 and Scopus CiteScore rank 2020: Histology is 31/60; Genetics is 205/325; Genetics (clinical) is 64/87; Molecular Biology is 285/382; Cell Biology is 208/279.

RESPONSIBLE EDITORS FOR THIS ISSUE

Production Editor: *Yan-Liang Zhang*; **Production Department Director:** *Xu Guo*; **Editorial Office Director:** *Ze-Mao Gong*.

NAME OF JOURNAL
World Journal of Stem Cells

ISSN
ISSN 1948-0210 (online)

LAUNCH DATE
December 31, 2009

FREQUENCY
Monthly

EDITORS-IN-CHIEF
Shengwen Calvin Li, Carlo Ventura

EDITORIAL BOARD MEMBERS
https://www.wjgnet.com/1948-0210/editorialboard.htm

PUBLICATION DATE
February 26, 2022

INSTRUCTIONS TO AUTHORS
https://www.wjgnet.com/bpg/gerinfo/204

GUIDELINES FOR ETHICS DOCUMENTS
https://www.wjgnet.com/bpg/GerInfo/287

GUIDELINES FOR NON-NATIVE SPEAKERS OF ENGLISH
https://www.wjgnet.com/bpg/gerinfo/240

PUBLICATION ETHICS
https://www.wjgnet.com/bpg/GerInfo/288

PUBLICATION MISCONDUCT
https://www.wjgnet.com/bpg/gerinfo/208

ARTICLE PROCESSING CHARGE
https://www.wjgnet.com/bpg/gerinfo/242

STEPS FOR SUBMITTING MANUSCRIPTS
https://www.wjgnet.com/bpg/GerInfo/239

ONLINE SUBMISSION
https://www.f6publishing.com

E-mail: bpgoffice@wjgnet.com https://www.wjgnet.com

World Journal of Stem Cells

Submit a Manuscript: https://www.f6publishing.com

World J Stem Cells 2022 February 26; 14(2): 146-162

DOI: 10.4252/wjsc.v14.i2.146

ISSN 1948-0210 (online)

REVIEW

Abnormal lipid synthesis as a therapeutic target for cancer stem cells

Si-Yu Wang, Qin-Chao Hu, Tong Wu, Juan Xia, Xiao-An Tao, Bin Cheng

Specialty type: Cell and tissue engineering

Provenance and peer review: Invited article; Externally peer reviewed.

Peer-review model: Single blind

Peer-review report's scientific quality classification

Grade A (Excellent): A
Grade B (Very good): 0
Grade C (Good): C, C
Grade D (Fair): 0
Grade E (Poor): 0

P-Reviewer: Li WJ, Li SC, Madamsetty VS

Received: March 16, 2021
Peer-review started: March 16, 2021
First decision: May 5, 2021
Revised: May 19, 2021
Accepted: February 14, 2022
Article in press: February 14, 2022
Published online: February 26, 2022

Si-Yu Wang, Qin-Chao Hu, Tong Wu, Juan Xia, Xiao-An Tao, Bin Cheng, Department of Oral Medicine, Hospital of Stomatology, Sun Yat-sen University, Guangzhou 510000, Guangdong Province, China

Si-Yu Wang, Qin-Chao Hu, Tong Wu, Juan Xia, Xiao-An Tao, Bin Cheng, Guangdong Provincial Key Laboratory of Stomatology, Guanghua School of Stomatology, Sun Yat-sen University, Guangzhou 510000, Guangdong Province, China

Corresponding author: Bin Cheng, MD, PhD, Dean, Department of Oral Medicine, Hospital of Stomatology, Sun Yat-sen University, No. 56 Lingyuanxi Road, Guangzhou 510000, Guangdong Province, China. chengbin@mail.sysu.edu.cn

Abstract

Cancer stem cells (CSCs) comprise a subpopulation of cancer cells with stem cell properties, which exhibit the characteristics of high tumorigenicity, self-renewal, and tumor initiation and are associated with the occurrence, metastasis, therapy resistance, and relapse of cancer. Compared with differentiated cells, CSCs have unique metabolic characteristics, and metabolic reprogramming contributes to the self-renewal and maintenance of stem cells. It has been reported that CSCs are highly dependent on lipid metabolism to maintain stemness and satisfy the requirements of biosynthesis and energy metabolism. In this review, we demonstrate that lipid anabolism alterations promote the survival of CSCs, including *de novo* lipogenesis, lipid desaturation, and cholesterol synthesis. In addition, we also emphasize the molecular mechanism underlying the relationship between lipid synthesis and stem cell survival, the signal transduction pathways involved, and the application prospect of lipid synthesis reprogramming in CSC therapy. It is demonstrated that the dependence on lipid synthesis makes targeting of lipid synthesis metabolism a promising therapeutic strategy for eliminating CSCs. Targeting key molecules in lipid synthesis will play an important role in anti-CSC therapy.

Key Words: Lipid synthesis; Cancer stem cells; Anti-cancer therapy; Stem cell survival; Lipid anabolism

Core Tip: Cancer stem cells (CSCs) are associated with the occurrence, metastasis, therapy resistance, and relapse of cancer. CSCs are highly dependent on lipid metabolism to maintain stemness and satisfy the requirements of biosynthesis and energy metabolism. Here, we review the molecular mechanism underlying the relationship between lipid synthesis and stem cell survival, the signal transduction pathways involved, and the application prospect of lipid synthesis reprogramming in CSC therapy. We demonstrate that lipid anabolism alterations promote the survival of CSCs.

Citation: Wang SY, Hu QC, Wu T, Xia J, Tao XA, Cheng B. Abnormal lipid synthesis as a therapeutic target for cancer stem cells. *World J Stem Cells* 2022; 14(2): 146-162
URL: https://www.wjgnet.com/1948-0210/full/v14/i2/146.htm
DOI: https://dx.doi.org/10.4252/wjsc.v14.i2.146

INTRODUCTION

Cancer stem cells (CSCs) comprise a subpopulation of cancer cells with stem cell properties, which exhibit the characteristics of high tumorigenicity, self-renewal, and tumor initiation. They may be responsible for cancer occurrence, metastasis, therapy resistance, and relapse of cancer[1,2]. CSCs are able to differentiate into diverse cancer cell progenies to maintain the hierarchical organization of a tumor[3].

In solid tumors, the expression of the CSC markers, including CD133, CD44, and aldehyde dehydrogenase (ALDH)1, is similar to that in normal human embryonic stem cells, thus transformed adult stem cells are one possible source of CSCs. Another possibility is differentiated cells under long-term stress conditions, which transform into CSCs through reprogramming due to genetic instability and epigenetic abnormalities[4-6] (Figure 1).

Various studies have shown that both CSC and non-CSC are plastic, and the interconversion between them may be a common phenomenon. Epithelial-to-mesenchymal transition (EMT) is the process by which epithelial cancer cells acquire a mesenchymal gene program that promotes migration and invasion. Many studies suggest that EMT promotes the transition from non-CSCs to CSC[7]. During EMT, cancer cells obtain stem cell-like properties to migrate and grow into distant tissues[8-10]. In a human model, the EMT major transcription factor Snail was elevated in cancer cells that displayed enhanced oncogenic capability and metastatic potential and was tightly associated with a CSC phenotype[11]. The plasticity of CSCs is also closely related to microenvironment. Angiogenesis, the hypoxic niche, and extracellular matrix are essential for maintaining the stemness of glioblastoma stem cells[12]. In addition, there is evidence that, in colon cancer, myofibroblasts enhance Wnt signaling through secreted factors, establishing a CSC niche and restoring the stemness of highly differentiated cancer cells[13]. In non-CSCs, the promoter of zinc-finger E-box-binding (ZEB)1, the key regulator of EMT, maintains the bivalent chromatin configuration, making non-CSCs respond readily to microenvironmental signals. When the promoter converts to active chromatin configuration, ZEB1 transcription increases and non-CSCs convert to the CSC state.

Independent of the origin, CSCs are important cancer cell subsets. The existence of CSCs is clearly demonstrated in different types of cancer, including leukemia[14,15], tongue squamous cell carcinoma [16], breast cancer[17], glioblastoma[18], lung cancer[19,20], and osteosarcoma[21]. They actuate tumorigenesis and progression, and promote therapy resistance, metastasis, and recurrence of cancers. A growing number of studies have shown that metabolic reprogramming of cancer cells caused by changes in the microenvironment exerts a marked effect on the properties of stem cells.

METABOLIC REPROGRAMMING IN CSCS

The interaction between CSCs and the tumor microenvironment (TME) is related to tumorigenesis and disease progression[22]. Due to the rapid proliferation of tumor cells and insufficient angiogenesis, the TME has the characteristics of hypoxic, acidic, and nutrient-poor conditions; therefore, tumor cells must adjust energy metabolism to deal with this adverse microenvironment, and maintain the rapid growth and proliferation of tumor cells[23-25], a process called metabolic reprogramming. The metabolic phenotype of CSCs may depend on the microenvironment to a great extent.

Several studies have been conducted on a variety of cancer types, such as nasopharyngeal carcinoma [26], leukemia[27], osteosarcoma[28], breast cancer[29], and ovarian cancer[30], which suggest that CSCs show a greater reliance on glycolysis for energy supply compared with other differentiated cancer cells *in vitro* and *in vivo*. Evidence suggests that paracrine hepatocyte growth factor/c-MET enhances the expression of hexokinase 2 and promotes glycolysis by activating Yes-associated protein (YAP)/hypoxia-inducible factor-1α in pancreatic cancer, which may facilitate CSC-like properties[31].

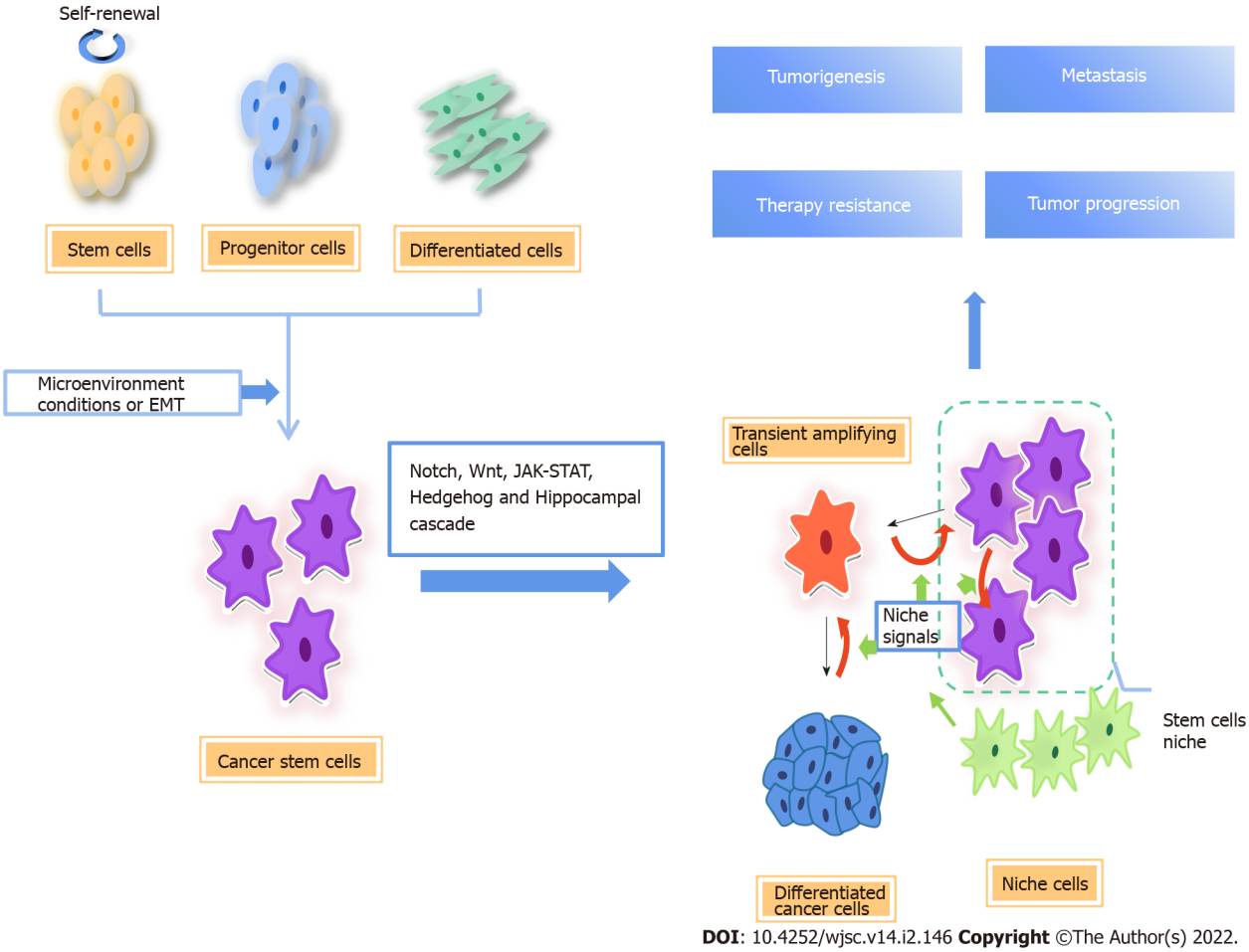

DOI: 10.4252/wjsc.v14.i2.146

Figure 1 Origin of cancer stem cells and regulatory pathways involved. There are two possible origins of cancer stem cells (CSCs), one is normal stem cells/progenitor cells, and the other is fully differentiated cells. CSCs are closely related to tumor microenvironmental factors. In the process of epithelial-mesenchymal transformation, cancer cells acquire stem cell-like characteristics. The differentiation direction of CSC progeny is determined by niche signal, and the available niche space determines the number of progeny stem cells. When there is no space available in the niche, the stem cells divide into transient amplifying (TA) cells, which divide and differentiate rapidly. At the same time, niche cells reprogram TA cells and differentiated cells into CSCs by niche signals[7]. CSCs are important subsets of tumor cells, which are regulated by a variety of signal pathways, including Notch, Wnt/β-catenin, Hippo, and Hedgehog signaling, which are the main causes of cancer initiation, progression, metastasis, therapy resistance, and relapse. EMT: Epithelial-to-mesenchymal transition.

However, there is also growing evidence that mitochondrial oxidative metabolism is the preferred form of energy production in CSCs, including CD133+ colon cancer cells[32], CD44+ and CD117+ ovarian cancer cells[33], cholangiocarcinoma cells[34], brain tumor cells[35], and leukemia cells[36]. In addition, it is found that pancreatic CSCs (PaCSCs) are enriched in the oxidative phosphorylation (OXPHOS) promotion system using galactose instead of glucose as carbon source *in vitro*. And significant CSC features are present, such as the expression of multiple CSC biomarkers, the overexpression of stem-related pathways, the enhancement of self-renewal ability, and the significant improvement of tumorigenicity *in vivo*. Meanwhile, OXPHOS promoted the immune escape properties of PaCSCs[37].

A large number of the above studies have shown that CSC metabolism is highly heterogeneous. CSCs exhibit a metabolic phenotype dependent on glycolysis or OXPHOS, which mainly depends on the heterogeneity of tumor origin and surrounding microenvironmental conditions.

In addition to glucose metabolism, alterations in lipid metabolism also modulate tumor development and progression. Lipid metabolism is related to the stem cell properties in cancers. A growing body of evidence suggests that alterations in metabolic pathways associated with lipids, including fatty acids (FA) and cholesterol, are crucial for maintaining the stemness of CSCs. Lipid synthesis and catabolism are strictly regulated by CSCs to maintain self-renewal, proliferation, and chemotherapy resistance of the CSCs. Increased *de novo* lipid biosynthesis and lipid storage, as well as enhanced lipid oxidation, are unique features of many CSCs. It has been reported that fatty acid oxidation (FAO) can support self-renewal and drug resistance of breast CSCs. The Leptin-LEPR-JAK-STAT3-dependent FAO pathway plays an important role in the self-renewal of breast cancer stem cell (BCSC) associated with chemotherapy resistance in breast cancer. Blocking FAO and/or Leptin re-sensitize them to chemotherapy and inhibit breast CSCs *in vivo*[38]. Furthermore, targeting FAO enhances the chemotherapy efficacy of cytarabine (AraC) in AraC-resistant acute myeloid leukemia enriched in

leukemic stem cells[39]. Mesenchymal stem cells promoted stemness and chemoresistance in gastric cancer cells through FAO *in vitro* and *in vivo*[40]. Lipid droplets (LDs), organelles that store neutral lipids, are accumulated in CSCs in numerous types of cancer[41,42]. LDs are more abundant in pancreatic and colorectal CSCs than in isogenic non-CSCs[43].

Lipid synthesis has been shown to play a significant role in maintaining the characteristics of CSCs during tumorigenesis. *De novo* lipid biosynthesis is one of the most targetable features of CSCs[44]. We will highlight the important role of lipid synthesis in CSCs, including the pathways involved and promising therapeutic targets (Figure 2).

ALTERATIONS AND KEY MODULATORS IN LIPID SYNTHESIS IN CSCS

Lipid synthesis includes *de novo* lipid biosynthesis, lipid desaturation, and cholesterol synthesis. Metabonomic analysis demonstrated that FA and cholesterol synthesis displays high activity in triple-negative breast CSCs (TNBCSCs). Cholesterol synthesis is essential for the survival and migration of CSCs, and inhibition of cholesterol synthesis induces cytotoxic effects on CSCs. For instance, pyridine pamoate (PP) can induce a cell killing effect on CSCs and prevent tumor metastasis by inhibiting cholesterol anabolic flux. By supplementing cholesterol to restore the level of free and bound cholesterol, the cytotoxicity induced by PP is effectively limited[45]. Compared with non-CSCs, the rates of lipid unsaturation in the CSCs were further increased[46,47]. In addition, in various cancers such as ovarian cancer, glioblastoma multiforme, and colon cancer, more monounsaturated FAs (MUFAs) are demanded by CSCs, which indicates that MUFAs may be involved in mediating various signaling pathways in CSCs and associated with stemness, and lipid desaturation may be an ideal and specific therapeutic target for CSCs[48,49].

FA synthesis in CSCs

Experimental investigation indicated that *de novo* FA synthesis is more active in CSCs than in differentiated cells, suggesting that it is essential for CSCs to maintain stemness. In CSCs, the key rate-limiting enzymes of *de novo* FA synthesis, including ATP-citrate lyase (ACLY), acetyl-CoA carboxylase (ACC), and fatty acid synthase (FASN), as well as sterol regulatory element-binding proteins (SREBPs), which regulate the expression level of lipid synthesis genes, are highly expressed.

ACLY

ACLY is principally located in the cytoplasm, which catalyzes the conversion of citrate to acetyl-CoA. Acetyl-CoA is not only an important substrate for the synthesis of FAs and cholesterol, but it is also necessary for protein acetylation reactions. Therefore, ACLY is a key enzyme of lipid synthesis that links catabolic pathways to biosynthesis. In many types of cancer, ACLY is upregulated or activated[50-52]. ACLY upregulation contributes to stemness maintenance and tumorigenesis[53,54]. ACLY overexpression increased the expression of Snail, which is known to promote EMT and stemness[55]. ACLY inhibition decreased the invasiveness of breast cancer cells, and targeting ACLY attenuated the proliferation potential and cisplatin resistance in ovarian cancer[56,57].

ACC

ACC catalyzes the ATP-dependent carboxylation of acetyl CoA to generate malonyl-CoA, which is a rate-limiting step in *de novo* FA synthesis. In pancreatic cancer cells, inhibition of ACC inhibits Wnt and Hedgehog (HH) signal transduction by inhibiting palmitoylation of their ligands, and inhibits the growth of pancreatic tumors *in vivo* and *in vitro*. ACC inhibitors can restore tumor cells to histological epithelial phenotype *in vitro*[58]. Moreover, ACC is highly expressed in induced pluripotent stem cells (iPSCs). Pharmacological inhibition of ACC significantly reduced reprogramming efficiency in iPSCs [59]. Research reveals that inhibiting the activation of ACC can effectively restore intracellular lipid levels, reduce EMT, and inhibit the features of CSCs[60].

FASN

FASN, the key enzyme of *de novo* lipogenesis, is highly expressed in human pluripotent stem cells (hPSCs) compared with that in hPSC-derived cardiomyocytes (hPSC-CMs)[61]. In addition, it is highly active in adult neural stem and progenitor cells, which require FASN-dependent lipogenesis for proliferation[62]. Data suggest that *de novo* lipogenesis is higher and FASN expression is upregulated in glioma stem cells (GCSs). Pharmacological inhibition of FASN dramatically decreases the expression of GSC stemness markers, including Sox2, Nestin, CD133, and FABP7, and thus inhibits cell proliferation and invasiveness of GSCs[63]. Moreover, downregulation of FASN suppresses CSCs in breast cancer[64] and pancreatic cancer[65].

SREBP1

SREBPs are a class of transcription factors that regulate lipid homeostasis by controlling the expression

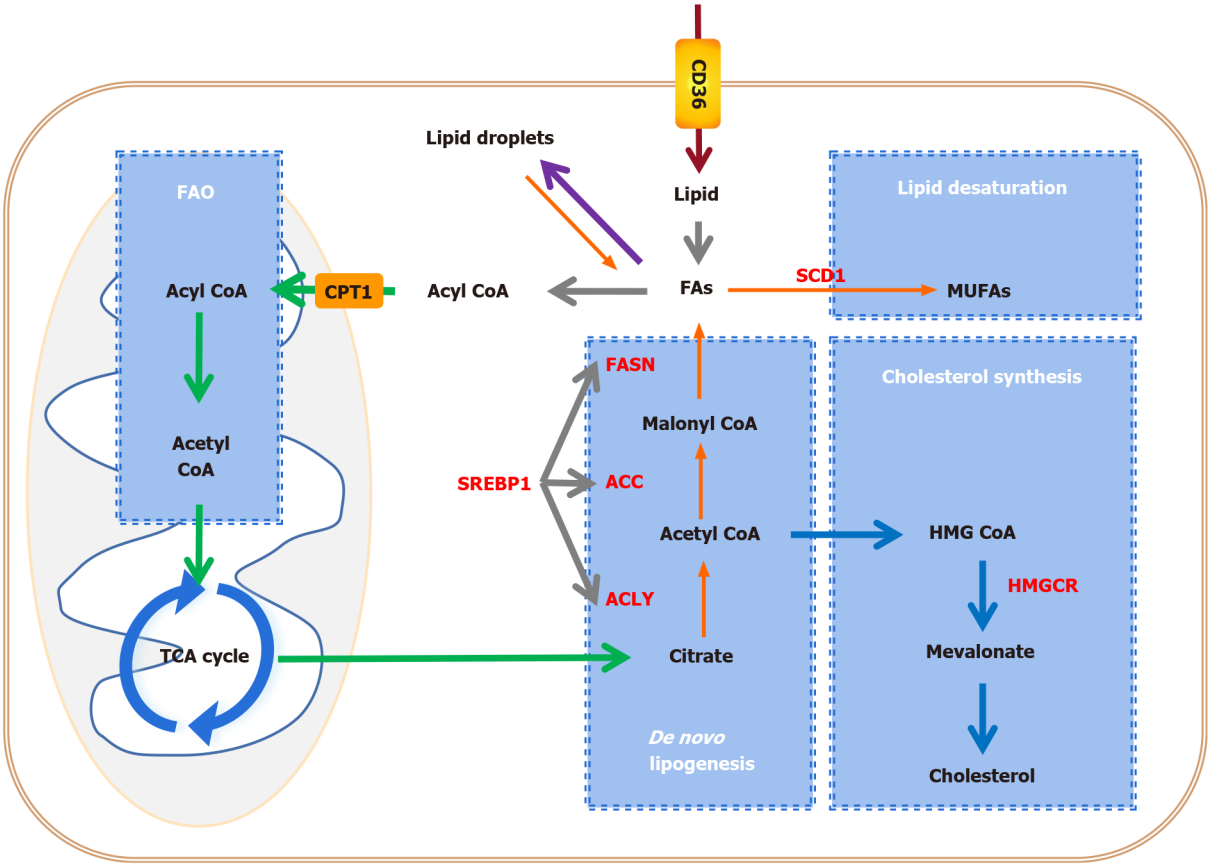

DOI: 10.4252/wjsc.v14.i2.146

Figure 2 Alteration of lipid metabolic pathways in tumors and cancer stem cells. Cancer stem cells (CSCs) enhance lipid metabolic activities, such as fatty acid synthesis, fatty acid oxidation, and lipid storage, to promote self-renewal and proliferation. Key enzymes that control lipid metabolism (red letters) are considered to be ideal therapeutic targets for CSCs. CPT1: Carnitine palmitoyl-transferase 1; FAO: Fatty acid oxidation; TCA cycle: Tricarboxylic acid cycle; CD36: Cluster of differentiation 36; FA: Fatty acid; FASN: Fatty acid synthase; ACC: Acetyl-CoA carboxylase; ACLY: ATP citrate lyase; SREBP1: Sterol-regulatory element binding protein 1; SCD1: Stearoyl-CoA desaturase 1; MUFA: Monounsaturated fatty acid; HMGCR: 3-hydroxy-3-methylglutaryl coenzyme A reductase.

of a series of key enzymes required for cholesterol and FA synthesis. Three SREBP subtypes have distinctive roles in lipid synthesis: SREBP1a regulates FA and cholesterol synthesis, and cholesterol absorption, SREBP1c regulates FA synthesis, and SREBP2 specifically regulates cholesterol synthesis and uptake. SREBPs are downstream molecules of the PI3K/AKT/mTOR signaling pathway. Regulation of SREBPs through the PI3K/AKT/mTOR pathway can regulate glucose production and FA synthesis, and affect the proliferation and invasion of cancer cells[66,67]. Downregulation of SREBP inhibited the growth of non-small-cell lung cancer cells and liver cancer cells[67,68]. SREBP1 targets key enzymes of FA synthesis, such as ACLY, ACC, FASN, and stearyl coenzyme A desaturase 1 (SCD1), to regulate lipid metabolism[69], and is highly expressed in various cancers[69-71]. Compared to differentiating melanosphere-derived cells, the expression of SREBP1 is enhanced in melanosphere-derived CSCs[42]. Gemcitabine is a standard treatment for advanced pancreatic cancer patients but can cause chemoresistance during treatment. The chemoresistant cells have features of CSCs. Gemcitabine is widely used in chemotherapy for advanced pancreatic cancer, but chemotherapy in turn promotes the stemness of CSCs. Resveratrol inhibits SREBP1, resulting in the inhibition of lipid synthesis and the stemness induced by gemcitabine, and enhances the sensitivity of gemcitabine[72].

Lipid desaturation in CSCs

MUFAs, such as palmitoleic acid and oleic acid, are key substrates in the formation of complex lipids such as phospholipids, triglycerides, and cholesterol esters, and maintain optimal fluidity of cellular membranes. Moreover, MUFAs have a protective function against the lipotoxicity caused by excess saturated FAs and other cellular stresses[73,74]. SCD catalyzes the committed step in the biosynthesis of MUFAs from saturated FAs[75,76]. There are two isoforms in humans, SCD1 and SCD5. The expression of SCD5 is high in the brain and pancreas, while SCD1 is the main subtype, and is highly expressed in adipose tissue, the brain, liver, heart, and lung[77]. SCD1 is overexpressed in a variety of tumors, including ovarian cancer[78], breast cancer[79], prostate cancer[80], and colon cancer[81]. The upregulation of SCD1, which increases lipid desaturation and relieves endoplasmic reticulum stress, promotes ovarian cancer progression and metastasis[82]. Inhibition of SCD1 can inhibit the growth of leukemic

cells in the central nervous system[83]. A growing number of studies on SCD1 have indicated that it plays a key role in tumorigenesis and maintenance of stemness[84-86]. SCD1 promotes the activation of NF-κB by increasing the synthesis of polyunsaturated FA (PUFAs) to promote CSC characteristics. In turn, the NF-κB pathway regulates the expression of lipid desaturase by regulating transcription. This supports a positive feedback loop involving the NF-κB pathway and lipid desaturase in ovarian CSCs [46]. Furthermore, SCD1 controls the fate of breast CSCs by regulating Wnt/β-catenin signaling[87].

Cholesterol synthesis in CSCs

Cholesterol is an important component of cell membranes and lipid rafts. Highly proliferating cancer cells require increased cholesterol synthesis to meet the need for rapid production of cell membranes. At the same time, metabolically active cancer cells need lipid rafts to form signal complexes for multiple complex signal transduction[88,89]. Cholesterol is produced by a variety of biosynthetic processes or obtained from the diet. Cholesterol synthesis occurs in most tissues and cells. The synthetic pathway involves the conversion of acetyl-CoA to cholesterol through a series of enzymatic reactions, including the biosynthesis of mevalonate (MVA) and squalene[90,91]. There are three crucial players in the cholesterol synthesis pathway, namely, SREBP2 and the two key rate-limiting enzymes, 3-hydroxy-3-methylglutaryl-CoA reductase (HMGCR) and squalene epoxidase (SQLE). Of these, SREBP2 is the master transcriptional regulator of cholesterol biosynthesis. HMGCR and SQLE reduce HMG-CoA to MVA and catalyze the oxidation of squalene to 2,3-epoxy-quinenone, respectively[92]. Increased cholesterol synthesis is considered to be a unique hallmark of many cancers[93]. Pharmacological inhibition of cholesterol biosynthesis dramatically suppressed crypt growth *in vivo* and *ex vivo*, which demonstrates that cholesterol itself acts as a mitogen for intestinal stem cells (ISCs). Cholesterol biosynthesis can drive ISC proliferation and tumorigenesis[94]. Proteomic analysis of tumor tissues, patient-derived xenograft, and mammospheres known to be enriched in CSCs revealed that the expression of proteins involved in the cholesterol synthesis pathway in CSCs increased. Simvastatin or siRNA blocking cholesterol biosynthesis reduced the formation of mammospheres. These results confirm that CSCs are highly dependent on metabolic processes associated with cholesterol biosynthesis, suggesting that the cholesterol biosynthesis pathway is a potential therapeutic target for the elimination of CSCs [95].

SREBP2

SREBP2 specifically regulates cholesterol synthesis and uptake to maintain intracellular cholesterol homeostasis. Evidence indicates that apoA-I binding protein-mediated cholesterol efflux activates endothelial SREBP2 which in turn transactivates Notch and promotes hematopoietic stem and progenitor cell (HSPC) emergence. SREBP2 inhibition impairs hypercholesterolemia-induced HSPC expansion[96]. Biofunctional analyses demonstrated that SREBP2 promotes stem cell-like characteristics and metastasis of prostate cancer cells. The overexpression of SREBP2 increases the population of prostate CSCs and promotes the tumorigenicity of prostate cancer cells *in vivo*, while gene silencing of SREBP2 inhibits the growth, metastasis, and stemness of prostate cancer cells[97]. In colon cancer, inhibition of SREBP2 blocked the proliferation of cancer cells and reduced CSC properties. Knockdown of SREBP inhibits the growth of xenograft tumor *in vivo*[98].

MVA pathway

The MVA pathway produces isoprenoids, such as cholesterol and vitamin D, which are essential for a variety of cellular functions from cholesterol synthesis to cell survival and growth[91]. Many studies have shown that numerous enzymes (HMGCR, FDPS, squalene synthase, and SQLE) required for cholesterol synthesis in the MVA pathway are overexpressed and overactivated in several cancers, including multiple myeloma, as well as breast, gastric, lung, colon, and prostate cancers. Targeting MVA can effectively inhibit the survival and proliferation ability of cancer cells and reduce the tumorigenic potential[99-104]. Overactivation of key enzymes in cholesterol synthesis in the MVA pathway is usually associated with a poor prognosis with shorter disease-free survival and reduced overall survival[105-107]. Statins inhibit HMGCR, the rate-limiting enzyme of the MVA pathway. Genetic variants associated with low HMG-CoA reductase function significantly reduced the risk of epithelial ovarian cancer[108]. Lovastatin inhibited SOX2 promoter transactivation and reduced the efficiency of mammosphere formation and the percentage of ALDH+ cells *in vitro*. Gene set enrichment analysis indicated that lovastatin downregulates genes that are involved in stemness and invasiveness of breast CSCs[109]. Atorvastatin has a stronger anti-proliferative effect on CSCs by inhibiting the MVA pathway[110]. Cholesterol and MVA increase the proliferation of breast CSCs and promote breast cancer progression, invasion, and chemotherapy resistance through activation of the estrogen-related receptor α pathway[111]. Long non-coding RNA (lncRNA)/mRNA microarray assays showed that a novel lncRNA (named lnc030) cooperates with poly (rC) binding protein 2 (PCBP2) to stabilize SQLE mRNA, resulting in increased cholesterol which activates PI3K/Akt signaling in governing BCSC stemness[112].

In addition, the MVA pathway is the only source of intracellular isopentenyl- diphosphate, which produces farnesyl-diphosphate and geranylgeranyl-diphosphate (GGPP) for the prenylation of proteins. For example, different types of preacylation enable the RasGTPase superfamily, including Ras and

Ral/Rho, to be correctly directed to specific subcellular membranes to function. The RasGTPase superfamily affects a variety of cellular processes in cancer progression and participates in EMT, tumor progression, metastasis, and chemotherapy resistance. Inhibition of the MVA pathway can reduce GTPases prenylation and can induce the death of cancer cells, suggesting that these MVA pathway metabolites are essential for cancer cell viability[91,110]. In addition, inhibiting the MVA pathway with small-molecule inhibitors such as statins has been shown to cause inhibition of YAP/transcriptional co-activator with PDZ-binding motif (TAZ) activity. Studies have shown that the activation of RhoGTPases requires GGPP, and the Rho-dependent YAP/TAZ regulatory pathway inhibits YAP/TAZ phosphorylation and promotes their nuclear accumulation to play a role[113-115]. Decreasing the activation of Rho-GTPases and Hippo-YAP/TAZ represses the expression of genes associated with breast cancer stemness[116]. YAP/TAZ nuclear accumulation and transcriptional activity are attenuated by Rho-GTPase/F-actin signaling to increase the sensitivity to chemotherapeutic drugs and suppress breast cancer chemoresistance[117].

MECHANISM OF LIPID SYNTHESIS REPROGRAMMING IN CSCS

In CSCs, there are a series of pathways involved in lipid metabolism to maintain cell stemness, and sustain their survival, proliferation, and invasion, including Notch, hippocampal cascade, HH, and Wnt signaling (Figure 3).

Notch signaling

Notch signaling is a highly conservative signal transduction pathway, which is closely related to various biological behaviors such as tumor metastasis and immune escape[22,118,119]. In terms of lipid metabolism, the Notch signaling pathway can regulate the expression of peroxisome proliferator-activated receptor α and lipid oxidation genes to achieve lipid homeostasis and redox homeostasis[120]. In colon cancer, targeting SCD1-dependent lipid desaturation selectively eliminates colon CSCs by inhibiting Notch signaling[49,121].

Wnt signaling pathway

The Wnt signal cascade includes three main pathways: The canonical Wnt pathway, which leads to the accumulation of β-catenin, activates the transactivation complex, and participates in tumorigenesis, the non-canonical planar cellular polarity pathway, and the non-canonical Wnt-calcium pathway[119]. At least 19 Wnt family members have been identified in humans, all of which are lipid-modified secretory glycoproteins. They are the ligands of ten Frizzled family receptors[22,122].

Wnt signaling plays a key role in regulating CSCs[13,123,124]. The canonical Wnt signaling pathway, activated by ligands such as Wnt2β and Wnt3, promotes the proliferation of CSC by up-regulating β-catenin and terminating target β-catenin and STOP-target proteins, such as FOXM1, MYC, and YAP/TAZ, while the non-canonical Wnt signaling pathway in CSCs is activated by non-canonical Wnt ligands such as Wnt5A and Wnt11, thus activating the PI3K/AKT signal and inducing YAP/TAZ-dependent transcriptional activation to promote survival and therapeutic resistance of CSCs[125]. In contrast, tumor invasion and metastasis are driven by both the canonical and non-canonical Wnt signaling cascades. Canonical Wnt/β-catenin and Wnt/STOP signaling cascades cooperatively upregulate SNAI1 to initiate EMT of CSCs[126].

Wnt signaling has also been associated with lipid synthesis in CSCs. The canonical Wnt/β-catenin pathway regulates *de novo* lipogenesis and fatty acid monounsaturation[127]. SCD could be a key regulator between the Wnt signaling pathway and lipid metabolism. In mouse liver CSCs, the expression of SCD is regulated by the Wnt-β-catenin signaling pathway, while MUFAs produced by SCD provide a positive feedback loop to amplify Wnt signaling by promoting the stability and expression of Lrp5/6 mRNA[128]. Another study suggests that MUFAs are crucial in the production and secretion of Wnt ligands[129]. Finally, FA metabolism, especially SCD1 activity, in YAP/TAZ signaling depends on the activity of the β-catenin pathway in CSCs[130].

Hippo signaling

The core of the Hippo signaling pathway is the kinase cascade involving mammalian STE20-like (MST)1/2 and LATS1/2. MST1/2 activates LATS1/2 by promoting autosphosphorylation of LATS1/2 or by phosphorylation of MOB1, resulting in degradation of the downstream transcriptional coactivators YAP1 and TAZ, thereby limiting YAP activity[22,131]. YAP/TAZ activation leads to the induction of CSC properties, including self-renewal, tumorigenic potential, anoikis resistance, EMT, drug resistance, and metastasis, in a wide range of human cancers[132,133]. As mentioned earlier, in lung CSCs, SCD1 regulates lung cancer stemness by stabilizing YAP/TAZ and nuclear localization [130]. The positive feedback loops of LATS2 and p53 inhibit cholesterol synthesis, and LATS2 binds to the endoplasmic reticulum tethered precursor (P-SREBP) of SREBP1 and SREBP2, and inhibits the transcription of SREBP mRNA, thus inhibiting the activity of cellular SREBP[134]. Recent studies have revealed that the cancer-promoting properties of YAP/TAZ depend on cholesterol biosynthesis activity

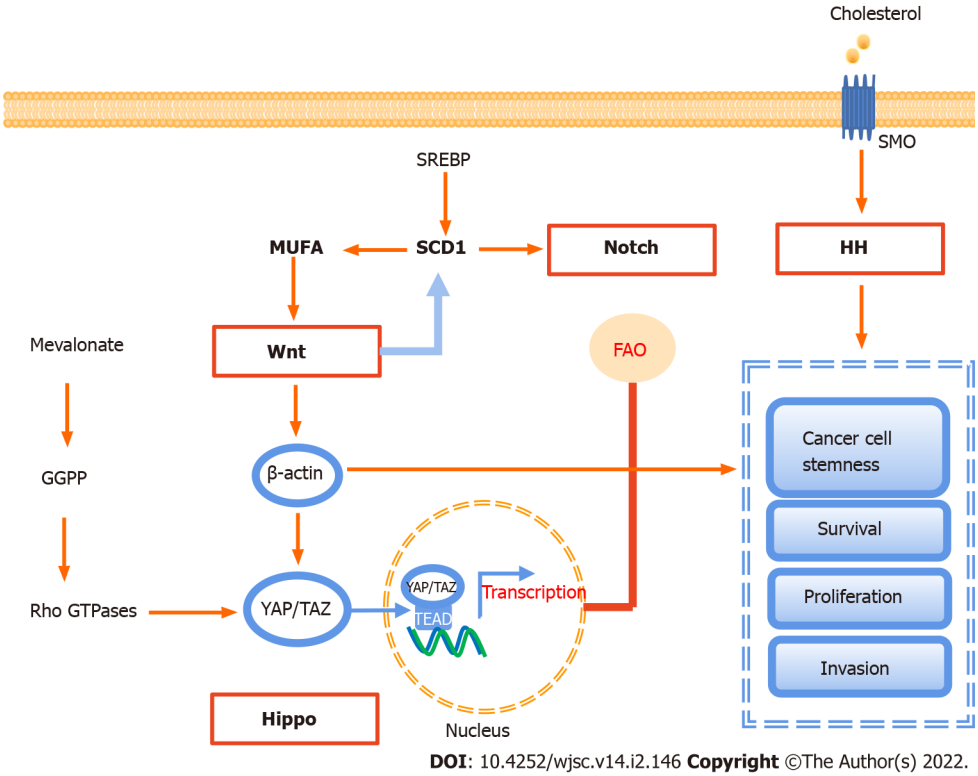

DOI: 10.4252/wjsc.v14.i2.146

Figure 3 Signaling pathways involved in lipid metabolism in cancer stem cells. There are four major signaling pathways, including Notch, Wnt, Hippo, and Hedgehog signaling, involved in lipid metabolism to maintain cell stemness, and sustain their survival, proliferation, and invasion. GGPP: Geranylgeranyl pyrophosphate; MUFA: Monounsaturated fatty acids; YAP: Yes-associated protein; TAZ: Transcriptional co-activator with PDZ-binding motif; SREBP: Sterol regulatory element-binding protein; SCD1: Stearyl coenzyme A desaturase 1; TEAD: Transcriptional enhanced associate domain; FAO: Fatty acid oxidation; SMO: Smoothened; HH: Hedgehog; SMP: Scalp micropigmentation.

and MVA-dependent nuclear localization and activity of YAP/TAZ[114]. YAP/TAZ-mediated lipid synthesis may be an important factor affecting the metabolic changes of CSCs[135].

HH signaling

The HH signaling pathway, which is responsible for the signal transmission from the cell membrane to the nucleus, is a highly conservative pathway. HH ligands mainly include Sonic hedgehog (SHH), Indian HH, and Desert HH. The HH signal pathway is activated by the binding of HH ligands to the transmembrane proteins Patched (PTCH)1/2, which release the inhibition of smoothened (SMO), leading to the activation of glioma transcription factors, thus inducing target gene transcription[22]. HH ligands have been found to be activated in CSCs. High fibrillar collagen content resulting from HH pathway activation promotes breast cancer cell stemness. In cholangiocarcinoma, hypoxia promoted SHH pathway activation. Inhibition of the SHH pathway by cyclopamine significantly attenuated the expression of CSC transcription factors, leading to the abrogation of CD133 expression and EMT[136].

Previous evidence suggested that lipids are key regulators of HH signaling. The cholesterol covalent modification of SMO is regulated by the HH signaling pathway and is very important for the signal transduction and cell biological function of HH. PTCH1 inhibits the cholesterol modification of SMO, while the overexpression of SHH increases the cholesterol modification of SMO[137]. In addition, SMO activates adenosine monophosphate kinase *via* the non-canonical pathway, directly or indirectly inhibiting FA and cholesterol synthesis[138].

APPLICATION PROSPECTS OF LIPID SYNTHESIS REPROGRAMMING IN THE TREATMENT OF CSCS

CSCs can adapt easily to changes in the nearby environment and are more resistant to conventional therapies than other cancer cells. However, their proliferation and survival are highly dependent on lipid synthesis, which provides a point of penetration for the establishment of efficient targeting strategies to eliminate CSCs. Targeted clearance of CSCs can be achieved by interfering with different aspects of lipid synthesis, such as FA synthesis, lipid desaturation, and cholesterol synthesis (Table 1).

Table 1 Inhibitors related to lipid synthesis enzymes of cancer stem cells

Metabolism type	Targeting enzyme	Drug	Cancer type	Metabolic processes or signaling pathways involved	Study type
Lipogenesis	FASN	Cerulenin	Glioma stem cells[63], pancreatic CSCs[65]	FASN	Preclinical trial
	FASN	TVB-2640	NSCLC and breast cancer[139]	FASN	Clinical trial
	ACC	Soraphen A	Breast CSCs[140]	FASN	Preclinical trial
	ACC	ND-646	Non-small-cell lung CSCs[142]	FASN	Preclinical trial
	ACC	Leptin	Breast CSCs[141]	TAK1-AMPK signaling	Preclinical trial
Lipid desaturation	SCD1	CAY10566	Ovarian CSCs[46], glioblastoma CSCs[84]	NF-κB pathway, ER stress	Preclinical trial
	SCD1	A939572	Liver cancer[146], *etc.*	MUFA synthesis	Preclinical trial
	SCD1	MF-438	Colon CSCs[121], lung CSCs[85]	Wnt, Notch, and YAP/TAZ signaling	Preclinical trial
	SCD1	PluriSIn#1	Colon CSCs[121], liver CSCs[150]	Wnt/β-catenin and Notch signaling	Preclinical trial
	Delta 6 desaturase	SC-26196	Ovarian CSCs[46]	Polyunsaturated fatty acid synthesis	Preclinical trial
Cholesterol synthesis	SREBPs	25-HC or fatostatin	Colon CSCs[98]	Fatty acid synthesis and cholesterol synthesis	Preclinical trial
		Pyrvinium pamoate	TNBC CSCs[45]	Cholesterol biosynthesis	Preclinical trial
	HMGCR	Simvastatin	Breast CSCs[95]	Cholesterol biosynthesis	FDA-approved cardiovascular system drug

HMGCR: 3-hydroxy-3-methylglutaryl-CoA reductase; CSCs: Cancer stem cells; FDA: Food and Drug Administration; TNBC: Triple negative breast cancer; ACC: Acetyl-CoA carboxylase; FASN: Fatty acid synthase; MUFA: Monounsaturated fatty acid; NSCLC: Non-small cell lung cancer; YAP: Yes-associated protein; TAZ: Transcriptional co-activator with PDZ-binding motif; SREBP: Sterol regulatory element-binding protein; SCD1: Stearyl coenzyme A desaturase 1.

Targeting FA synthesis

FASN is the most targetable among the lipogenesis genes. Some FASN inhibitors have shown anti-CSC and anti-tumor activities. Both inhibitor and RNA silencing of FASN decreased invasiveness, sphere formation, and expression of stemness markers to kill various CSCs[63,65]. A new generation of FASN inhibitors is being developed, and data from early clinical trials on TVB-2640, a FASN inhibitor, show a partial tumor response in patients with non-small-cell lung cancer and breast cancer when TVB-2640 was used in combination with paclitaxel[139]. Similarly, Soraphen A, an ACC inhibitor, suppressed mammosphere formation. Sorafen A treatment inhibited the self-renewal and growth of CSC-like cells by blocking FA synthesis and eliminated the promoting effect of human epidermal growth factor receptor 2 on CSC proliferation[140]. Moreover, inhibition of ACC suppresses tumor growth, metastasis, and recurrence in non-small-cell lung cancer and breast cancer[141,142], indicating that ACC has great significance and potential in inhibiting CSCs and cancer.

However, in addition to being produced through the ACLY pathway, acetyl-CoA can also be produced by glucose or acetate metabolism to enter the process of fatty acid synthesis[143,144]. In cancer cells, ACLY silencing increases the expression of ACC2, which maintains lipid synthesis in an acetate-dependent manner[145]. Despite the knockdown of ACLY diminishing the number of breast CSCs, the effect of ACLY deficiency remains to be studied in CSCs.

Targeting lipid desaturation

Targeting SCD1, which converts fully saturated fatty acids to MUFAs, can selectively kill CSCs. It is reported that SCD1 inhibitors, such as CAY10566 and A939572, suppress cancer stemness and prevent tumorigenesis, and can counteract cancer cell chemoresistance[46,146]. Significantly, MF-438 and PluriSIn #1, as SCD1 inhibitors, selectively eliminate colon CSCs but not the bulk cancer cells[121]. Furthermore, inhibition of SCD1 increased the sensitivity of CSCs to cisplatin and reduced drug resistance[85]. Therefore, combining SCD1 inhibitors with chemotherapy may be a more effective

treatment strategy. Other studies have shown that miR-600 targeting SCD1 regulates Wnt/β-catenin signaling, thereby inhibiting the self-renewal and differentiation of mammary CSCs. Therefore, in addition to SCD1 inhibitors, nanovectorized miR-600 agonists (promiRNAs) may serve as a targeted tumor stem cell therapy[87]. Delta 6-desaturase inhibitors block the globular formation and tumor-initiating ability of ovarian CSCs by inhibiting the synthesis of PUFAs[46].

Targeting cholesterol synthesis

Activation of cholesterol synthesis could be relevant to the aggressive and metastatic potential in CSCs. Inhibition of SREBP activation by 25-HC or fatostatin inhibits lipogenesis, including FA and cholesterol, and decreases the expression of genes associated with CSCs[98]. PP significantly inhibits lipid anabolism in CSCs. In triple-negative breast cancer, PP exerts cytotoxic effects on TNBCSCs by inhibiting cholesterol synthesis[45]. Simvastatin significantly reduced mammosphere formation and growth through inhibition of cholesterol biosynthesis[96]. In addition, statins target CSCs by inhibiting the signaling associated with protein farnesylation, and protein geranylgeranylation in the MVA pathway[147,148]. Similarly, metformin suppresses CSCs through inhibiting protein prenylation of the MVA pathway in colorectal cancer[149].

CONCLUSION

In the past few years, many studies have shown that CSCs are responsible for tumor occurrence and development, distant metastasis, and therapy resistance. Metabolic alterations are the main pathways for cancer cells and CSCs to escape from adverse environmental effects. Among the reprogrammed metabolic pathways, alterations in lipid synthesis such as *de novo* lipogenesis, lipid desaturation, and cholesterol synthesis are closely related to CSC generation and stemness maintenance. Furthermore, lipid synthesis is also involved in the activation of several important oncogenic signaling pathways, including Notch, Wnt/β-catenin, Hippo, and HH signaling. Taking the key molecules of lipid synthesis as the target shows promising application potential in the elimination of CSCs. Therefore, we believe that altered lipid synthesis metabolism is a promising target for CSC elimination and tumor therapy.

FOOTNOTES

Author contributions: Wang SY was responsible for conceptualizing this review and writing the original draft; Hu QC was involved in the conceptualization, funding acquisition, and review and editing of the manuscript; Wu T participated in the conceptualization and review of the manuscript; Tao XA, Xia J, and Cheng B contributed to the editing, improving, and finalizing of the manuscript; all authors approved the final version of the manuscript and agreed to be accountable for this work.

Supported by the National Natural Science Foundation of China, No. 82001044 and No. 81630025; the China Postdoctoral Science Foundation, No. 2020M673019; the Guangdong Basic and Applied Basic Research Foundation, No. 2019A1515110071; and the Natural Science Foundation of Guangdong Province, No. 2017A030311033.

Conflict-of-interest statement: The research was conducted in the absence of any commercial or financial relationships that could be construed as a potential conflict of interest.

Country/Territory of origin: China

ORCID number: Si-Yu Wang 0000-0001-9690-5514; Qin-Chao Hu 0000-0002-4969-0589; Tong Wu 0000-0001-7455-9083; Juan Xia 0000-0002-4966-7119; Xiao-An Tao 0000-0003-1114-9698; Bin Cheng 0000-0001-7288-806X.

S-Editor: Wang JJ
L-Editor: Wang TQ
P-Editor: Wang JJ

REFERENCES

1 **Clevers H**. The cancer stem cell: premises, promises and challenges. *Nat Med* 2011; **17**: 313-319 [PMID: 21386835 DOI: 10.1038/nm.2304]
2 **Najafi M**, Mortezaee K, Majidpoor J. Cancer stem cell (CSC) resistance drivers. *Life Sci* 2019; **234**: 116781 [PMID: 31430455 DOI: 10.1016/j.lfs.2019.116781]
3 **Vlashi E**, Pajonk F. Cancer stem cells, cancer cell plasticity and radiation therapy. *Semin Cancer Biol* 2015; **31**: 28-35 [PMID: 25025713 DOI: 10.1016/j.semcancer.2014.07.001]
4 **Feinberg AP**, Koldobskiy MA, Göndör A. Epigenetic modulators, modifiers and mediators in cancer aetiology and progression. *Nat Rev Genet* 2016; **17**: 284-299 [PMID: 26972587 DOI: 10.1038/nrg.2016.13]
5 **Plaks V**, Kong N, Werb Z. The cancer stem cell niche: how essential is the niche in regulating stemness of tumor cells? *Cell Stem Cell* 2015; **16**: 225-238 [PMID: 25748930 DOI: 10.1016/j.stem.2015.02.015]
6 **Batlle E**, Clevers H. Cancer stem cells revisited. *Nat Med* 2017; **23**: 1124-1134 [PMID: 28985214 DOI: 10.1038/nm.4409]
7 **Nieto MA**, Huang RY, Jackson RA, Thiery JP. EMT: 2016. *Cell* 2016; **166**: 21-45 [PMID: 27368099 DOI: 10.1016/j.cell.2016.06.028]
8 **Eun K**, Ham SW, Kim H. Cancer stem cell heterogeneity: origin and new perspectives on CSC targeting. *BMB Rep* 2017; **50**: 117-125 [PMID: 27998397 DOI: 10.5483/bmbrep.2017.50.3.222]
9 **Najafi M**, Mortezaee K, Ahadi R. Cancer stem cell (a)symmetry & plasticity: Tumorigenesis and therapy relevance. *Life Sci* 2019; **231**: 116520 [PMID: 31158379 DOI: 10.1016/j.lfs.2019.05.076]
10 **Zhou P**, Li B, Liu F, Zhang M, Wang Q, Liu Y, Yao Y, Li D. The epithelial to mesenchymal transition (EMT) and cancer stem cells: implication for treatment resistance in pancreatic cancer. *Mol Cancer* 2017; **16**: 52 [PMID: 28245823 DOI: 10.1186/s12943-017-0624-9]
11 **Ye X**, Tam WL, Shibue T, Kaygusuz Y, Reinhardt F, Ng Eaton E, Weinberg RA. Distinct EMT programs control normal mammary stem cells and tumour-initiating cells. *Nature* 2015; **525**: 256-260 [PMID: 26331542 DOI: 10.1038/nature14897]
12 **Sattiraju A**, Sai KKS, Mintz A. Glioblastoma Stem Cells and Their Microenvironment. *Adv Exp Med Biol* 2017; **1041**: 119-140 [PMID: 29204831 DOI: 10.1007/978-3-319-69194-7_7]
13 **Vermeulen L**, De Sousa E Melo F, van der Heijden M, Cameron K, de Jong JH, Borovski T, Tuynman JB, Todaro M, Merz C, Rodermond H, Sprick MR, Kemper K, Richel DJ, Stassi G, Medema JP. Wnt activity defines colon cancer stem cells and is regulated by the microenvironment. *Nat Cell Biol* 2010; **12**: 468-476 [PMID: 20418870 DOI: 10.1038/ncb2048]
14 **Zhou H**, Xu R. Leukemia stem cells: the root of chronic myeloid leukemia. *Protein Cell* 2015; **6**: 403-412 [PMID: 25749979 DOI: 10.1007/s13238-015-0143-7]
15 **Chopra M**, Bohlander SK. The cell of origin and the leukemia stem cell in acute myeloid leukemia. *Genes Chromosomes Cancer* 2019; **58**: 850-858 [PMID: 31471945 DOI: 10.1002/gcc.22805]
16 **Xie SL**, Fan S, Zhang SY, Chen WX, Li QX, Pan GK, Zhang HQ, Wang WW, Weng B, Zhang Z, Li JS, Lin ZY. SOX8 regulates cancer stem-like properties and cisplatin-induced EMT in tongue squamous cell carcinoma by acting on the Wnt/β-catenin pathway. *Int J Cancer* 2018; **142**: 1252-1265 [PMID: 29071717 DOI: 10.1002/ijc.31134]
17 **Yang F**, Xu J, Tang L, Guan X. Breast cancer stem cell: the roles and therapeutic implications. *Cell Mol Life Sci* 2017; **74**: 951-966 [PMID: 27530548 DOI: 10.1007/s00018-016-2334-7]
18 **Janiszewska M**, Suvà ML, Riggi N, Houtkooper RH, Auwerx J, Clément-Schatlo V, Radovanovic I, Rheinbay E, Provero P, Stamenkovic I. Imp2 controls oxidative phosphorylation and is crucial for preserving glioblastoma cancer stem cells. *Genes Dev* 2012; **26**: 1926-1944 [PMID: 22899010 DOI: 10.1101/gad.188292.112]
19 **Heng WS**, Gosens R, Kruyt FAE. Lung cancer stem cells: origin, features, maintenance mechanisms and therapeutic targeting. *Biochem Pharmacol* 2019; **160**: 121-133 [PMID: 30557553 DOI: 10.1016/j.bcp.2018.12.010]
20 **Leon G**, MacDonagh L, Finn SP, Cuffe S, Barr MP. Cancer stem cells in drug resistant lung cancer: Targeting cell surface markers and signaling pathways. *Pharmacol Ther* 2016; **158**: 71-90 [PMID: 26706243 DOI: 10.1016/j.pharmthera.2015.12.001]
21 **Brown HK**, Tellez-Gabriel M, Heymann D. Cancer stem cells in osteosarcoma. *Cancer Lett* 2017; **386**: 189-195 [PMID: 27894960 DOI: 10.1016/j.canlet.2016.11.019]
22 **Clara JA**, Monge C, Yang Y, Takebe N. Targeting signalling pathways and the immune microenvironment of cancer stem cells - a clinical update. *Nat Rev Clin Oncol* 2020; **17**: 204-232 [PMID: 31792354 DOI: 10.1038/s41571-019-0293-2]
23 **Li L**, Bi Z, Wadgaonkar P, Lu Y, Zhang Q, Fu Y, Thakur C, Wang L, Chen F. Metabolic and epigenetic reprogramming in the arsenic-induced cancer stem cells. *Semin Cancer Biol* 2019; **57**: 10-18 [PMID: 31009762 DOI: 10.1016/j.semcancer.2019.04.003]
24 **Viale A**, Pettazzoni P, Lyssiotis CA, Ying H, Sánchez N, Marchesini M, Carugo A, Green T, Seth S, Giuliani V, Kost-Alimova M, Muller F, Colla S, Nezi L, Genovese G, Deem AK, Kapoor A, Yao W, Brunetto E, Kang Y, Yuan M, Asara JM, Wang YA, Heffernan TP, Kimmelman AC, Wang H, Fleming JB, Cantley LC, DePinho RA, Draetta GF. Oncogene ablation-resistant pancreatic cancer cells depend on mitochondrial function. *Nature* 2014; **514**: 628-632 [PMID: 25119024 DOI: 10.1038/nature13611]
25 **Pavlova NN**, Thompson CB. The Emerging Hallmarks of Cancer Metabolism. *Cell Metab* 2016; **23**: 27-47 [PMID: 26771115 DOI: 10.1016/j.cmet.2015.12.006]
26 **Shen YA**, Wang CY, Hsieh YT, Chen YJ, Wei YH. Metabolic reprogramming orchestrates cancer stem cell properties in nasopharyngeal carcinoma. *Cell Cycle* 2015; **14**: 86-98 [PMID: 25483072 DOI: 10.4161/15384101.2014.974419]
27 **Qing Y**, Dong L, Gao L, Li C, Li Y, Han L, Prince E, Tan B, Deng X, Wetzel C, Shen C, Gao M, Chen Z, Li W, Zhang B, Braas D, Ten Hoeve J, Sanchez GJ, Chen H, Chan LN, Chen CW, Ann D, Jiang L, Müschen M, Marcucci G, Plas DR, Li Z, Su R, Chen J. R-2-hydroxyglutarate attenuates aerobic glycolysis in leukemia by targeting the FTO/m^{6}A/PFKP/LDHB

axis. *Mol Cell* 2021; **81**: 922-939.e9 [PMID: 33434505 DOI: 10.1016/j.molcel.2020.12.026]

28 **Palorini R**, Votta G, Balestrieri C, Monestiroli A, Olivieri S, Vento R, Chiaradonna F. Energy metabolism characterization of a novel cancer stem cell-like line 3AB-OS. *J Cell Biochem* 2014; **115**: 368-379 [PMID: 24030970 DOI: 10.1002/jcb.24671]

29 **Peng F**, Wang JH, Fan WJ, Meng YT, Li MM, Li TT, Cui B, Wang HF, Zhao Y, An F, Guo T, Liu XF, Zhang L, Lv L, Lv DK, Xu LZ, Xie JJ, Lin WX, Lam EW, Xu J, Liu Q. Glycolysis gatekeeper PDK1 reprograms breast cancer stem cells under hypoxia. *Oncogene* 2018; **37**: 1062-1074 [PMID: 29106390 DOI: 10.1038/onc.2017.368]

30 **Liao J**, Qian F, Tchabo N, Mhawech-Fauceglia P, Beck A, Qian Z, Wang X, Huss WJ, Lele SB, Morrison CD, Odunsi K. Ovarian cancer spheroid cells with stem cell-like properties contribute to tumor generation, metastasis and chemotherapy resistance through hypoxia-resistant metabolism. *PLoS One* 2014; **9**: e84941 [PMID: 24409314 DOI: 10.1371/journal.pone.0084941]

31 **Yan B**, Jiang Z, Cheng L, Chen K, Zhou C, Sun L, Qian W, Li J, Cao J, Xu Q, Ma Q, Lei J. Paracrine HGF/c-MET enhances the stem cell-like potential and glycolysis of pancreatic cancer cells *via* activation of YAP/HIF-1α. *Exp Cell Res* 2018; **371**: 63-71 [PMID: 30056064 DOI: 10.1016/j.yexcr.2018.07.041]

32 **Song IS**, Jeong YJ, Han J. Mitochondrial metabolism in cancer stem cells: a therapeutic target for colon cancer. *BMB Rep* 2015; **48**: 539-540 [PMID: 26350748 DOI: 10.5483/bmbrep.2015.48.10.179]

33 **Foo BJ**, Eu JQ, Hirpara JL, Pervaiz S. Interplay between Mitochondrial Metabolism and Cellular Redox State Dictates Cancer Cell Survival. *Oxid Med Cell Longev* 2021; **2021**: 1341604 [PMID: 34777681 DOI: 10.1155/2021/1341604]

34 **Raggi C**, Taddei ML, Sacco E, Navari N, Correnti M, Piombanti B, Pastore M, Campani C, Pranzini E, Iorio J, Lori G, Lottini T, Peano C, Cibella J, Lewinska M, Andersen JB, di Tommaso L, Viganò L, Di Maira G, Madiai S, Ramazzotti M, Orlandi I, Arcangeli A, Chiarugi P, Marra F. Mitochondrial oxidative metabolism contributes to a cancer stem cell phenotype in cholangiocarcinoma. *J Hepatol* 2021; **74**: 1373-1385 [PMID: 33484774 DOI: 10.1016/j.jhep.2020.12.031]

35 **Strzyz P**. Immortalizing switch to OXPHOS. *Nat Rev Mol Cell Biol* 2020; **21**: 658-659 [PMID: 32978604 DOI: 10.1038/s41580-020-00301-1]

36 **Long NA**, Golla U, Sharma A, Claxton DF. Acute Myeloid Leukemia Stem Cells: Origin, Characteristics, and Clinical Implications. *Stem Cell Rev Rep* 2022 [PMID: 35050458 DOI: 10.1007/s12015-021-10308-6]

37 **Valle S**, Alcalá S, Martin-Hijano L, Cabezas-Sáinz P, Navarro D, Muñoz ER, Yuste L, Tiwary K, Walter K, Ruiz-Cañas L, Alonso-Nocelo M, Rubiolo JA, González-Arnay E, Heeschen C, Garcia-Bermejo L, Hermann PC, Sánchez L, Sancho P, Fernández-Moreno MÁ, Sainz B Jr. Exploiting oxidative phosphorylation to promote the stem and immunoevasive properties of pancreatic cancer stem cells. *Nat Commun* 2020; **11**: 5265 [PMID: 33067432 DOI: 10.1038/s41467-020-18954-z]

38 **Wang T**, Fahrmann JF, Lee H, Li YJ, Tripathi SC, Yue C, Zhang C, Lifshitz V, Song J, Yuan Y, Somlo G, Jandial R, Ann D, Hanash S, Jove R, Yu H. JAK/STAT3-Regulated Fatty Acid β-Oxidation Is Critical for Breast Cancer Stem Cell Self-Renewal and Chemoresistance. *Cell Metab* 2018; **27**: 136-150.e5 [PMID: 29249690 DOI: 10.1016/j.cmet.2017.11.001]

39 **Farge T**, Saland E, de Toni F, Aroua N, Hosseini M, Perry R, Bosc C, Sugita M, Stuani L, Fraisse M, Scotland S, Larrue C, Boutzen H, Féliu V, Nicolau-Travers ML, Cassant-Sourdy S, Broin N, David M, Serhan N, Sarry A, Tavitian S, Kaoma T, Vallar L, Iacovoni J, Linares LK, Montersino C, Castellano R, Griessinger E, Collette Y, Duchamp O, Barreira Y, Hirsch P, Palama T, Gales L, Delhommeau F, Garmy-Susini BH, Portais JC, Vergez F, Selak M, Danet-Desnoyers G, Carroll M, Récher C, Sarry JE. Chemotherapy-Resistant Human Acute Myeloid Leukemia Cells Are Not Enriched for Leukemic Stem Cells but Require Oxidative Metabolism. *Cancer Discov* 2017; **7**: 716-735 [PMID: 28416471 DOI: 10.1158/2159-8290.CD-16-0441]

40 **He W**, Liang B, Wang C, Li S, Zhao Y, Huang Q, Liu Z, Yao Z, Wu Q, Liao W, Zhang S, Liu Y, Xiang Y, Liu J, Shi M. MSC-regulated lncRNA MACC1-AS1 promotes stemness and chemoresistance through fatty acid oxidation in gastric cancer. *Oncogene* 2019; **38**: 4637-4654 [PMID: 30742067 DOI: 10.1038/s41388-019-0747-0]

41 **Tirinato L**, Liberale C, Di Franco S, Candeloro P, Benfante A, La Rocca R, Potze L, Marotta R, Ruffilli R, Rajamanickam VP, Malerba M, De Angelis F, Falqui A, Carbone E, Todaro M, Medema JP, Stassi G, Di Fabrizio E. Lipid droplets: a new player in colorectal cancer stem cells unveiled by spectroscopic imaging. *Stem Cells* 2015; **33**: 35-44 [PMID: 25186497 DOI: 10.1002/stem.1837]

42 **Giampietri C**, Petrungaro S, Cordella M, Tabolacci C, Tomaipitinca L, Facchiano A, Eramo A, Filippini A, Facchiano F, Ziparo E. Lipid Storage and Autophagy in Melanoma Cancer Cells. *Int J Mol Sci* 2017; **18** [PMID: 28617309 DOI: 10.3390/ijms18061271]

43 **Kuramoto K**, Yamamoto M, Suzuki S, Togashi K, Sanomachi T, Kitanaka C, Okada M. Inhibition of the Lipid Droplet-Peroxisome Proliferator-Activated Receptor α Axis Suppresses Cancer Stem Cell Properties. *Genes (Basel)* 2021; **12** [PMID: 33466690 DOI: 10.3390/genes12010099]

44 **Yi M**, Li J, Chen S, Cai J, Ban Y, Peng Q, Zhou Y, Zeng Z, Peng S, Li X, Xiong W, Li G, Xiang B. Emerging role of lipid metabolism alterations in Cancer stem cells. *J Exp Clin Cancer Res* 2018; **37**: 118 [PMID: 29907133 DOI: 10.1186/s13046-018-0784-5]

45 **Dattilo R**, Mottini C, Camera E, Lamolinara A, Auslander N, Doglioni G, Muscolini M, Tang W, Planque M, Ercolani C, Buglioni S, Manni I, Trisciuoglio D, Boe A, Grande S, Luciani AM, Iezzi M, Ciliberto G, Ambs S, De Maria R, Fendt SM, Ruppin E, Cardone L. Pyrvinium Pamoate Induces Death of Triple-Negative Breast Cancer Stem-Like Cells and Reduces Metastases through Effects on Lipid Anabolism. *Cancer Res* 2020; **80**: 4087-4102 [PMID: 32718996 DOI: 10.1158/0008-5472.CAN-19-1184]

46 **Li J**, Condello S, Thomes-Pepin J, Ma X, Xia Y, Hurley TD, Matei D, Cheng JX. Lipid Desaturation Is a Metabolic Marker and Therapeutic Target of Ovarian Cancer Stem Cells. *Cell Stem Cell* 2017; **20**: 303-314.e5 [PMID: 28041894 DOI: 10.1016/j.stem.2016.11.004]

47 **Song M**, Lee H, Nam MH, Jeong E, Kim S, Hong Y, Kim N, Yim HY, Yoo YJ, Kim JS, Cho YY, Mills GB, Kim WY, Yoon S. Loss-of-function screens of druggable targetome against cancer stem-like cells. *FASEB J* 2017; **31**: 625-635 [PMID: 27811063 DOI: 10.1096/fj.201600953]

48 **Lo Re O**, Douet J, Buschbeck M, Fusilli C, Pazienza V, Panebianco C, Castracani CC, Mazza T, Li Volti G, Vinciguerra

M. Histone variant macroH2A1 rewires carbohydrate and lipid metabolism of hepatocellular carcinoma cells towards cancer stem cells. *Epigenetics* 2018; **13**: 829-845 [PMID: 30165787 DOI: 10.1080/15592294.2018.1514239]

49 **Choi S**, Yoo YJ, Kim H, Lee H, Chung H, Nam MH, Moon JY, Lee HS, Yoon S, Kim WY. Clinical and biochemical relevance of monounsaturated fatty acid metabolism targeting strategy for cancer stem cell elimination in colon cancer. *Biochem Biophys Res Commun* 2019; **519**: 100-105 [PMID: 31481234 DOI: 10.1016/j.bbrc.2019.08.137]

50 **Khwairakpam AD**, Shyamananda MS, Sailo BL, Rathnakaram SR, Padmavathi G, Kotoky J, Kunnumakkara AB. ATP citrate lyase (ACLY): a promising target for cancer prevention and treatment. *Curr Drug Targets* 2015; **16**: 156-163 [PMID: 25537655 DOI: 10.2174/1389450115666141224125117]

51 **Granchi C**. ATP citrate lyase (ACLY) inhibitors: An anti-cancer strategy at the crossroads of glucose and lipid metabolism. *Eur J Med Chem* 2018; **157**: 1276-1291 [PMID: 30195238 DOI: 10.1016/j.ejmech.2018.09.001]

52 **Icard P**, Wu Z, Fournel L, Coquerel A, Lincet H, Alifano M. ATP citrate lyase: A central metabolic enzyme in cancer. *Cancer Lett* 2020; **471**: 125-134 [PMID: 31830561 DOI: 10.1016/j.canlet.2019.12.010]

53 **Clementino M**, Xie J, Yang P, Li Y, Lin HP, Fenske WK, Tao H, Kondo K, Yang C, Wang Z. A Positive Feedback Loop Between c-Myc Upregulation, Glycolytic Shift, and Histone Acetylation Enhances Cancer Stem Cell-like Property and Tumorigenicity of Cr(VI)-transformed Cells. *Toxicol Sci* 2020; **177**: 71-83 [PMID: 32525551 DOI: 10.1093/toxsci/kfaa086]

54 **Yang D**, Peng M, Hou Y, Qin Y, Wan X, Zhu P, Liu S, Yang L, Zeng H, Jin T, Qiu Y, Li Q, Liu M. Oxidized ATM promotes breast cancer stem cell enrichment through energy metabolism reprogram-mediated acetyl-CoA accumulation. *Cell Death Dis* 2020; **11**: 508 [PMID: 32641713 DOI: 10.1038/s41419-020-2714-7]

55 **Hanai JI**, Doro N, Seth P, Sukhatme VP. ATP citrate lyase knockdown impacts cancer stem cells in vitro. *Cell Death Dis* 2013; **4**: e696 [PMID: 23807225 DOI: 10.1038/cddis.2013.215]

56 **Lucenay KS**, Doostan I, Karakas C, Bui T, Ding Z, Mills GB, Hunt KK, Keyomarsi K. Cyclin E Associates with the Lipogenic Enzyme ATP-Citrate Lyase to Enable Malignant Growth of Breast Cancer Cells. *Cancer Res* 2016; **76**: 2406-2418 [PMID: 26928812 DOI: 10.1158/0008-5472.CAN-15-1646]

57 **Wei X**, Shi J, Lin Q, Ma X, Pang Y, Mao H, Li R, Lu W, Wang Y, Liu P. Targeting ACLY Attenuates Tumor Growth and Acquired Cisplatin Resistance in Ovarian Cancer by Inhibiting the PI3K-AKT Pathway and Activating the AMPK-ROS Pathway. *Front Oncol* 2021; **11**: 642229 [PMID: 33816292 DOI: 10.3389/fonc.2021.642229]

58 **Petrova E**, Scholz A, Paul J, Sturz A, Haike K, Siegel F, Mumberg D, Liu N. Acetyl-CoA carboxylase inhibitors attenuate WNT and Hedgehog signaling and suppress pancreatic tumor growth. *Oncotarget* 2017; **8**: 48660-48670 [PMID: 27750213 DOI: 10.18632/oncotarget.12650]

59 **Vazquez-Martin A**, Corominas-Faja B, Cufi S, Vellon L, Oliveras-Ferraros C, Menendez OJ, Joven J, Lupu R, Menendez JA. The mitochondrial H(+)-ATP synthase and the lipogenic switch: new core components of metabolic reprogramming in induced pluripotent stem (iPS) cells. *Cell Cycle* 2013; **12**: 207-218 [PMID: 23287468 DOI: 10.4161/cc.23352]

60 **Bort A**, Sánchez BG, de Miguel I, Mateos-Gómez PA, Diaz-Laviada I. Dysregulated lipid metabolism in hepatocellular carcinoma cancer stem cells. *Mol Biol Rep* 2020; **47**: 2635-2647 [PMID: 32125560 DOI: 10.1007/s11033-020-05352-3]

61 **Tanosaki S**, Tohyama S, Fujita J, Someya S, Hishiki T, Matsuura T, Nakanishi H, Ohto-Nakanishi T, Akiyama T, Morita Y, Kishino Y, Okada M, Tani H, Soma Y, Nakajima K, Kanazawa H, Sugimoto M, Ko MSH, Suematsu M, Fukuda K. Fatty Acid Synthesis Is Indispensable for Survival of Human Pluripotent Stem Cells. *iScience* 2020; **23**: 101535 [PMID: 33083764 DOI: 10.1016/j.isci.2020.101535]

62 **Knobloch M**, Braun SM, Zurkirchen L, von Schoultz C, Zamboni N, Araúzo-Bravo MJ, Kovacs WJ, Karalay O, Suter U, Machado RA, Roccio M, Lutolf MP, Semenkovich CF, Jessberger S. Metabolic control of adult neural stem cell activity by Fasn-dependent lipogenesis. *Nature* 2013; **493**: 226-230 [PMID: 23201681 DOI: 10.1038/nature11689]

63 **Yasumoto Y**, Miyazaki H, Vaidyan LK, Kagawa Y, Ebrahimi M, Yamamoto Y, Ogata M, Katsuyama Y, Sadahiro H, Suzuki M, Owada Y. Inhibition of Fatty Acid Synthase Decreases Expression of Stemness Markers in Glioma Stem Cells. *PLoS One* 2016; **11**: e0147717 [PMID: 26808816 DOI: 10.1371/journal.pone.0147717]

64 **Pandey PR**, Okuda H, Watabe M, Pai SK, Liu W, Kobayashi A, Xing F, Fukuda K, Hirota S, Sugai T, Wakabayashi G, Koeda K, Kashiwaba M, Suzuki K, Chiba T, Endo M, Fujioka T, Tanji S, Mo YY, Cao D, Wilber AC, Watabe K. Resveratrol suppresses growth of cancer stem-like cells by inhibiting fatty acid synthase. *Breast Cancer Res Treat* 2011; **130**: 387-398 [PMID: 21188630 DOI: 10.1007/s10549-010-1300-6]

65 **Brandi J**, Dando I, Pozza ED, Biondani G, Jenkins R, Elliott V, Park K, Fanelli G, Zolla L, Costello E, Scarpa A, Cecconi D, Palmieri M. Proteomic analysis of pancreatic cancer stem cells: Functional role of fatty acid synthesis and mevalonate pathways. *J Proteomics* 2017; **150**: 310-322 [PMID: 27746256 DOI: 10.1016/j.jprot.2016.10.002]

66 **Shimano H**, Sato R. SREBP-regulated lipid metabolism: convergent physiology - divergent pathophysiology. *Nat Rev Endocrinol* 2017; **13**: 710-730 [PMID: 28849786 DOI: 10.1038/nrendo.2017.91]

67 **Zhang B**, Wu J, Guo P, Wang Y, Fang Z, Tian J, Yu Y, Teng W, Luo Y, Li Y. Down-Regulation of SREBP *via* PI3K/AKT/mTOR Pathway Inhibits the Proliferation and Invasion of Non-Small-Cell Lung Cancer Cells. *Onco Targets Ther* 2020; **13**: 8951-8961 [PMID: 32982287 DOI: 10.2147/OTT.S266073]

68 **Guo D**, Wang Y, Wang J, Song L, Wang Z, Mao B, Tan N. RA-XII Suppresses the Development and Growth of Liver Cancer by Inhibition of Lipogenesis *via* SCAP-dependent SREBP Supression. *Molecules* 2019; **24** [PMID: 31083642 DOI: 10.3390/molecules24091829]

69 **Sun Q**, Yu X, Peng C, Liu N, Chen W, Xu H, Wei H, Fang K, Dong Z, Fu C, Xu Y, Lu W. Activation of SREBP-1c alters lipogenesis and promotes tumor growth and metastasis in gastric cancer. *Biomed Pharmacother* 2020; **128**: 110274 [PMID: 32464305 DOI: 10.1016/j.biopha.2020.110274]

70 **Chen M**, Zhang J, Sampieri K, Clohessy JG, Mendez L, Gonzalez-Billalabeitia E, Liu XS, Lee YR, Fung J, Katon JM, Menon AV, Webster KA, Ng C, Palumbieri MD, Diolombi MS, Breitkopf SB, Teruya-Feldstein J, Signoretti S, Bronson RT, Asara JM, Castillo-Martin M, Cordon-Cardo C, Pandolfi PP. An aberrant SREBP-dependent lipogenic program promotes metastatic prostate cancer. *Nat Genet* 2018; **50**: 206-218 [PMID: 29335545 DOI: 10.1038/s41588-017-0027-2]

71 **Zhang Y**, Li C, Hu C, Wu Q, Cai Y, Xing S, Lu H, Wang L, Huang, Sun L, Li T, He X, Zhong X, Wang J, Gao P, Smith

ZJ, Jia W, Zhang H. Lin28 enhances de novo fatty acid synthesis to promote cancer progression *via* SREBP-1. *EMBO Rep* 2019; **20**: e48115 [PMID: 31379107 DOI: 10.15252/embr.201948115]

72 **Zhou C**, Qian W, Ma J, Cheng L, Jiang Z, Yan B, Li J, Duan W, Sun L, Cao J, Wang F, Wu E, Wu Z, Ma Q, Li X. Resveratrol enhances the chemotherapeutic response and reverses the stemness induced by gemcitabine in pancreatic cancer cells *via* targeting SREBP1. *Cell Prolif* 2019; **52**: e12514 [PMID: 30341797 DOI: 10.1111/cpr.12514]

73 **Flowers MT**, Ntambi JM. Role of stearoyl-coenzyme A desaturase in regulating lipid metabolism. *Curr Opin Lipidol* 2008; **19**: 248-256 [PMID: 18460915 DOI: 10.1097/MOL.0b013e3282f9b54d]

74 **Liu G**, Kuang S, Cao R, Wang J, Peng Q, Sun C. Sorafenib kills liver cancer cells by disrupting SCD1-mediated synthesis of monounsaturated fatty acids *via* the ATP-AMPK-mTOR-SREBP1 signaling pathway. *FASEB J* 2019; **33**: 10089-10103 [PMID: 31199678 DOI: 10.1096/fj.201802619RR]

75 **Peck B**, Schulze A. Lipid desaturation - the next step in targeting lipogenesis in cancer? *FEBS J* 2016; **283**: 2767-2778 [PMID: 26881388 DOI: 10.1111/febs.13681]

76 **Zhang L**, Ge L, Parimoo S, Stenn K, Prouty SM. Human stearoyl-CoA desaturase: alternative transcripts generated from a single gene by usage of tandem polyadenylation sites. *Biochem J* 1999; **340** (Pt 1): 255-264 [PMID: 10229681]

77 **ALJohani AM**, Syed DN, Ntambi JM. Insights into Stearoyl-CoA Desaturase-1 Regulation of Systemic Metabolism. *Trends Endocrinol Metab* 2017; **28**: 831-842 [PMID: 29089222 DOI: 10.1016/j.tem.2017.10.003]

78 **Tesfay L**, Paul BT, Konstorum A, Deng Z, Cox AO, Lee J, Furdui CM, Hegde P, Torti FM, Torti SV. Stearoyl-CoA Desaturase 1 Protects Ovarian Cancer Cells from Ferroptotic Cell Death. *Cancer Res* 2019; **79**: 5355-5366 [PMID: 31270077 DOI: 10.1158/0008-5472.CAN-19-0369]

79 **Angelucci C**, Maulucci G, Colabianchi A, Iacopino F, D'Alessio A, Maiorana A, Palmieri V, Papi M, De Spirito M, Di Leone A, Masetti R, Sica G. Stearoyl-CoA desaturase 1 and paracrine diffusible signals have a major role in the promotion of breast cancer cell migration induced by cancer-associated fibroblasts. *Br J Cancer* 2015; **112**: 1675-1686 [PMID: 25880005 DOI: 10.1038/bjc.2015.135]

80 **Galbraith L**, Leung HY, Ahmad I. Lipid pathway deregulation in advanced prostate cancer. *Pharmacol Res* 2018; **131**: 177-184 [PMID: 29466694 DOI: 10.1016/j.phrs.2018.02.022]

81 **Chen L**, Ren J, Yang L, Li Y, Fu J, Tian Y, Qiu F, Liu Z, Qiu Y. Stearoyl-CoA desaturase-1 mediated cell apoptosis in colorectal cancer by promoting ceramide synthesis. *Sci Rep* 2016; **6**: 19665 [PMID: 26813308 DOI: 10.1038/srep19665]

82 **Zhang Q**, Yu S, Lam MMT, Poon TCW, Sun L, Jiao Y, Wong AST, Lee LTO. Angiotensin II promotes ovarian cancer spheroid formation and metastasis by upregulation of lipid desaturation and suppression of endoplasmic reticulum stress. *J Exp Clin Cancer Res* 2019; **38**: 116 [PMID: 30845964 DOI: 10.1186/s13046-019-1127-x]

83 **Savino AM**, Fernandes SI, Olivares O, Zemlyansky A, Cousins A, Markert EK, Barel S, Geron I, Frishman L, Birger Y, Eckert C, Tumanov S, MacKay G, Kamphorst JJ, Herzyk P, Fernández-García J, Abramovich I, Mor I, Bardini M, Barin E, Janaki-Raman S, Cross JR, Kharas MG, Gottlieb E, Izraeli S, Halsey C. Metabolic adaptation of acute lymphoblastic leukemia to the central nervous system microenvironment is dependent on Stearoyl CoA desaturase. *Nat Cancer* 2020; **1**: 998-1009 [PMID: 33479702 DOI: 10.1038/s43018-020-00115-2]

84 **Pinkham K**, Park DJ, Hashemiaghdam A, Kirov AB, Adam I, Rosiak K, da Hora CC, Teng J, Cheah PS, Carvalho L, Ganguli-Indra G, Kelly A, Indra AK, Badr CE. Stearoyl CoA Desaturase Is Essential for Regulation of Endoplasmic Reticulum Homeostasis and Tumor Growth in Glioblastoma Cancer Stem Cells. *Stem Cell Reports* 2019; **12**: 712-727 [PMID: 30930246 DOI: 10.1016/j.stemcr.2019.02.012]

85 **Pisanu ME**, Noto A, De Vitis C, Morrone S, Scognamiglio G, Botti G, Venuta F, Diso D, Jakopin Z, Padula F, Ricci A, Mariotta S, Giovagnoli MR, Giarnieri E, Amelio I, Agostini M, Melino G, Ciliberto G, Mancini R. Blockade of Stearoyl-CoA-desaturase 1 activity reverts resistance to cisplatin in lung cancer stem cells. *Cancer Lett* 2017; **406**: 93-104 [PMID: 28797843 DOI: 10.1016/j.canlet.2017.07.027]

86 **Bruschini S**, di Martino S, Pisanu ME, Fattore L, De Vitis C, Laquintana V, Buglioni S, Tabbì E, Cerri A, Visca P, Alessandrini G, Facciolo F, Napoli C, Trombetta M, Santoro A, Crescenzi A, Ciliberto G, Mancini R. CytoMatrix for a reliable and simple characterization of lung cancer stem cells from malignant pleural effusions. *J Cell Physiol* 2020; **235**: 1877-1887 [PMID: 31397494 DOI: 10.1002/jcp.29121]

87 **El Helou R**, Pinna G, Cabaud O, Wicinski J, Bhajun R, Guyon L, Rioualen C, Finetti P, Gros A, Mari B, Barbry P, Bertucci F, Bidaut G, Harel-Bellan A, Birnbaum D, Charafe-Jauffret E, Ginestier C. miR-600 Acts as a Bimodal Switch that Regulates Breast Cancer Stem Cell Fate through WNT Signaling. *Cell Rep* 2017; **18**: 2256-2268 [PMID: 28249169 DOI: 10.1016/j.celrep.2017.02.016]

88 **Ray S**, Kassan A, Busija AR, Rangamani P, Patel HH. The plasma membrane as a capacitor for energy and metabolism. *Am J Physiol Cell Physiol* 2016; **310**: C181-C192 [PMID: 26771520 DOI: 10.1152/ajpcell.00087.2015]

89 **Pike LJ**. The challenge of lipid rafts. *J Lipid Res* 2009; **50** Suppl: S323-S328 [PMID: 18955730 DOI: 10.1194/jlr.R800040-JLR200]

90 **Xu H**, Zhou S, Tang Q, Xia H, Bi F. Cholesterol metabolism: New functions and therapeutic approaches in cancer. *Biochim Biophys Acta Rev Cancer* 2020; **1874**: 188394 [PMID: 32698040 DOI: 10.1016/j.bbcan.2020.188394]

91 **Mullen PJ**, Yu R, Longo J, Archer MC, Penn LZ. The interplay between cell signalling and the mevalonate pathway in cancer. *Nat Rev Cancer* 2016; **16**: 718-731 [PMID: 27562463 DOI: 10.1038/nrc.2016.76]

92 **Luo J**, Yang H, Song BL. Mechanisms and regulation of cholesterol homeostasis. *Nat Rev Mol Cell Biol* 2020; **21**: 225-245 [PMID: 31848472 DOI: 10.1038/s41580-019-0190-7]

93 **Huang B**, Song BL, Xu C. Cholesterol metabolism in cancer: mechanisms and therapeutic opportunities. *Nat Metab* 2020; **2**: 132-141 [PMID: 32694690 DOI: 10.1038/s42255-020-0174-0]

94 **Wang B**, Rong X, Palladino END, Wang J, Fogelman AM, Martín MG, Alrefai WA, Ford DA, Tontonoz P. Phospholipid Remodeling and Cholesterol Availability Regulate Intestinal Stemness and Tumorigenesis. *Cell Stem Cell* 2018; **22**: 206-220.e4 [PMID: 29395055 DOI: 10.1016/j.stem.2017.12.017]

95 **Ehmsen S**, Pedersen MH, Wang G, Terp MG, Arslanagic A, Hood BL, Conrads TP, Leth-Larsen R, Ditzel HJ. Increased Cholesterol Biosynthesis Is a Key Characteristic of Breast Cancer Stem Cells Influencing Patient Outcome. *Cell Rep* 2019;

27: 3927-3938.e6 [PMID: 31242424 DOI: 10.1016/j.celrep.2019.05.104]

96 **Gu Q**, Yang X, Lv J, Zhang J, Xia B, Kim JD, Wang R, Xiong F, Meng S, Clements TP, Tandon B, Wagner DS, Diaz MF, Wenzel PL, Miller YI, Traver D, Cooke JP, Li W, Zon LI, Chen K, Bai Y, Fang L. AIBP-mediated cholesterol efflux instructs hematopoietic stem and progenitor cell fate. *Science* 2019; **363**: 1085-1088 [PMID: 30705153 DOI: 10.1126/science.aav1749]

97 **Li X**, Wu JB, Li Q, Shigemura K, Chung LW, Huang WC. SREBP-2 promotes stem cell-like properties and metastasis by transcriptional activation of c-Myc in prostate cancer. *Oncotarget* 2016; **7**: 12869-12884 [PMID: 26883200 DOI: 10.18632/oncotarget.7331]

98 **Wen YA**, Xiong X, Zaytseva YY, Napier DL, Vallee E, Li AT, Wang C, Weiss HL, Evers BM, Gao T. Downregulation of SREBP inhibits tumor growth and initiation by altering cellular metabolism in colon cancer. *Cell Death Dis* 2018; **9**: 265 [PMID: 29449559 DOI: 10.1038/s41419-018-0330-6]

99 **Longo J**, Smirnov P, Li Z, Branchard E, van Leeuwen JE, Licht JD, Haibe-Kains B, Andrews DW, Keats JJ, Pugh TJ, Trudel S, Penn LZ. The mevalonate pathway is an actionable vulnerability of t(4;14)-positive multiple myeloma. *Leukemia* 2021; **35**: 796-808 [PMID: 32665698 DOI: 10.1038/s41375-020-0962-2]

100 **Sethunath V**, Hu H, De Angelis C, Veeraraghavan J, Qin L, Wang N, Simon LM, Wang T, Fu X, Nardone A, Pereira R, Nanda S, Griffith OL, Tsimelzon A, Shaw C, Chamness GC, Reis-Filho JS, Weigelt B, Heiser LM, Hilsenbeck SG, Huang S, Rimawi MF, Gray JW, Osborne CK, Schiff R. Targeting the Mevalonate Pathway to Overcome Acquired Anti-HER2 Treatment Resistance in Breast Cancer. *Mol Cancer Res* 2019; **17**: 2318-2330 [PMID: 31420371 DOI: 10.1158/1541-7786.MCR-19-0756]

101 **Chushi L**, Wei W, Kangkang X, Yongzeng F, Ning X, Xiaolei C. HMGCR is up-regulated in gastric cancer and promotes the growth and migration of the cancer cells. *Gene* 2016; **587**: 42-47 [PMID: 27085483 DOI: 10.1016/j.gene.2016.04.029]

102 **Fatehi Hassanabad A**, Mina F. Targeting the Mevalonate Pathway for Treating Lung Cancer. *Am J Clin Oncol* 2020; **43**: 69-70 [PMID: 31842152 DOI: 10.1097/COC.0000000000000630]

103 **Longo J**, Mullen PJ, Yu R, van Leeuwen JE, Masoomian M, Woon DTS, Wang Y, Chen EX, Hamilton RJ, Sweet JM, van der Kwast TH, Fleshner NE, Penn LZ. An actionable sterol-regulated feedback loop modulates statin sensitivity in prostate cancer. *Mol Metab* 2019; **25**: 119-130 [PMID: 31023626 DOI: 10.1016/j.molmet.2019.04.003]

104 **Zhou S**, Xu H, Tang Q, Xia H, Bi F. Dipyridamole Enhances the Cytotoxicities of Trametinib against Colon Cancer Cells through Combined Targeting of HMGCS1 and MEK Pathway. *Mol Cancer Ther* 2020; **19**: 135-146 [PMID: 31554653 DOI: 10.1158/1535-7163.MCT-19-0413]

105 **Brown DN**, Caffa I, Cirmena G, Piras D, Garuti A, Gallo M, Alberti S, Nencioni A, Ballestrero A, Zoppoli G. Squalene epoxidase is a bona fide oncogene by amplification with clinical relevance in breast cancer. *Sci Rep* 2016; **6**: 19435 [PMID: 26777065 DOI: 10.1038/srep19435]

106 **Wang X**, Xu W, Zhan P, Xu T, Jin J, Miu Y, Zhou Z, Zhu Q, Wan B, Xi G, Ye L, Liu Y, Gao J, Li H, Lv T, Song Y. Overexpression of geranylgeranyl diphosphate synthase contributes to tumour metastasis and correlates with poor prognosis of lung adenocarcinoma. *J Cell Mol Med* 2018; **22**: 2177-2189 [PMID: 29377583 DOI: 10.1111/jcmm.13493]

107 **Yang YF**, Jan YH, Liu YP, Yang CJ, Su CY, Chang YC, Lai TC, Chiou J, Tsai HY, Lu J, Shen CN, Shew JY, Lu PJ, Lin YF, Huang MS, Hsiao M. Squalene synthase induces tumor necrosis factor receptor 1 enrichment in lipid rafts to promote lung cancer metastasis. *Am J Respir Crit Care Med* 2014; **190**: 675-687 [PMID: 25152164 DOI: 10.1164/rccm.201404-0714OC]

108 **Yarmolinsky J**, Bull CJ, Vincent EE, Robinson J, Walther A, Smith GD, Lewis SJ, Relton CL, Martin RM. Association Between Genetically Proxied Inhibition of HMG-CoA Reductase and Epithelial Ovarian Cancer. *JAMA* 2020; **323**: 646-655 [PMID: 32068819 DOI: 10.1001/jama.2020.0150]

109 **Vásquez-Bochm LX**, Velázquez-Paniagua M, Castro-Vázquez SS, Guerrero-Rodríguez SL, Mondragon-Peralta A, De La Fuente-Granada M, Pérez-Tapia SM, González-Arenas A, Velasco-Velázquez MA. Transcriptome-based identification of lovastatin as a breast cancer stem cell-targeting drug. *Pharmacol Rep* 2019; **71**: 535-544 [PMID: 31026757 DOI: 10.1016/j.pharep.2019.02.011]

110 **Göbel A**, Rauner M, Hofbauer LC, Rachner TD. Cholesterol and beyond - The role of the mevalonate pathway in cancer biology. *Biochim Biophys Acta Rev Cancer* 2020; **1873**: 188351 [PMID: 32007596 DOI: 10.1016/j.bbcan.2020.188351]

111 **Brindisi M**, Fiorillo M, Frattaruolo L, Sotgia F, Lisanti MP, Cappello AR. Cholesterol and Mevalonate: Two Metabolites Involved in Breast Cancer Progression and Drug Resistance through the ERRα Pathway. *Cells* 2020; **9** [PMID: 32751976 DOI: 10.3390/cells9081819]

112 **Qin Y**, Hou Y, Liu S, Zhu P, Wan X, Zhao M, Peng M, Zeng H, Li Q, Jin T, Cui X, Liu M. A Novel Long Non-Coding RNA lnc030 Maintains Breast Cancer Stem Cell Stemness by Stabilizing SQLE mRNA and Increasing Cholesterol Synthesis. *Adv Sci (Weinh)* 2021; **8**: 2002232 [PMID: 33511005 DOI: 10.1002/advs.202002232]

113 **Totaro A**, Panciera T, Piccolo S. YAP/TAZ upstream signals and downstream responses. *Nat Cell Biol* 2018; **20**: 888-899 [PMID: 30050119 DOI: 10.1038/s41556-018-0142-z]

114 **Sorrentino G**, Ruggeri N, Specchia V, Cordenonsi M, Mano M, Dupont S, Manfrin A, Ingallina E, Sommaggio R, Piazza S, Rosato A, Piccolo S, Del Sal G. Metabolic control of YAP and TAZ by the mevalonate pathway. *Nat Cell Biol* 2014; **16**: 357-366 [PMID: 24658687 DOI: 10.1038/ncb2936]

115 **Reggiani F**, Gobbi G, Ciarrocchi A, Ambrosetti DC, Sancisi V. Multiple roles and context-specific mechanisms underlying YAP and TAZ-mediated resistance to anti-cancer therapy. *Biochim Biophys Acta Rev Cancer* 2020; **1873**: 188341 [PMID: 31931113 DOI: 10.1016/j.bbcan.2020.188341]

116 **Zhang S**, Zhang H, Ghia EM, Huang J, Wu L, Zhang J, Lam S, Lei Y, He J, Cui B, Widhopf GF 2nd, Yu J, Schwab R, Messer K, Jiang W, Parker BA, Carson DA, Kipps TJ. Inhibition of chemotherapy resistant breast cancer stem cells by a ROR1 specific antibody. *Proc Natl Acad Sci U S A* 2019; **116**: 1370-1377 [PMID: 30622177 DOI: 10.1073/pnas.1816262116]

117 **Zheng L**, Xiang C, Li X, Guo Q, Gao L, Ni H, Xia Y, Xi T. STARD13-correlated ceRNA network-directed inhibition on YAP/TAZ activity suppresses stemness of breast cancer *via* co-regulating Hippo and Rho-GTPase/F-actin signaling. *J Hematol Oncol* 2018; **11**: 72 [PMID: 29848346 DOI: 10.1186/s13045-018-0613-5]

118 **Bocci F**, Gearhart-Serna L, Boareto M, Ribeiro M, Ben-Jacob E, Devi GR, Levine H, Onuchic JN, Jolly MK. Toward understanding cancer stem cell heterogeneity in the tumor microenvironment. *Proc Natl Acad Sci U S A* 2019; **116**: 148-157 [PMID: 30587589 DOI: 10.1073/pnas.1815345116]

119 **Takebe N**, Miele L, Harris PJ, Jeong W, Bando H, Kahn M, Yang SX, Ivy SP. Targeting Notch, Hedgehog, and Wnt pathways in cancer stem cells: clinical update. *Nat Rev Clin Oncol* 2015; **12**: 445-464 [PMID: 25850553 DOI: 10.1038/nrclinonc.2015.61]

120 **Song NJ**, Yun UJ, Yang S, Wu C, Seo CR, Gwon AR, Baik SH, Choi Y, Choi BY, Bahn G, Kim S, Kwon SM, Park JS, Baek SH, Park TJ, Yoon K, Kim BJ, Mattson MP, Lee SJ, Jo DG, Park KW. Notch1 deficiency decreases hepatic lipid accumulation by induction of fatty acid oxidation. *Sci Rep* 2016; **6**: 19377 [PMID: 26786165 DOI: 10.1038/srep19377]

121 **Yu Y**, Kim H, Choi S, Yu J, Lee JY, Lee H, Yoon S, Kim WY. Targeting a Lipid Desaturation Enzyme, SCD1, Selectively Eliminates Colon Cancer Stem Cells through the Suppression of Wnt and NOTCH Signaling. *Cells* 2021; **10** [PMID: 33430034 DOI: 10.3390/cells10010106]

122 **Takebe N**, Ivy SP. Controversies in cancer stem cells: targeting embryonic signaling pathways. *Clin Cancer Res* 2010; **16**: 3106-3112 [PMID: 20530695 DOI: 10.1158/1078-0432.CCR-09-2934]

123 **Fendler A**, Bauer D, Busch J, Jung K, Wulf-Goldenberg A, Kunz S, Song K, Myszczyszyn A, Elezkurtaj S, Erguen B, Jung S, Chen W, Birchmeier W. Inhibiting WNT and NOTCH in renal cancer stem cells and the implications for human patients. *Nat Commun* 2020; **11**: 929 [PMID: 32066735 DOI: 10.1038/s41467-020-14700-7]

124 **Patel S**, Alam A, Pant R, Chattopadhyay S. Wnt Signaling and Its Significance Within the Tumor Microenvironment: Novel Therapeutic Insights. *Front Immunol* 2019; **10**: 2872 [PMID: 31921137 DOI: 10.3389/fimmu.2019.02872]

125 **Cho YH**, Ro EJ, Yoon JS, Mizutani T, Kang DW, Park JC, Il Kim T, Clevers H, Choi KY. 5-FU promotes stemness of colorectal cancer *via* p53-mediated WNT/β-catenin pathway activation. *Nat Commun* 2020; **11**: 5321 [PMID: 33087710 DOI: 10.1038/s41467-020-19173-2]

126 **Katoh M**. Canonical and non-canonical WNT signaling in cancer stem cells and their niches: Cellular heterogeneity, omics reprogramming, targeted therapy and tumor plasticity (Review). *Int J Oncol* 2017; **51**: 1357-1369 [PMID: 29048660 DOI: 10.3892/ijo.2017.4129]

127 **Bagchi DP**, Nishii A, Li Z, DelProposto JB, Corsa CA, Mori H, Hardij J, Learman BS, Lumeng CN, MacDougald OA. Wnt/β-catenin signaling regulates adipose tissue lipogenesis and adipocyte-specific loss is rigorously defended by neighboring stromal-vascular cells. *Mol Metab* 2020; **42**: 101078 [PMID: 32919095 DOI: 10.1016/j.molmet.2020.101078]

128 **Lai KKY**, Kweon SM, Chi F, Hwang E, Kabe Y, Higashiyama R, Qin L, Yan R, Wu RP, Lai K, Fujii N, French S, Xu J, Wang JY, Murali R, Mishra L, Lee JS, Ntambi JM, Tsukamoto H. Stearoyl-CoA Desaturase Promotes Liver Fibrosis and Tumor Development in Mice *via* a Wnt Positive-Signaling Loop by Stabilization of Low-Density Lipoprotein-Receptor-Related Proteins 5 and 6. *Gastroenterology* 2017; **152**: 1477-1491 [PMID: 28143772 DOI: 10.1053/j.gastro.2017.01.021]

129 **Rios-Esteves J**, Resh MD. Stearoyl CoA desaturase is required to produce active, lipid-modified Wnt proteins. *Cell Rep* 2013; **4**: 1072-1081 [PMID: 24055053 DOI: 10.1016/j.celrep.2013.08.027]

130 **Noto A**, De Vitis C, Pisanu ME, Roscilli G, Ricci G, Catizone A, Sorrentino G, Chianese G, Taglialatela-Scafati O, Trisciuoglio D, Del Bufalo D, Di Martile M, Di Napoli A, Ruco L, Costantini S, Jakopin Z, Budillon A, Melino G, Del Sal G, Ciliberto G, Mancini R. Stearoyl-CoA-desaturase 1 regulates lung cancer stemness *via* stabilization and nuclear localization of YAP/TAZ. *Oncogene* 2017; **36**: 4573-4584 [PMID: 28368399 DOI: 10.1038/onc.2017.75]

131 **Yu FX**, Zhao B, Guan KL. Hippo Pathway in Organ Size Control, Tissue Homeostasis, and Cancer. *Cell* 2015; **163**: 811-828 [PMID: 26544935 DOI: 10.1016/j.cell.2015.10.044]

132 **Park JH**, Shin JE, Park HW. The Role of Hippo Pathway in Cancer Stem Cell Biology. *Mol Cells* 2018; **41**: 83-92 [PMID: 29429151 DOI: 10.14348/molcells.2018.2242]

133 **Maugeri-Saccà M**, De Maria R. Hippo pathway and breast cancer stem cells. *Crit Rev Oncol Hematol* 2016; **99**: 115-122 [PMID: 26725175 DOI: 10.1016/j.critrevonc.2015.12.004]

134 **Aylon Y**, Oren M. The Hippo pathway, p53 and cholesterol. *Cell Cycle* 2016; **15**: 2248-2255 [PMID: 27419353 DOI: 10.1080/15384101.2016.1207840]

135 **Koo JH**, Guan KL. Interplay between YAP/TAZ and Metabolism. *Cell Metab* 2018; **28**: 196-206 [PMID: 30089241 DOI: 10.1016/j.cmet.2018.07.010]

136 **Bhuria V**, Xing J, Scholta T, Bui KC, Nguyen MLT, Malek NP, Bozko P, Plentz RR. Hypoxia induced Sonic Hedgehog signaling regulates cancer stemness, epithelial-to-mesenchymal transition and invasion in cholangiocarcinoma. *Exp Cell Res* 2019; **385**: 111671 [PMID: 31634481 DOI: 10.1016/j.yexcr.2019.111671]

137 **Hu A**, Song BL. The interplay of Patched, Smoothened and cholesterol in Hedgehog signaling. *Curr Opin Cell Biol* 2019; **61**: 31-38 [PMID: 31369952 DOI: 10.1016/j.ceb.2019.06.008]

138 **Blassberg R**, Jacob J. Lipid metabolism fattens up hedgehog signaling. *BMC Biol* 2017; **15**: 95 [PMID: 29073896 DOI: 10.1186/s12915-017-0442-y]

139 **Jones SF**, Infante JR. Molecular Pathways: Fatty Acid Synthase. *Clin Cancer Res* 2015; **21**: 5434-5438 [PMID: 26519059 DOI: 10.1158/1078-0432.CCR-15-0126]

140 **Corominas-Faja B**, Cuyàs E, Gumuzio J, Bosch-Barrera J, Leis O, Martin ÁG, Menendez JA. Chemical inhibition of acetyl-CoA carboxylase suppresses self-renewal growth of cancer stem cells. *Oncotarget* 2014; **5**: 8306-8316 [PMID: 25246709 DOI: 10.18632/oncotarget.2059]

141 **Schug ZT**, Peck B, Jones DT, Zhang Q, Grosskurth S, Alam IS, Goodwin LM, Smethurst E, Mason S, Blyth K, McGarry L, James D, Shanks E, Kalna G, Saunders RE, Jiang M, Howell M, Lassailly F, Thin MZ, Spencer-Dene B, Stamp G, van den Broek NJ, Mackay G, Bulusu V, Kamphorst JJ, Tardito S, Strachan D, Harris AL, Aboagye EO, Critchlow SE, Wakelam MJ, Schulze A, Gottlieb E. Acetyl-CoA synthetase 2 promotes acetate utilization and maintains cancer cell growth under metabolic stress. *Cancer Cell* 2015; **27**: 57-71 [PMID: 25584894 DOI: 10.1016/j.ccell.2014.12.002]

142 **Svensson RU**, Parker SJ, Eichner LJ, Kolar MJ, Wallace M, Brun SN, Lombardo PS, Van Nostrand JL, Hutchins A, Vera L, Gerken L, Greenwood J, Bhat S, Harriman G, Westlin WF, Harwood HJ Jr, Saghatelian A, Kapeller R, Metallo CM, Shaw RJ. Inhibition of acetyl-CoA carboxylase suppresses fatty acid synthesis and tumor growth of non-small-cell lung cancer in preclinical models. *Nat Med* 2016; **22**: 1108-1119 [PMID: 27643638 DOI: 10.1038/nm.4181]

143 **Diaz-Moralli S**, Aguilar E, Marin S, Coy JF, Dewerchin M, Antoniewicz MR, Meca-Cortés O, Notebaert L, Ghesquière B, Eelen G, Thomson TM, Carmeliet P, Cascante M. A key role for transketolase-like 1 in tumor metabolic reprogramming. *Oncotarget* 2016; **7**: 51875-51897 [PMID: 27391434 DOI: 10.18632/oncotarget.10429]

144 **Schug ZT**, Vande Voorde J, Gottlieb E. The metabolic fate of acetate in cancer. *Nat Rev Cancer* 2016; **16**: 708-717 [PMID: 27562461 DOI: 10.1038/nrc.2016.87]

145 **Zaidi N**, Royaux I, Swinnen JV, Smans K. ATP citrate lyase knockdown induces growth arrest and apoptosis through different cell- and environment-dependent mechanisms. *Mol Cancer Ther* 2012; **11**: 1925-1935 [PMID: 22718913 DOI: 10.1158/1535-7163.MCT-12-0095]

146 **Tracz-Gaszewska Z**, Dobrzyn P. Stearoyl-CoA Desaturase 1 as a Therapeutic Target for the Treatment of Cancer. *Cancers (Basel)* 2019; **11** [PMID: 31284458 DOI: 10.3390/cancers11070948]

147 **Ginestier C**, Monville F, Wicinski J, Cabaud O, Cervera N, Josselin E, Finetti P, Guille A, Larderet G, Viens P, Sebti S, Bertucci F, Birnbaum D, Charafe-Jauffret E. Mevalonate metabolism regulates Basal breast cancer stem cells and is a potential therapeutic target. *Stem Cells* 2012; **30**: 1327-1337 [PMID: 22605458 DOI: 10.1002/stem.1122]

148 **Iannelli F**, Roca MS, Lombardi R, Ciardiello C, Grumetti L, De Rienzo S, Moccia T, Vitagliano C, Sorice A, Costantini S, Milone MR, Pucci B, Leone A, Di Gennaro E, Mancini R, Ciliberto G, Bruzzese F, Budillon A. Synergistic antitumor interaction of valproic acid and simvastatin sensitizes prostate cancer to docetaxel by targeting CSCs compartment *via* YAP inhibition. *J Exp Clin Cancer Res* 2020; **39**: 213 [PMID: 33032653 DOI: 10.1186/s13046-020-01723-7]

149 **Seo Y**, Kim J, Park SJ, Park JJ, Cheon JH, Kim WH, Kim TI. Metformin Suppresses Cancer Stem Cells through AMPK Activation and Inhibition of Protein Prenylation of the Mevalonate Pathway in Colorectal Cancer. *Cancers (Basel)* 2020; **12** [PMID: 32911743 DOI: 10.3390/cancers12092554]

150 **Ma XL**, Sun YF, Wang BL, Shen MN, Zhou Y, Chen JW, Hu B, Gong ZJ, Zhang X, Cao Y, Pan BS, Zhou J, Fan J, Guo W, Yang XR. Sphere-forming culture enriches liver cancer stem cells and reveals Stearoyl-CoA desaturase 1 as a potential therapeutic target. *BMC Cancer* 2019; **19**: 760 [PMID: 31370822 DOI: 10.1186/s12885-019-5963-z]

World Journal of Stem Cells

Submit a Manuscript: https://www.f6publishing.com

World J Stem Cells 2022 February 26; 14(2): 163-182

DOI: 10.4252/wjsc.v14.i2.163

ISSN 1948-0210 (online)

ORIGINAL ARTICLE

Basic Study

Transcription regulators differentiate mesenchymal stem cells into chondroprogenitors, and their *in vivo* implantation regenerated the intervertebral disc degeneration

Shumaila Khalid, Sobia Ekram, Asmat Salim, G. Rasul Chaudhry, Irfan Khan

Specialty type: Cell Biology

Provenance and peer review: Invited article; Externally peer reviewed.

Peer-review model: Single blind

Peer-review report's scientific quality classification

Grade A (Excellent): 0
Grade B (Very good): 0
Grade C (Good): C
Grade D (Fair): 0
Grade E (Poor): 0

P-Reviewer: Nikcevic G

Received: February 28, 2021
Peer-review started: February 28, 2021
First decision: April 19, 2021
Revised: May 2, 2021
Accepted: January 6, 2022
Article in press: January 6, 2022
Published online: February 26, 2022

Shumaila Khalid, Sobia Ekram, Asmat Salim, Irfan Khan, Dr. Panjwani Center for Molecular Medicine and Drug Research, International Center for Chemical and Biological Sciences, University of Karachi, Karachi 75270, Sindh, Pakistan

G. Rasul Chaudhry, Department of Biological Sciences, Oakland University, Rochester, MI 48309, United States

Corresponding author: Irfan Khan, PhD, Assistant Professor, Dr. Panjwani Center for Molecular Medicine and Drug Research, International Center for Chemical and Biological Sciences, University of Karachi, KU Circular Rd, Karachi 75270, Sindh, Pakistan. khan@iccs.edu

Abstract

BACKGROUND

Intervertebral disc degeneration (IVDD) is the leading cause of lower back pain. Disc degeneration is characterized by reduced cellularity and decreased production of extracellular matrix (ECM). Mesenchymal stem cells (MSCs) have been envisioned as a promising treatment for degenerative illnesses. Cell-based therapy using ECM-producing chondrogenic derivatives of MSCs has the potential to restore the functionality of the intervertebral disc (IVD).

AIM

To investigate the potential of chondrogenic transcription factors to promote differentiation of human umbilical cord MSCs into chondrocytes, and to assess their therapeutic potential in IVD regeneration.

METHODS

MSCs were isolated and characterized morphologically and immunologically by the expression of specific markers. MSCs were then transfected with *Sox-9* and *Six-1* transcription factors to direct differentiation and were assessed for chondrogenic lineage based on the expression of specific markers. These differentiated MSCs were implanted in the rat model of IVDD. The regenerative potential of transplanted cells was investigated using histochemical and molecular analyses of IVDs.

RESULTS

Isolated cells showed fibroblast-like morphology and expressed CD105, CD90,

CD73, CD29, and Vimentin but not CD45 antigens. Overexpression of *Sox-9* and *Six-1* greatly enhanced the gene expression of *transforming growth factor beta-1* gene, *BMP, Sox-9, Six-1,* and *Aggrecan,* and protein expression of Sox-9 and Six-1. The implanted cells integrated, survived, and homed in the degenerated intervertebral disc. Histological grading showed that the transfected MSCs regenerated the IVD and restored normal architecture.

CONCLUSION

Genetically modified MSCs accelerate cartilage regeneration, providing a unique opportunity and impetus for stem cell-based therapeutic approach for degenerative disc diseases.

Key Words: Intervertebral disc degeneration; Human umbilical cord; Transcription factors; Mesenchymal stem cells; Gene expression; Regeneration

Core Tip: In this study, we highlighted that overexpression of chondrogenic transcription factors in human umbilical cord derived mesenchymal stem cells (hUC-MSCs) accelerated their differentiation into chondroprogenitor cells. The synergistic effect of *Sox-9* and *Six-1* transcription factors leads the MSCs to differentiate into chondrogenic cells in the basal medium, which produced the same effect as the chondro-induction medium. *In vivo* transplantation of these transfected cells leads to their homing, integration, and differentiation into nucleus pulposus cells of the intervertebral disc. This approach could help to develop a better treatment option for degenerative disc diseases.

Citation: Khalid S, Ekram S, Salim A, Chaudhry GR, Khan I. Transcription regulators differentiate mesenchymal stem cells into chondroprogenitors, and their *in vivo* implantation regenerated the intervertebral disc degeneration. *World J Stem Cells* 2022; 14(2): 163-182
URL: https://www.wjgnet.com/1948-0210/full/v14/i2/163.htm
DOI: https://dx.doi.org/10.4252/wjsc.v14.i2.163

INTRODUCTION

Severe lower back pain (LBP) is the major disability responsible for physical discomfort, emotional distress, and significant decline in social life. Intervertebral disc (IVD) degeneration is a consequence of LBP affecting 80% of the world's population and economy[1]. IVD provides cushioning between vertebrae and absorbs pressure placed on the spine. It is an avascular and aneural site consisting of central nucleus pulposus (NP) containing a limited number of notochondral cells and a high volume of proteoglycans and glycosaminoglycans (GAGs)[2], with surrounding concentric rings of annular fibrosus (AF)[3] and cartilaginous endplate (CEP)[4]. The disc nourishes with the nutrients and metabolites provided by CEP, which is the prime region for controlled diffusion[5]. The main function of IVDs is to transmit load between the spinal column and body weight, and helps in body flexion and torsion[6]. Degeneration of IVD starts with the disintegration of resident cells which is ultimately followed by a reduction in the proteoglycan and water content. The degenerative process intensifies with age, injury, and genetic factors[7]. These factors decrease the synthesis of extracellular matrix (ECM) in the NP region[8]. Additionally, loss of notochondral cells disturbs the balance of anabolic and catabolic processes, resulting in disc degeneration[9]. These drastic changes also release cytokines and accelerate the secretion of matrix metalloproteinases. Current approaches to rejuvenate the tissue infrastructure and improve biochemical homeostasis of IVD using pharmacological and conventional or surgical treatments do not provide long-lasting relief from LBP caused by degenerative disc disease (DDD)[10,11].

Stem cell therapy has been considered a promising therapeutic option for degenerative diseases, including DDD. Stem cells can be isolated from various sources like bone marrow, umbilical cord, adipose tissues, *etc.*[12]. Mesenchymal stem cells (MSCs) are the most preferred population because of their proliferation, differentiation, and immunomodulatory potential[13]. The concept of inducing differentiation of MSCs through the overexpression of chondro-specific genes before injecting them into IVD disease (IVDD) model is novel which is likely to significantly improve the microenvironment for the regeneration of the disc[14]. One of the significant advantages of the stem cell-based gene therapy approach is that it can exhibit a long-lasting effect. However, the genetically modified cells need to be analyzed for safety and effectiveness. Nevertheless, such genetic modifications have been explored for targeting traditional inheritable genetic disorders, such as cystic fibrosis, hemophilia, and hypercholesteremia, and to treat acute and chronic diseases[15].

Murine MSCs have been transduced by the adenovirus-mediated *transforming growth factor beta-2* (*TGFβ2*) gene that led to the synthesis of proteoglycans and downregulation of markers for hypertrophy [16], while *BMP2* is responsible for cartilage production when transduced *via* retroviral vector promoting chondrogenesis[17]. Gene overexpression proved to be a powerful tool to differentiate MSCs into chondroprogenitors (CPCs) which, upon transplantation, healed the degenerated region of IVD [18]. Similarly, collagen synthesis was upregulated in the osteoarthritis imperfecta mice model by transduction of bone marrow MSCs with retroviral-mediated transcription of *procollagen alpha 2*[19].

The novel role of *Six-1* and other transcription factors, including *pitx1,* and *ttf1,* for differentiation of MSCs, resulted in cell progression towards the early stages of cartilage differentiation[20]. Additionally, different genes have been targeted by researchers to treat IVDs. For example, *IL-1* and *BMP2* co-transduced *via* adenovirus vector showed positive biological activity by enhancing ECM at the site of inflamed articular cartilage[21]. Similarly, when *Sox* tri-genes (*Sox-9, Sox-6, Sox-7*) were electroporated to MSCs for transplantation in the IVDD model, it enhanced chondrogenesis and suppressed hypertrophy of MSCs compared to the normal non transfected MSCs[22].

In the present study, we hypothesized that damaged IVD could be regenerated, and its normal physiological function can be restored if MSCs are preconditioned by overexpressing chondrogenic transcription factors *Six-1* and *Sox-9* or by their synergistic combination, as well as by MSCs pre-differentiated into CPCs, transplanted into the damaged disc in the form of induced chondro-progenitor cells (iCPCs).

MATERIALS AND METHODS

Isolation and propagation of human umbilical cord derived MSCs

The study protocol (IEC-009-UCB-2015) was approved by the institutional ethical committee on human subjects. Human umbilical cord samples (n = 20) were collected from Zainab Panjwani Memorial Hospital following cesarean section. Formal ethical consent was obtained from the donor parents. The cord was washed with phosphate buffered saline (PBS) to remove blood clots. This was followed by mincing the cord tissue into approximately 1–3 mm pieces. The minced tissue was then transferred to a T-75 culture flask containing 12 mL complete medium (Dulbecco's Modified Eagle's Medium [DMEM]) supplemented with 10% fetal bovine serum, 1 mmol/L L-glutamine, 1 mmol/L sodium pyruvate, and 1% penicillin-streptomycin, and kept in a humidified incubator at 37 °C, maintained at 5% CO_2. The growth medium was refreshed every 3rd day. After 14 d, cell outgrowth was observed from explants. Upon reaching 70%-80% confluency, sub-culturing was performed.

Immunocytochemistry for characterization of MSCs

Cells at passage 2 (P_2) were grown on the coverslip, fixed with 4% paraformaldehyde for 15 min at room temperature (RT) and permeabilized with 0.1% Triton X-100 in PBS. Blocking was performed with 2% bovine serum albumin (BSA) and 0.1% Tween-20 in PBS for 30 min at RT. The primary antibodies against CD73, CD105, Vimentin, CD29, and CD90 at recommended dilutions were added and incubated at 4 °C overnight. The cells were washed three times with PBS and then subjected to secondary antibodies, Alexa fluor-546 or 488 at a dilution of 1:200 for 1 h at 37 °C. Nuclei were stained with DAPI for 10 min. Finally, cells were mounted with an aqueous mounting medium and visualized under a fluorescent microscope (NiE, Nikon, Japan).

Immunophenotyping of MSCs

Cells were analyzed for the presence of MSC specific markers by flow cytometry using standard protocol. Briefly, the cells were washed with PBS and blocked using a blocking solution (2% BSA). This was followed by incubation with primary antibodies against CD45, Vimentin, CD105, and CD73 at RT for 2 h, and then with the secondary antibody, Alexa fluor 546. Cells were analyzed by flow cytometer (FACS Celesta, Becton Dickinson, Franklin Lakes, NJ, United States).

Tri-lineage differentiation of MSCs

To validate that the isolated cells from human umbilical cord tissues are MSCs, the differentiation potential of these cells into adipogenic, osteogenic, and chondrogenic lineages was assessed. Cells at passage P_2 were seeded in a 6-well plate and grown in DMEM until they reached 60%-70% confluency, then DMEM was replaced with adipogenic induction medium (1 μM dexamethasone, 10 μM insulin, and 200 μM indomethacin), osteogenic differentiation medium (0.1 μM dexamethasone, 10 μM β-glycerophosphate, and 50 M ascorbate phosphate), and chondrogenic medium (1 μM dexamethasone, 10 ng insulin, 20 ng TGFβ1 and 100 μM ascorbic acid). Cells in the induction media were cultured for 3 wk. Cells were stained with Oil Red O, Alizarin Red S, and Alcian blue stains for the detection of adipogenic, osteogenic, and chondrogenic differentiation, respectively, and observed under a bright-field microscope. Images were captured with a CCD camera (TE2000, Nikon).

Amplification and isolation of plasmid vectors

Plasmid constructs for *Sox-9* and *Six-1* in the form of *E. coli* stab cultures were obtained from Addgene (www.addgene.org; plasmid No. 62972 and 49263, respectively). *E. coli* was grown in Luria broth and plasmid DNA was isolated by using a maxiprep plasmid DNA isolation kit (Thermo Scientific, Waltham, MA, United States) according to the manufacturer's instructions. Plasmid DNA was quantified using a nano-drop spectrophotometer and resolved on 1% agarose gel to check purity.

Transfection of human umbilical cord derived MSCs by electroporation

To transfect MSCs with plasmids (pcDNA3.1 HA-rn*Sox-9* and MSCV-*Six-1* tagged GFP), MSCs were suspended in sterile R buffer containing 30 μg plasmids and were electroporated at 1200 volts; 10 ms and 1 pulse with Neon Transfection System (Thermo Scientific). MSCs were transfected separately with *Sox-9* and *Six-1*, and co-transfected with 15 μg each of *Sox-9* and *Six-1* plasmids. Each subset of transfected MSCs was cultured in a basic growth medium for 48 h, followed by incubation in a chondrogenic induction and standard growth media till day 21. MSCs grown in the chondrogenic induction medium were used as positive control, while non-electroporated MSCs in the basal medium was used as negative control.

Evaluation of transfection efficiency

After 48 h of electroporation, MSCV-*Six-1* GFP labeled plasmid was analyzed for GFP expression under fluorescent microscope. HA-rn*Sox-9* and MSCV-*Six-1* transfected MSCs were analyzed for protein expression by immunocytochemical staining. To evaluate the transfection efficiency, the fluorescent intensity of Six-1 and Sox-9 expressing cells was quantified with Image J software and plotted with MS excel.

Protein expression analysis

Normal and transfected MSCs cultured in the basal and chondro-induction media for 21 d were evaluated for chondrogenic protein expression by immunocytochemical analysis as described in the above section for the presence of chondrogenic markers Six-1, Sox-9, TGFβ1, TGFβ2, and aggrecan, as well as a stem cell potency marker Stro-1 at the recommended dilutions. Phalloidin labeled with Alexa fluor 488 or 546 was used to visualize the cellular cytoskeleton. Slides were observed under a fluorescent microscope (NiE, Nikon). Fluorescent cells were quantified with Image J software and plotted with Microsoft Excel.

Gene expression dynamics

RNA was isolated using 1 mL TRIzol for lysis, followed by 200 μL of chloroform for aqueous phase separation, and centrifugation at 12000 rpm for 10 min. The aqueous phase was collected and 1 mL of absolute ethanol was added for overnight incubation at -20 ˚C. The suspension was centrifuged, and the pellet was washed with 70% ethanol. Finally, the pellet was dissolved in 20 μL nuclease-free water and stored at -20 ˚C. Quantification and purity of RNA were determined at 260 nm and 280 nm, respectively. First-strand cDNA was prepared by using 1 μg RNA by RevertAidTM First Strand cDNA synthesis kit (K1622, Thermo Scientific). qPCR amplification was performed in three biological replicates in 96-well plates using qPCR master mix (A600A, Promega, Madison, WI, United States) for genes provided in Table 1. β-actin and GAPDH were used as internal controls.

Experimental animals

A total of 21 Wistar rats (aged 3-5 mo) were used for *in vivo* experiments under the guidelines for the care and use of laboratory animals. Local ethical approval was obtained under protocol number (#20170051) from the Institutional Animal Care and Use Committee of Dr. Panjwani Center for Molecular Medicine and Drug Research, University of Karachi, Pakistan. Animals weighting between 200-250 g were used for experiments to ensure equal size of IVDs to minimize variation in results.

Establishment of needle punctured IVDD model

Rats were anesthetized by injecting a mixture of ketamine hydrochloride (60 mg/kg) and xylazine hydrochloride (7 mg/kg), intraperitoneally. To ensure complete anesthesia, reflexes were checked by tail pinch test. The tail was sterilized with 70% ethanol and three sequential intervertebral disc spaces were manually located and marked. Sterile 21 G × 1-inch needle was penetrated in between the coccygeal vertebrae (Co); Co5/Co6 (unpunctured disc or negative control), Co6/Co7 (punctured disc or positive control), and Co7/Co8 (cells transplanted disc), through the level of an upper region (annulus fibrosus) to the middle section of the disc to aspire nucleus pulposus to induce degeneration. The needle was perpendicularly kept for about 20 s for rapid degeneration. Animals were placed back into their respective cages and observed on daily basis for changes in diet uptake and behavior till 14 d.

Cell labeling for transplantation

For *in vivo* cell tracking, transfected and non-transfected cells were detached, washed, and centrifuged

Table 1 Primer sequences used in the study with their annealing temperatures

Gene	Primer sequences (5'-3')	Annealing temperature (°C)
GAPDH	(F) 5′-CACCATGGGGAAGGTGAAGG-3′; (R) 5′- AGCATCGCCCCACTTGATTT -3′	58
β-actin	(F) 5′-CACTGGCATCGTGATGGACT -3′; (R) 5′-TGGCCATCTCTTGCTCGAAG -3′	58
Sox-9	(F) 5′-CATCTCCCCCAACGCCA-3′; (R) 5′-TGGGATTGCCCCGAGTG-3′	58
Six-1	(F) 5′-CTCCAGTCTGGTGGACTTGG-3′; (R) 5′-AGCTTGAGATCGCTGTTGGT -3′	58
BMP2	(F) 5′-AGCTGGGCCGCAGGA -3′; (R) 5′-TCGGCTGGCTGCCCT -3′	58
Aggrecan	(F) 5′-AATCTCACAATGCCACGCTG -3′; (R) 5′-GAGGCTGCATACCTCGGAAG -3′	58
TGFβ1	(F) 5′-CAAGGCACAGGGGACCAG -3′; (R) 5′-CAGGTTCCTGGTGGGCAG -3′	58

to obtain a cell pellet. Cells were labeled with red fluorescent lipophilic cationic indocarbocyanine (DiI) membrane labeling dye (V-22885, Vybrant® DiI cell-labeling solution, Invitrogen, Carlsbad, CA, United States) according to the manufacturer's instructions. The activity of unbound dye was instantly inhibited by adding 5 mL complete medium, followed by washing with PBS and dissolving in 50 μL PBS. To check the labeling efficiency, these cells were observed under a fluorescent microscope and flow cytometer.

Cellular transplantation in the IVDD model

There were seven experimental groups; normal, degenerated, MSC transplanted, *Sox-9* MSC transplanted, *Six-1* MSC transplanted, *Sox-9* and *Six-1* MSC transplanted (synergistic), and iCPC transplanted groups (n = 3). One million cells suspended in 50 μL PBS were transplanted into the site of injury. After 2 wk of transplantation, animals were decapitated and tail discs were carefully harvested and demineralized in 11% formic acid for 2 h. Tissues were transferred into small molds containing optimal cutting temperature (OCT) medium (Surgipath, FSC22, Leica Microsystems, Wetzlar, Germany), and immediately stored at -20 °C to turn it into a frozen block.

Histological analysis

Sectioning of frozen blocks was performed using a cryostat machine (Shandon, Thermo Electron Corporation, UK) with a sharp cutting blade. Ten μm thick sections were cut and loaded on gelatin coated slides, and further classified by hematoxylin-eosin and Alcian blue staining. Images were captured with a bright field microscope (NiE, Nikon). Histological grading was performed and plotted.

Tracking of DiI labeled cells in the transplanted IVDs

Cryosections were observed under a fluorescent microscope to track the presence of transplanted DiI labeled cells. To check the viability, long term survival and distribution of the transplanted cells in the IVDD model, the sections were stained with Alexa fluor 488 labeled phalloidin to stain the cytoskeleton protein F-actin. Images were captured with fluorescent microscope. Fluorescent intensity was measured with Image J software and plotted with Microsoft Excel.

Statistical analysis

All statistical evaluations were performed using IBM SPSS version 21. Each experiment was run in triplicate and presented as mean ± SD. Multiple comparative analysis was performed using One Way-ANOVA and Bonferroni post hoc test, considering $P < 0.05$, $P < 0.01$, and $P < 0.001$ as statistically significant.

RESULTS

Isolation, proliferation, and characterization of MSCs from a primary culture of human umbilical cord tissue

Cell growth observed after the 15th day of explant culture is termed P_0 cells, as shown in Figure 1A. Fibroblast-like cells of the homogenous population were detached upon reaching 70% confluency and sub-cultured; this is termed as P_1 cells propagated further until passage P_2. These cells showed expression of stem cell markers CD73, CD105, Vimentin, CD29, and CD90 as depicted in Figure 1B. The immunophenotypic analysis was performed using flow cytometry to analyze the expression of CD45, Vimentin, CD105, and CD73, as shown in Figure 1C. The isolated cells were analyzed for tri-lineage differentiation by culturing in the induction media for 3 wk; MSCs differentiated into osteogenic, adipogenic, and chondrogenic lineages revealed respectively by Alizarin Red S which indicated mineral

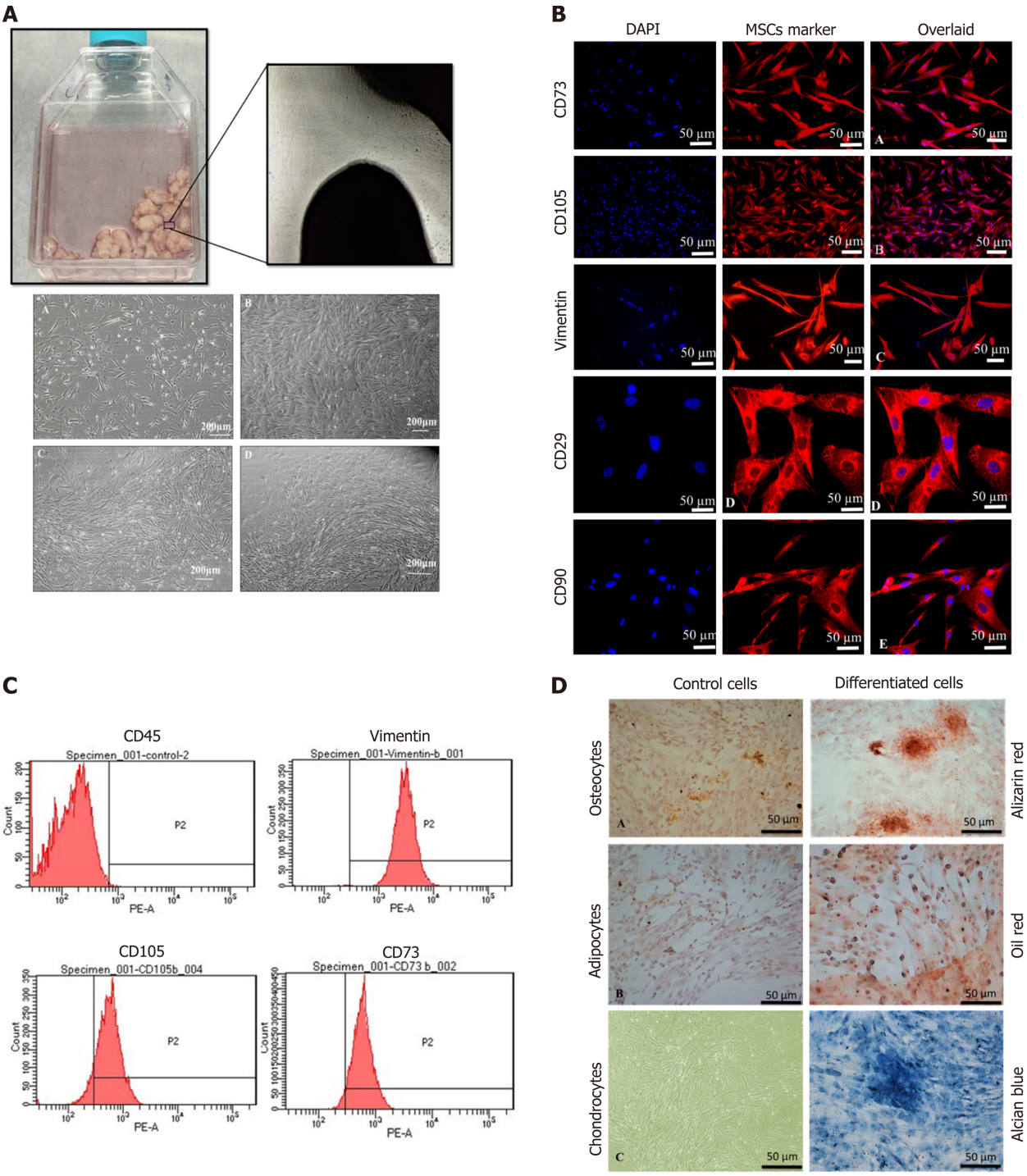

Figure 1 Characterization of human umbilical cord mesenchymal stem cells. A: Culture of human umbilical cord mesenchymal stem cells (hUC-MSCs) showed spindle-shaped fibroblast-like morphology at passage P_1 to P_4; B: MSCs showed positive expression of CD73, CD105, Vimentin, CD29, and CD90. Nuclei were stained with DAPI; C: Histogram of MSCs with specific markers. MSCs showed negative expression of CD45, while positive expression for Vimentin, CD105, and CD73; D: Tri-lineage differentiation of hUC-MSCs. Alizarin Red stained calcium deposits produced by osteocytes, Oil red O-stained lipid vacuoles produced by adipocytes, and Alcian blue stained proteoglycans and glycosaminoglycans secreted by chondrocytes.

deposits, Oil Red O, which positively stained oil droplets, and Alcian blue which stained ECM of chondrocytes, as shown in Figure 1D.

Transfection efficiency of MSCs

Sox-9 and *Six-1* transfected MSCs were characterized for transfection efficiency. MSCs were successfully transfected as shown by the expression of Sox-9 and Six-1 proteins after 48 h of transfection compared to control, as shown in Figure 2.

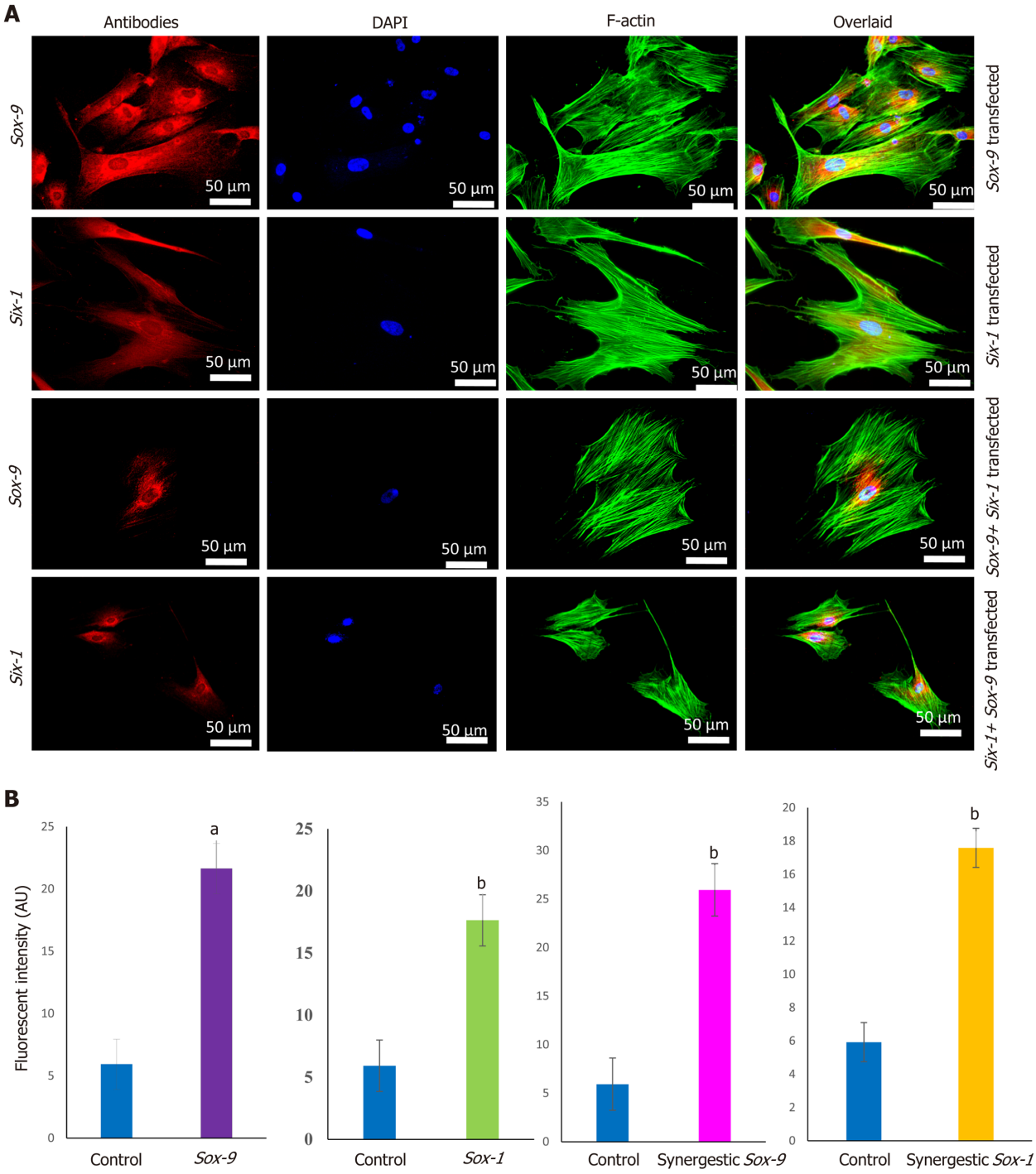

Figure 2 Transfection efficiency of human umbilical cord mesenchymal stem cells. A: Positive expression of Sox-9, and Six-1 proteins was observed after 48 h of electroporation, as analyzed by immunocytochemical staining; B: Quantification of fluorescent intensities showed that *Sox-9* transfected cells expressed Sox-9 protein, *Six-1* transfected mesenchymal stem cells (MSCs) expressed Six-1 protein, and *Sox-9*+*Six-1* transfected MSCs expressed Sox-9, and Six-1 proteins. [a]$P < 0.05$ *vs* control; [b]$P < 0.01$ *vs* control.

Characterization of differentiated transfected MSCs

MSCs analyzed by immunocytochemical staining indicated that they did not express chondro-markers Sox-9, TGFβ2, and aggrecan as shown in Figure 3A, whereas MSCs cultured in chondrogenic medium expressed TGFβ2 and aggrecan as shown in Figure 3B. The later cells are termed iCPCs. The cellular cytoskeleton of F-actin was stained with Alexa fluor 488/546 labeled phalloidin. After day 21 of transfection, striking differences in the morphological features of the differentiated cells were noted. The transfected cells completely lost their fibroblast-like appearance. Cells displayed a broad and polygonal shape similar to the iCPCs as shown in Figure 4. Transfected MSCs after 21 d of culture in the normal and chondro-induction media were immunostained for the expression of Sox-9 and Six-1 proteins, as shown in Figure 5. The fluorescent intensity was quantified, and the results showed that MSCs transfected with *Sox-9, Six-1*, and their combination expressed chondrogenic markers following 21 d of

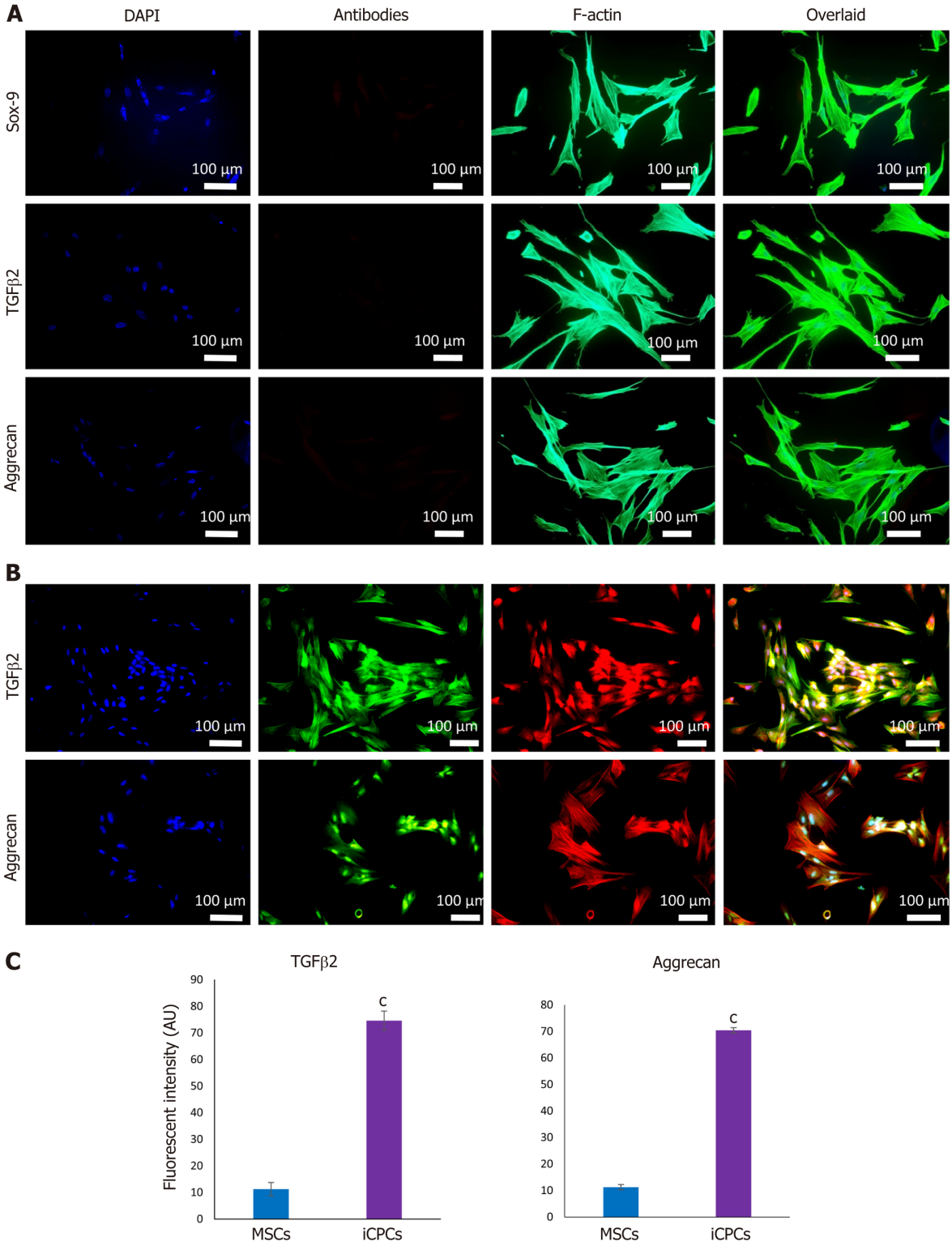

Figure 3 Expression of chondrogenic markers in human umbilical cord mesenchymal stem cells and induced chondro-progenitor cells.
A: Human umbilical cord (hUC)-mesenchymal stem cells (MSCs) did not express Sox-9, transforming growth factor beta-2 (TGFβ2), and aggrecan, which indicates that MSCs are negative for the expression of early and late chondrogenic markers; B: Induced chondro-progenitor cells expressed aggrecan, and TGFβ2, showing that MSCs were differentiated into chondrocytes; C: The quantification of fluorescent intensities for aggrecan and TGFβ2 showed their significantly higher expression in differentiated cells as compared to control. $^{c}P < 0.001$ *vs* MSCs.

culture in the basal medium. Similarly, the transfected MSCs in the chondro-induction medium also expressed chondrogenic markers Sox-9 and Six-1 after 21 d of culture as shown in Figure 5.

Stemness of MSCs

Immunostaining of MSCs showed positive expression of stemness marker Stro-1 in the control cells, whereas transfected MSCs lost the expression of Stro-1 after 21 d of culture in normal and chondro-

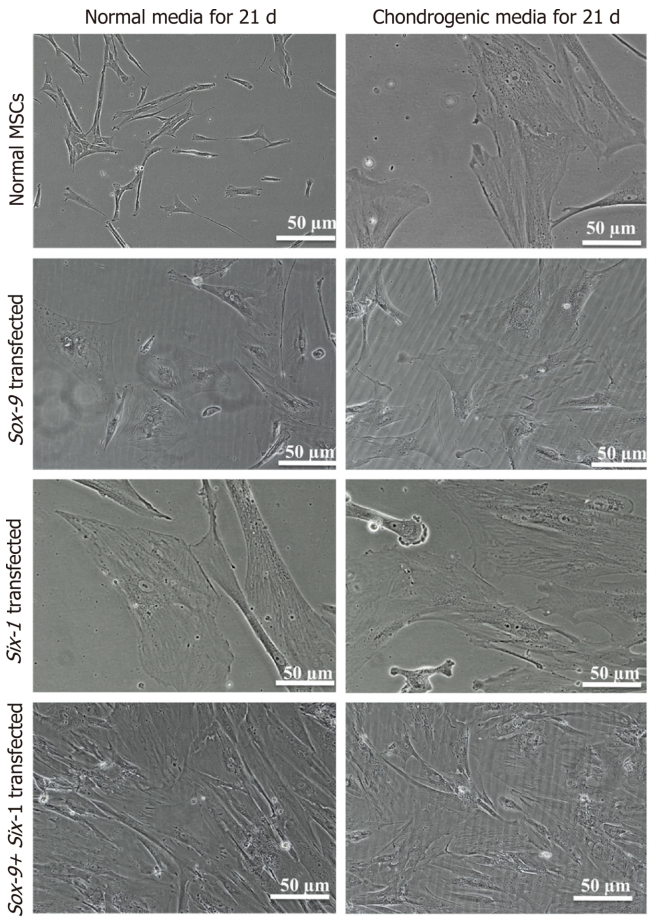

Figure 4 Morphology of transfected human umbilical cord mesenchymal stem cells. Transfected human umbilical cord mesenchymal stem cells (MSCs) after 21 d of culture in the normal and chondro-induction media under phase contrast microscope showed broad and polygonal morphology which is similar to the morphology of induced chondroprogenitor cells, indicating that differentiation is induced in the transfected cells.

induction media. The immunofluorescence quantification showed a significant reduction in Stro-1 protein expression in all the transfected and differentiated cells, as shown in Figure 6.

Gene expression dynamics of Sox-9 and Six-1 transfected MSCs

To check the transcriptional changes of transfected MSCs in comparison to the control MSCs, fold change regulation ($2^{-\Delta\Delta Ct}$) of chondro-specific genes was analyzed. Expression of *TGFβ1*, *BMP*, *Sox-9,* and *Six-1* at 48 h showed that these genes were significantly up-regulated in *Sox-9*, *Six-1* and their combination (*Sox-9* + *Six-1*) groups as shown in Figure 7. Expression of *Sox-9* was significantly up-regulated at day 21 post-transfection in the basal medium in *Sox-9* and the combination group, while no significant difference was observed in the *Six-1* transfected group. The expression of *Six-1* has shown no effect in any of the transfected groups after 21 d of transfection. *BMP*, *aggrecan*, and *TGFβ1* were significantly up-regulated in the *Sox-9, Six-1,* and the combination group at 21 d of transfection in the basal and chondro-induction media, as shown in the Figure 7.

Histological examination

Immunohistochemical staining after 2 wk of transplantation showed that the implanted cells homed, distributed, and integrated into the IVD. The quantification of fluorescently labeled cells in the IVD sections showed that the transfected MSC group has significantly higher fluorescent intensity than normal MSCs. The sections were stained for F-actin to visualize the cellular cytoskeleton, which showed that the DiI labeled implanted cells were stained with phalloidin, as evident by co-localization of red and green fluorescence in Figure 8. H and E staining of the degenerated intervertebral disc displayed complete shrinkage of the NP region with fissuring morphology at NP-AF interface compared to normal IVD. Cells surrounded by the matrix in healthy NP were not present in the degenerated IVD. Transfected MSC and iCPC transplanted IVD sections showed better cellularity than degenerated IVDs as shown in Figure 9. However, the partial deformity was observed in the MSC transplanted IVD sections. Alcian blue staining of IVDD showed negligible presence of glucosaminoglycans in the degenerated and MSC transplanted groups. In contrast, transfected MSC and iCPC transplanted IVDDs showed a significant amount of glucosaminoglycans as shown in Figure 9. Histological scoring showed

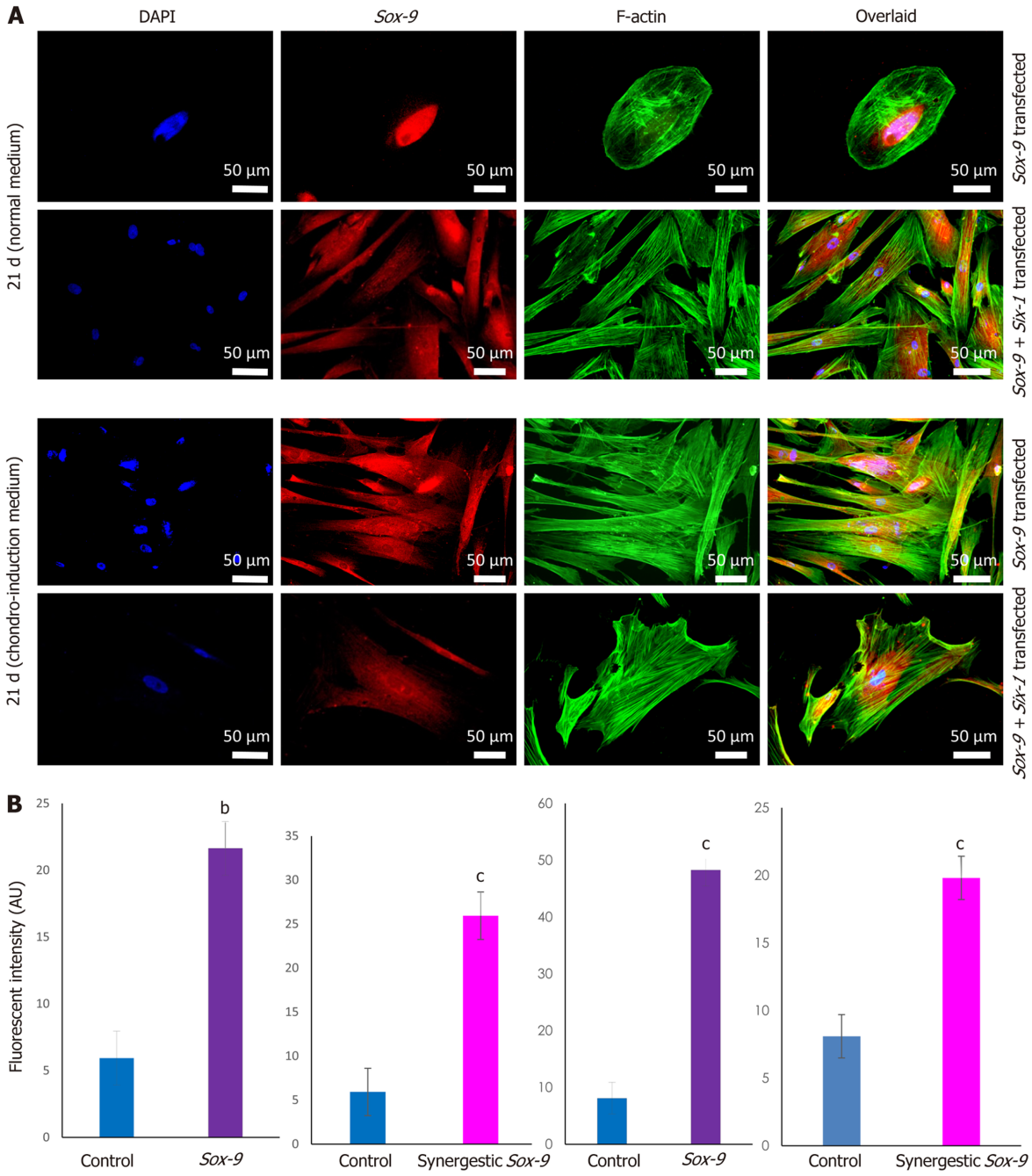
A
DAPI
Sox-9
F-actin
Overlaid
21 d (normal medium)
21 d (chondro-induction medium)
Sox-9 transfected
Sox-9 + Six-1 transfected
50 μm
B
Fluorescent intensity (AU)
Control
Sox-9
Synergestic Sox-9
b
c

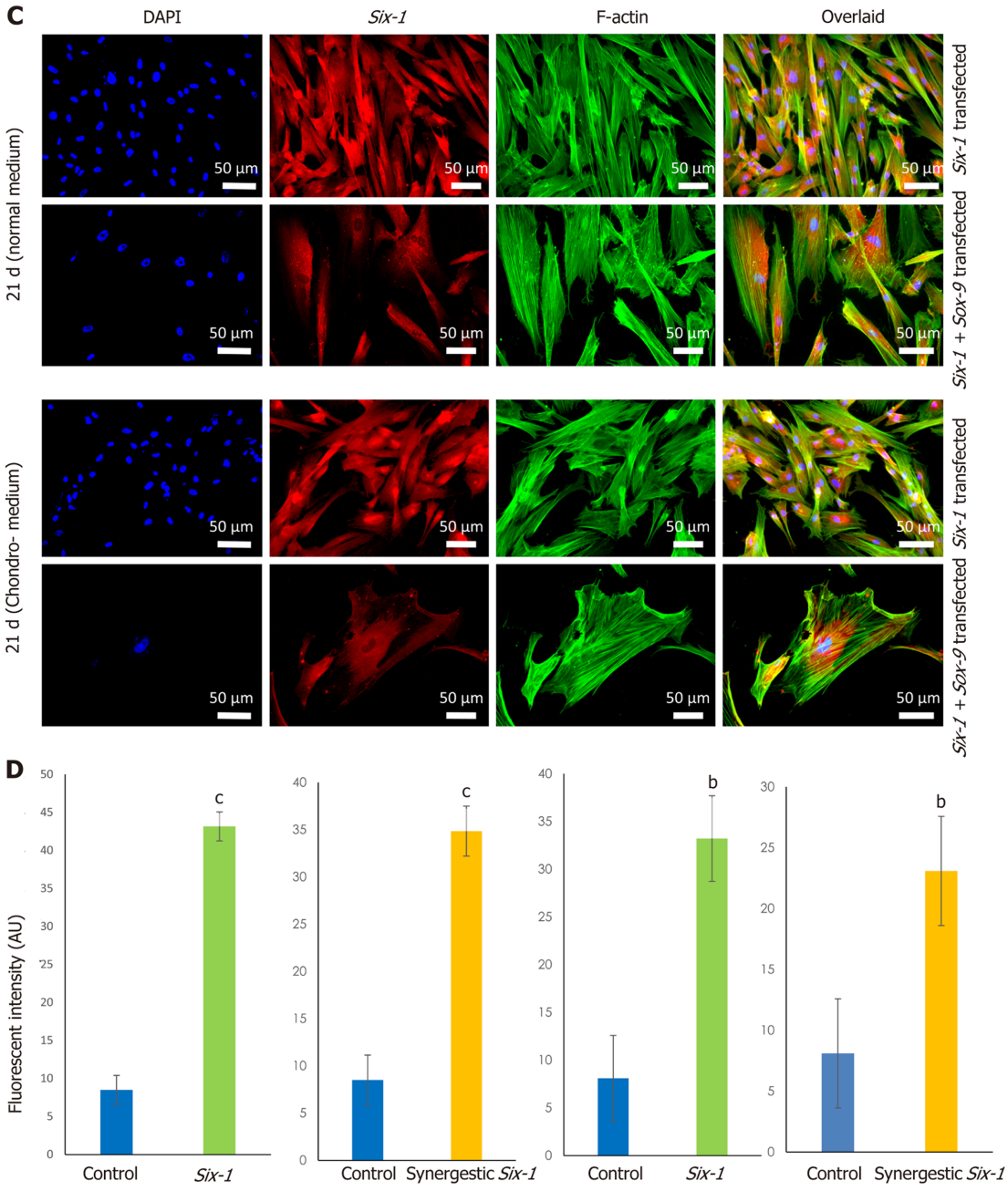

Figure 5 Expression of Sox-9 and Six-1 proteins in transfected human umbilical cord mesenchymal stem cells. Human umbilical cord mesenchymal stem cells transfected with *Sox-9*, *Six-1* or both in combination (*Sox-9* + *Six-1*) were cultured in the normal and chondro-induction media for 21 d. Cells were stained for the expression of Sox-9 and Six-1 proteins by immunocytochemical staining. Alexa fluor 488 labeled phalloidin was used to visualize F-actin of the cellular cytoskeleton. A, B: The expression of Sox-9 in *Sox-9* and synergistic transfected group in normal and chondro-induction media, and their fluorescent intensities, respectively; C, D: The expression of Six-1 in *Six-1* and synergistic transfected group in normal and chondro-induction media, and their fluorescent intensities, respectively. $^{b}P < 0.01$ *vs* control; $^{c}P < 0.001$ *vs* control.

that transfected MSCs better regenerated the IVD as compared to normal MSCs.

DISCUSSION

Discogenic pain arising from the degenerated intervertebral disc is considered one of the leading causes of chronic low back pain. Analgesics and physiotherapy are the only treatment options, which only reduce the symptoms; pathological progression of intervertebral disc degeneration cannot be precluded by these methods. A normal healthy disc is an avascular tissue with a consistent cell density of 5.5×10^3 cells/mm^3 that greatly reduces with age and injury. In disc degeneration morphology, the disc water content and matrix composition is significantly reduced[23]. Once the damage is initiated, it ultimately leads to cell loss in the nucleus pulposus region of the disc, which leads to deterioration as cartilage

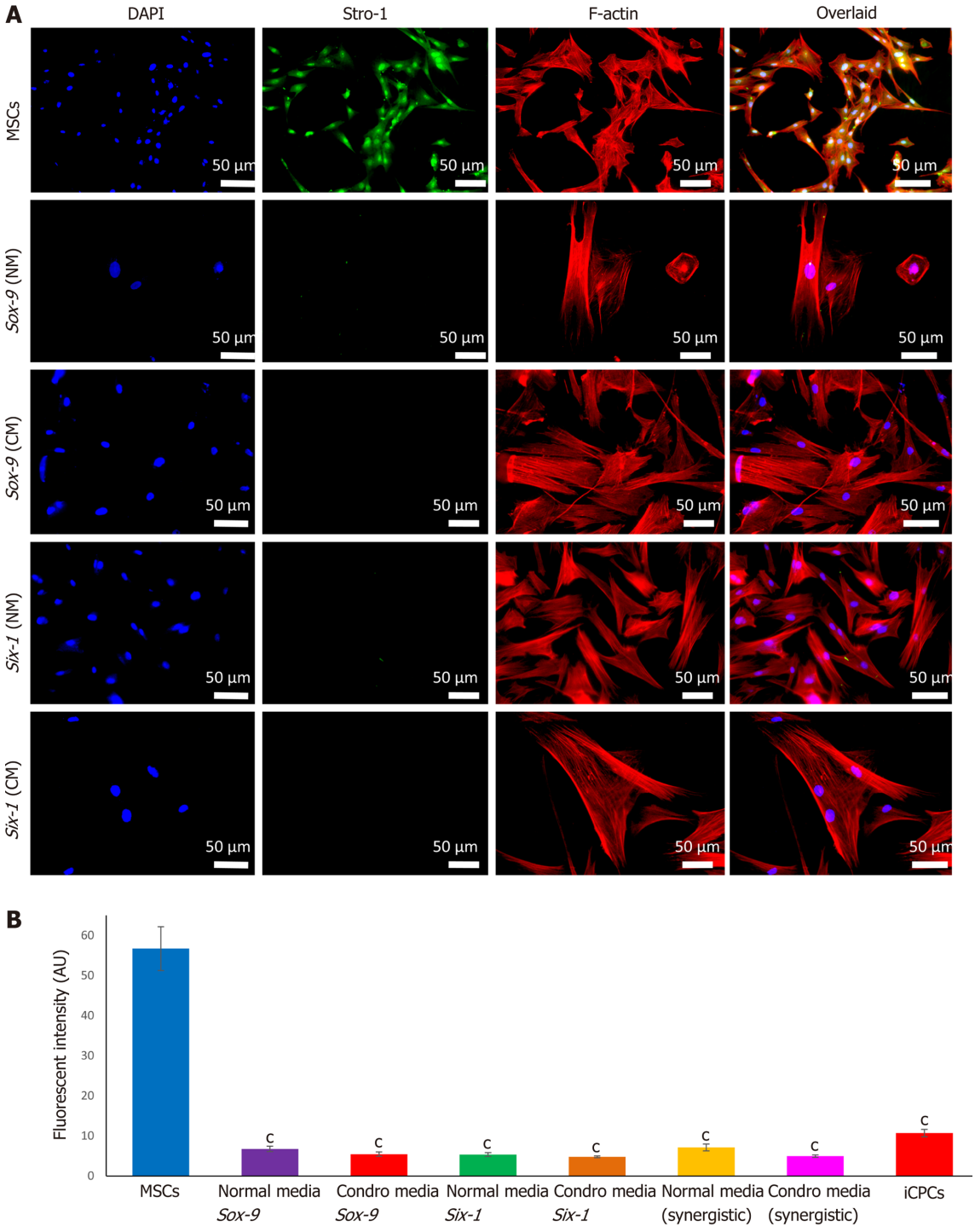

Figure 6 Stemness of transfected human umbilical cord mesenchymal stem cells. A: After 21 d of *in vitro* culture in normal and chondro-induction media, transfected cells were immunocytochemically stained for the expression of mesenchymal stem cell (MSC) stemness marker Stro-1. Alexa fluor 546 labeled phalloidin was used to visualize F-actin of the cellular cytoskeleton. The nuclei were stained with DAPI; B: The fluorescent intensity of Stro-1 was quantified and showed the expression of Stro-1 protein. $^{c}P < 0.001$ *vs* MSCs. iCPCs: Induced chondro-progenitor cells.

tissue has limited mending capability. Because cartilage in the intervertebral disc contributes to overall body movements and flexion, dysfunction in the disc prominently affects the body motions, including flexion and bending. It may cause severe back pain leading to a decline in the quality of life[24]. Recently, advances in understanding disc biology led to the interest in fixing the degeneration of disc by gene therapy combined with stem cells which may support the regeneration by overcoming the drawbacks of the self-renewal process[25].

This study was focused on determining the role of specific chondrogenic transcription factors *Sox-9* and *Six-1* in differentiating the MSCs into chondrocytes *in vitro*. Transfected MSCs after transplantation were analyzed for their enhanced role in homing, production of the extracellular matrix, and regeneration of the degenerated intervertebral disc.

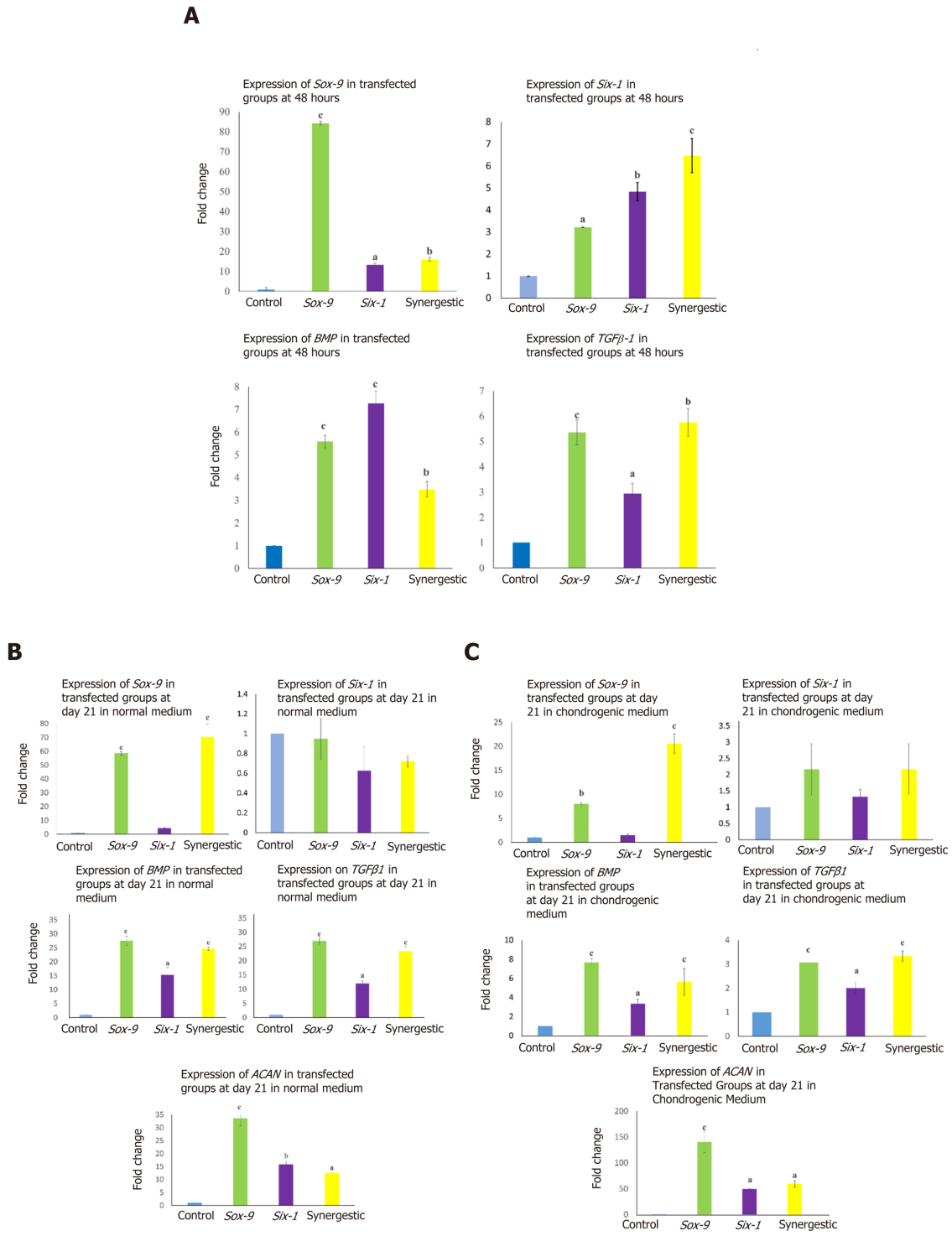

Figure 7 Gene expression analysis of transfected human umbilical cord mesenchymal stem cells *via* quantitative polymerase chain reaction. A: Bar graphs with significant transcriptional expression of transforming growth factor beta-1 gene (*TGFβ1*), *BMP*, *Sox-9*, and *Six-1* at 48 h post-transfection; B, C: Significant expression of *TGFβ1*, *BMP*, *Sox-9*, and *aggrecan* observed at 21 d post-transfection shows long term sustainability in the expression pattern. However, the expression was time-dependent, *Six-1* was significantly downregulated in both normal and chondro-induction media at day 21. $^{a}P < 0.05$ *vs* control; $^{b}P < 0.01$ *vs* control; $^{c}P < 0.001$ *vs* control.

Human umbilical cord tissue was used as a source of MSCs. Cord explants were cultured, and MSCs were isolated and grown in culture. They were passaged to obtain a pure population and their proliferative ability was analyzed. Further, cells showed typical spindle shape fibroblast-like morphology and positive expression of specific surface markers CD73, CD105, and Vimentin, as reported in other studies [26]. Harvested cells also exhibited significant expression of Stro-1 marker. Since Stro-1 is a well reported MSC marker, once MSCs are differentiated, they lose its expression[27]. Stro-1 is not expressed in iCPCs[28], which is in agreement with our findings. The presence of MSC antigens CD73, CD105, and Vimentin were also confirmed by flow cytometric analysis, while CD45 which is a hematopoietic

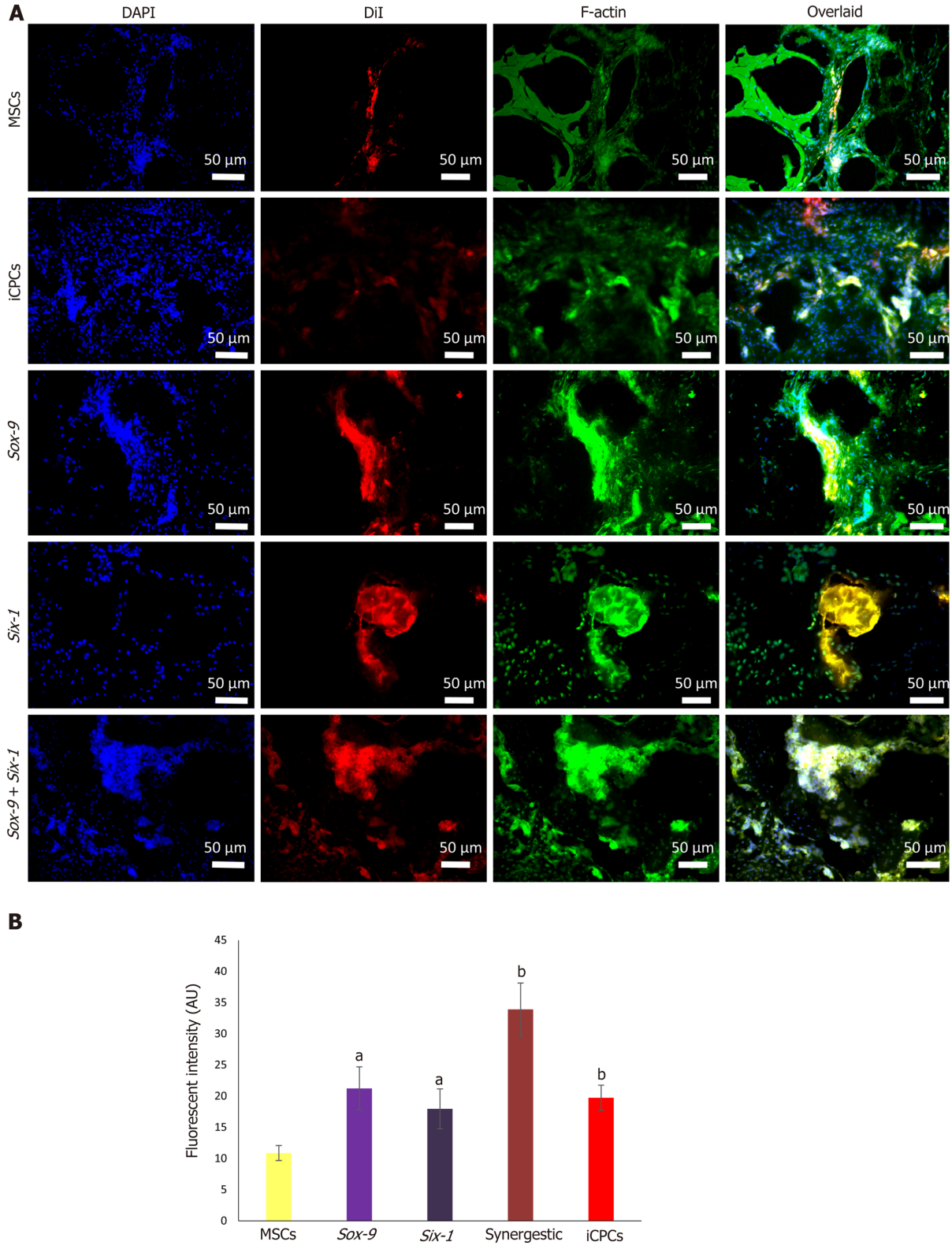

Figure 8 Tracking of transplanted cells in rat intervertebral disc degeneration model. A: Tracking of the Dil-labeled normal and transfected mesenchymal stem cells (MSCs), and induced chondro-progenitor cells transplanted disc indicated the co-localization of red fluorescence originating from the Dil-labeled cells and green fluorescence from Alexa fluor 488 labeled phalloidin (F-actin), confirming their distribution, and homing in the intervertebral discs; B: Fluorescence intensities of the group transplanted with transfected cells showed significantly high fluorescence compared to normal MSCs. $^{a}P < 0.05$ *vs* MSCs; $^{b}P < 0.01$ *vs* MSCs. iCPCs: Induced chondro-progenitor cells.

marker was used as a negative control; similar observations were also reported previously[29,30]. Additionally, human umbilical cord cells showed great potential of differentiation into chondrocytes, adipocytes, and osteocytes[31]. The differentiated cells showed irregular, broad-shaped morphology and presence of proteoglycans for chondrocytes, calcium deposits for osteocytes, and lipid molecules for adipocytes. Successful *in vitro* multilineage differentiation proved that the isolated cells were MSCs. All

A

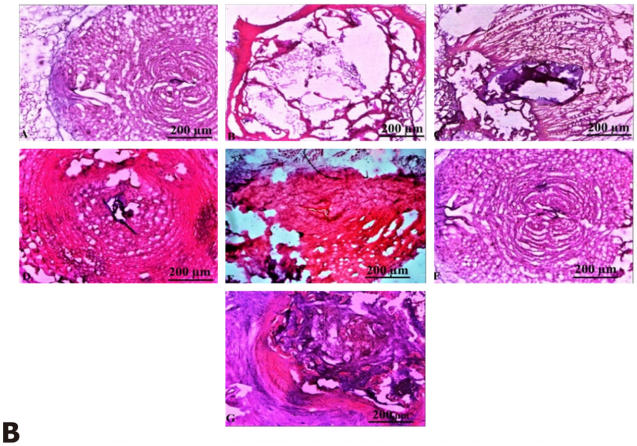

B

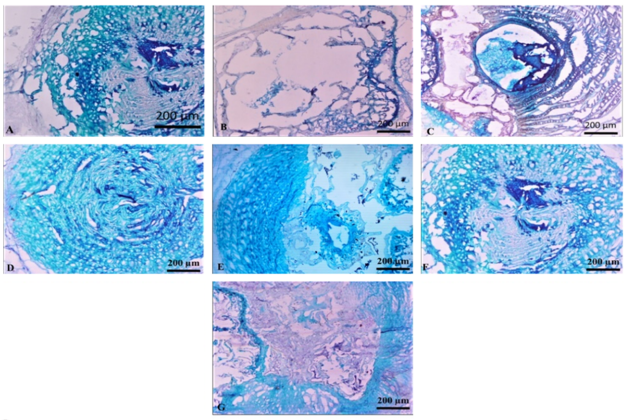

C

Treatment group	Score	Interpretation
Normal disc	5	Deep blue stain in peri-NP region; deep blue stain between AF lamellae.
MSCs transplanted	3	Normal pattern no longer present; large areas of faded blue centrally and in AF, but inconsistent and patchy
Degenerated disc	1	Entire stain washed out from the center; NP of the IVD.
iCPCs transplanted	5	Deep blue stain in peri-NP region; deep blue stain between AF lamellae.
Sox9 transfected	4	Pattern of stain similar to grade 5, but with less Prominent peri-NP stain and more rapid fading of stain between AF lamellae.
Six1 transfected	5	Deep blue stain in peri-NP region; deep blue stain between AF lamellae.
Synergistic combination	4	Pattern of stain similar to grade 5, but with less Prominent peri-NP stain and more rapid fading of stain between AF lamellae.
-	2	Only one third small patches of faded blue stain either centrally or in AF

Figure 9 Histological examination of intervertebral disc. A: (A-G) Bright field imaging of intervertebral discs (IVDs) showing nucleus pulposus (NP) content of the healthy (Co6/7), and degenerated disc (Co5/6) treated with normal mesenchymal stem cells (MSCs), transfected MSCs, and induced chondro-progenitor cells (iCPCs) (Co5/6) IVDs, in each group. Bright-field microscopic images of IVDs were captured from the cryosections stained by hematoxylin and eosin; normal healthy disc, degenerated disc, and degenerated disc transplanted with normal MSCs, *Six-1* transfected MSCs, *Sox-9* transfected MSCs, iCPCs, and *Sox-9* + *Six-1* transfected MSCs, respectively; B: (A-G) Bright-field microscopic images of IVDs were captured from the cryosections stained by Alcian blue displayed glycoproteins secreted by the transplanted cells compared to the degenerated disc; normal healthy disc, degenerated disc, and degenerated disc transplanted with normal MSCs, *Six-1* transfected MSCs, *Sox-9* transfected MSCs, iCPCs, and *Sox-9* + *Six-1* transfected MSCs, respectively; C: Histological grading with a score for regeneration. AF: Annular fibrosus.

these morphological, cytological, and biochemical properties were in agreement with previous studies and strongly favored the existence of a pure MSC population[32].

On day 21, the morphology of transfected cells showed a large, broad, and flat shape, similar to the morphology of iCPCs, unlike non-transfected MSCs that showed typical adult stem cell features. Similar morphological differences of *Sox-9* transfected cells at different days were also reported in a prior

investigation[33]. We also observed that the differentiation of cells has significantly reduced the expression of Stro-1, compared to normal MSCs, in agreement with previous findings[28].

Gene expression dynamics of normal and transfected MSCs and MSCs induced to chondrocytes showed that the chondrogenic markers, *Sox-9, Six-1, BMP,* and *TGFβ2* were significantly upregulated, indicating that the cellular differentiation towards chondrogenic lineage has been initiated. The mRNA expression is downregulated after sufficient protein expression is achieved or once the early induction into a particular lineage is initiated. Prior studies reported that the *Six-1* mRNA expression is downregulated after few hours. On day 21, it did not show any change; however, the Six-1 protein was found to be at a significant level[34]. Transcription factors have been reported to induce differentiation in human umbilical cord derived MSCs (hUC-MSCs) into chondrocytes[35,37]. *Sox-9* and *Six-1* are well-documented transcription factors to initiate chondrogenesis[38,39]. It has been found that overexpression of *Sox-9* and *Six-1* induced the transcription of *BMP2, TGFβ1, Sox-9,* and *Six-1* after 48 h of transfection which efficiently directed the fate of MSCs towards chondrocytes[40]. In the differentiated cells, *Six-1* expression downregulates, and aggrecan which is a late chondrogenesis marker, is reported to be upregulated[34,41]. *Sox-9* and *Six-1* triggered hUC-MSCs to undergo morphological changes and induce differentiation in MSCs[42].

To elucidate the effect of chondrogenic transcription factors, transfected MSCs, non-transfected MSCs, and iCPCs were analyzed for the regeneration of the intervertebral disc after 2 wk of transplantation. Fluorescently labeled cells were tracked in the harvested disc with fluorescence microscopy, which showed that MSCs transfected with *Sox-9 and Six-1,* as well as the co-transfected MSCs, did better homing, integration, distribution, and differentiation into notochordal cell types and regenerated the degenerated disc. To analyze the potential of differentiated MSCs, a histological assessment was performed for cellularity and ECM and GAG content. H and E staining of the degenerated intervertebral disc displayed NP ossification, reduced cell density, and diminished extracellular matrix in the form of shrunken shape. It has been documented that in the degenerated disc, interconnection with AF is lost and fissuring manifestation in the NP area is prominent[43,44]. The disc transplanted with MSCs only exhibited slight improvement in preserving structural integrity. However, disc injected with transfected MSCs showed remarkable difference in contrast to the IVDD. The overall appearance resembled the normal intervertebral disc IVD morphology. Alcian blue staining showed significant amount of GAG content in the disc transplanted with transfected MSCs, which is in agreement with previous findings[10,45]. Additionally, xenogenic transplanted MSCs were selectively investigated by measuring specific chondrogenic markers which contribute to restore IVD integrity[46].

Tracking of labeled cells with DiI showed better survival, homing and integration of transfected hUC-MSCs into the punctured rat model of IVDD. Regeneration of NP region showed better delivery of cells to the site of injury. Significantly, the effect of transfected cells on nucleus pulposus content was more noticeable than non-transfected hUC-MSCs. Immunohistochemistry revealed co-localized expression of Sox-9 and Six-1 with actin (used as internal control). Previous reports have shown similar findings that xenogenic MSCs home and integrate in the IVD[47,48]. The studies showed that the disc transplanted with genetically modified MSCs did home, survive, and were functionally active in the NP area[49].

The findings in the current study elucidated that gene modification or overexpression in stem cells has immense potential for the regeneration of degenerated disc, compared to normal MSCs. Genetically modified MSCs survived long and better regenerated the degenerated NP of the disc. The enforced expression of *Six-1, Sox-9*, and their synergistic *(Six-1 + Sox-9)* co-transfection enhanced the chondrogenic differentiation of human cord MSCs into chondrogenic lineage in the normal growth medium.

CONCLUSION

Overexpression of the chondrogenic transcription factors in hUC-MSCs accelerated their differentiation potential into chondroprogenitor cells. The synergistic effect of *Sox-9* and *Six-1* transcription factors led the MSCs to differentiate into chondrogenic cells in the basal medium and produced the same effect as the chondro-induction medium. The *in vivo* implantation of these transfected cells leads to their better homing, integration, and differentiation into NP cells of the IVD. Histological observation and grading score showed that cellular transplanted group significantly regenerated the degenerated disc. This approach could be further developed for treating DDD.

ARTICLE HIGHLIGHTS

Research background

Genetic manipulation is now considered the safest and promising approach in the field of regenerative medicine. Mesenchymal stem cells (MSCs) are the potential candidates for the clinical use of genetically engineered stem cells. They are non-immunogenic, proliferative, and possess multiple lineage differen-

tiation potential. Gene modification of MSCs using chondrogenic transcription factors may lead to the use of this strategy to treat debilitating diseases related to cartilage.

Research motivation

Genetic modification of MSCs offers a competent source for the sustained translation of therapeutic proteins. Transfection of human umbilical cord derived MSCs (hUC-MSCs) using chondro-specific transcription factors may lead to enhance chondrogenesis and efficient regeneration of cartilage-related injuries.

Research objectives

The main objective of the study was to analyze the effect of transcription factors *Sox-9* and *Six-1* in chondrogenesis by transfecting them into hUC-MSCs and determining successful intervertebral disc (IVD) regeneration.

Research methods

MSCs were isolated from cord tissue and characterized using their specific markers. MSCs were transfected using transcription factors *Sox-9* and *Six-1*. Cell differentiation was analyzed at the transcriptional and translational levels, while the regeneration potential of transfected MSCs was observed by transplanting them into the degenerated rat IVD model. Post-transplantation histology and cell tracking analysis were performed to evaluate cartilage regeneration.

Research results

In vitro analysis showed that transcription and translation of chondrogenic markers were significantly higher in transfected MSCs at 24 h, and 21 d in comparison to control MSCs. Transfected MSCs at the site of degenerated IVD differentiated into chondrocytes which secreted chondro-proteins. The cells homed and regenerated the injured cartilage as that of normal cartilage, as evident from immunohistological and histological analyses.

Research conclusions

Genetic modification of hUC-MSCs with two chondrogenic transcriptional factors *Sox-9* and *Six-1* enhances their chondrogenic differentiation. Their synergistic effect on MSCs accelerated the regeneration of degenerated cartilage with complete restoration of tissue architecture.

Research perspectives

The present manuscript offers a promising therapeutic approach to revolutionize the treatment of cartilaginous defects and spinal cord injuries. The outcomes discussed in this study accentuates the advances towards the clinical translation of such approaches.

ACKNOWLEDGEMENTS

We acknowledge International Center for Chemical and Biological Sciences, University of Karachi, Karachi-75270, Pakistan for providing imaging facility.

FOOTNOTES

Author contributions: Khalid S performed the experiment and wrote the first draft of manuscript; Ekram S helped in experimentation and data acquisition; Salim A and Chaudhry GR evaluated the data and helped in manuscript preparation; Khan I designed the experiment, evaluated and analyzed the data, secured the funding, and finalized the manuscript.

Supported by Higher Education Commission Pakistan, No. 7083.

Institutional review board statement: IEC approval for the protocol ICCBS/IEC-009-UCB-2015/protocol/1.0. Informed consent was obtained from donor parents for the use of umbilical cord tissue in research.

Institutional animal care and use committee statement: Approval for Animal Study Protocol, No. 2018-0016.

Conflict-of-interest statement: No conflict of interest.

Data sharing statement: No extra data to share.

ARRIVE guidelines statement: ARRIVE guidelines were followed.

Country/Territory of origin: Pakistan

ORCID number: Shumaila Khalid 0000-0002-4523-6936; Sobia Ekram 0000-0003-0073-8729; Asmat Salim 0000-0001-5181-0458; G Rasul Chaudhry 0000-0003-1692-8420; Irfan Khan 0000-0003-1878-7836.

S-Editor: Wang JL
L-Editor: Filipodia
P-Editor: Zhang YL

REFERENCES

1 **Rustenburg CME**, Emanuel KS, Peeters M, Lems WF, Vergroesen PA, Smit TH. Osteoarthritis and intervertebral disc degeneration: Quite different, quite similar. *JOR Spine* 2018; **1**: e1033 [PMID: 31463450 DOI: 10.1002/jsp2.1033]
2 **Boden SD**, Davis DO, Dina TS, Patronas NJ, Wiesel SW. Abnormal magnetic-resonance scans of the lumbar spine in asymptomatic subjects. A prospective investigation. *J Bone Joint Surg Am* 1990; **72**: 403-408 [PMID: 2312537]
3 **Cassidy JJ**, Hiltner A, Baer E. Hierarchical structure of the intervertebral disc. *Connect Tissue Res* 1989; **23**: 75-88 [PMID: 2632144 DOI: 10.3109/03008208909103905]
4 **van Uden S**, Silva-Correia J, Oliveira JM, Reis RL. Current strategies for treatment of intervertebral disc degeneration: substitution and regeneration possibilities. *Biomater Res* 2017; **21**: 22 [PMID: 29085662 DOI: 10.1186/s40824-017-0106-6]
5 **Wong J**, Sampson SL, Bell-Briones H, Ouyang A, Lazar AA, Lotz JC, Fields AJ. Nutrient supply and nucleus pulposus cell function: effects of the transport properties of the cartilage endplate and potential implications for intradiscal biologic therapy. *Osteoarthritis Cartilage* 2019; **27**: 956-964 [PMID: 30721733 DOI: 10.1016/j.joca.2019.01.013]
6 **Twomey LT**, Taylor JR. Age changes in lumbar vertebrae and intervertebral discs. *Clin Orthop Relat Res* 1987; 97-104 [PMID: 3665259 DOI: 10.1097/00003086-198711000-00013]
7 **Buckwalter JA**. Aging and degeneration of the human intervertebral disc. *Spine (Phila Pa 1976)* 1995; **20**: 1307-1314 [PMID: 7660243]
8 **Ishihara H**, Urban JP. Effects of low oxygen concentrations and metabolic inhibitors on proteoglycan and protein synthesis rates in the intervertebral disc. *J Orthop Res* 1999; **17**: 829-835 [PMID: 10632449 DOI: 10.1002/jor.1100170607]
9 **Zehra U**, Noel-Barker N, Marshall J, Adams MA, Dolan P. Associations Between Intervertebral Disc Degeneration Grading Schemes and Measures of Disc Function. *J Orthop Res* 2019; **37**: 1946-1955 [PMID: 31042314 DOI: 10.1002/jor.24326]
10 **Wang F**, Shi R, Cai F, Wang YT, Wu XT. Stem Cell Approaches to Intervertebral Disc Regeneration: Obstacles from the Disc Microenvironment. *Stem Cells Dev* 2015; **24**: 2479-2495 [PMID: 26228642 DOI: 10.1089/scd.2015.0158]
11 **Yim RL**, Lee JT, Bow CH, Meij B, Leung V, Cheung KM, Vavken P, Samartzis D. A systematic review of the safety and efficacy of mesenchymal stem cells for disc degeneration: insights and future directions for regenerative therapeutics. *Stem Cells Dev* 2014; **23**: 2553-2567 [PMID: 25050446 DOI: 10.1089/scd.2014.0203]
12 **Kozlowska U**, Krawczenko A, Futoma K, Jurek T, Rorat M, Patrzalek D, Klimczak A. Similarities and differences between mesenchymal stem/progenitor cells derived from various human tissues. *World J Stem Cells* 2019; **11**: 347-374 [PMID: 31293717 DOI: 10.4252/wjsc.v11.i6.347]
13 **Aiuti A**, Slavin S, Aker M, Ficara F, Deola S, Mortellaro A, Morecki S, Andolfi G, Tabucchi A, Carlucci F, Marinello E, Cattaneo F, Vai S, Servida P, Miniero R, Roncarolo MG, Bordignon C. Correction of ADA-SCID by stem cell gene therapy combined with nonmyeloablative conditioning. *Science* 2002; **296**: 2410-2413 [PMID: 12089448 DOI: 10.1126/science.1070104]
14 **Zhao B**, Yu Q, Li H, Guo X, He X. Characterization of microRNA expression profiles in patients with intervertebral disc degeneration. *Int J Mol Med* 2014; **33**: 43-50 [PMID: 24173697 DOI: 10.3892/ijmm.2013.1543]
15 **Mulligan RC**. The basic science of gene therapy. *Science* 1993; **260**: 926-932 [PMID: 8493530 DOI: 10.1126/science.8493530]
16 **Izadpanah R**, Bunnell BA. Gene delivery to mesenchymal stem cells. *Methods Mol Biol* 2008; **449**: 153-167 [PMID: 18370090 DOI: 10.1007/978-1-60327-169-1_11]
17 **Evans CH**, Robbins PD, Ghivizzani SC, Herndon JH, Kang R, Bahnson AB, Barranger JA, Elders EM, Gay S, Tomaino MM, Wasko MC, Watkins SC, Whiteside TL, Glorioso JC, Lotze MT, Wright TM. Clinical trial to assess the safety, feasibility, and efficacy of transferring a potentially anti-arthritic cytokine gene to human joints with rheumatoid arthritis. *Hum Gene Ther* 1996; **7**: 1261-1280 [PMID: 8793551 DOI: 10.1089/hum.1996.7.10-1261]
18 **Sampara P**, Banala RR, Vemuri SK, Av GR, Gpv S. Understanding the molecular biology of intervertebral disc degeneration and potential gene therapy strategies for regeneration: a review. *Gene Ther* 2018; **25**: 67-82 [PMID: 29567950 DOI: 10.1038/s41434-018-0004-0]
19 **Ning H**, Lin G, Lue TF, Lin CS. Mesenchymal stem cell marker Stro-1 is a 75 kd endothelial antigen. *Biochem Biophys Res Commun* 2011; **413**: 353-357 [PMID: 21903091 DOI: 10.1016/j.bbrc.2011.08.104]

20 **Cole AG**. A review of diversity in the evolution and development of cartilage: the search for the origin of the chondrocyte. *Eur Cell Mater* 2011; **21**: 122-129 [PMID: 21305475 DOI: 10.22203/eCM.v021a10]

21 **Smith LJ**, Fazzalari NL. The elastic fibre network of the human lumbar anulus fibrosus: architecture, mechanical function and potential role in the progression of intervertebral disc degeneration. *Eur Spine J* 2009; **18**: 439-448 [PMID: 19263091 DOI: 10.1007/s00586-009-0918-8]

22 **Im GI**, Kim HJ. Electroporation-mediated gene transfer of SOX trio to enhance chondrogenesis in adipose stem cells. *Osteoarthritis Cartilage* 2011; **19**: 449-457 [PMID: 21251990 DOI: 10.1016/j.joca.2011.01.005]

23 **Beeravolu N**, Brougham J, Khan I, McKee C, Perez-Cruet M, Chaudhry GR. Human umbilical cord derivatives regenerate intervertebral disc. *J Tissue Eng Regen Med* 2018; **12**: e579-e591 [PMID: 27690334 DOI: 10.1002/term.2330]

24 **Iwamoto M**, Ohta Y, Larmour C, Enomoto-Iwamoto M. Toward regeneration of articular cartilage. *Birth Defects Res C Embryo Today* 2013; **99**: 192-202 [PMID: 24078496 DOI: 10.1002/bdrc.21042]

25 **Hodgkinson T**, Shen B, Diwan A, Hoyland JA, Richardson SM. Therapeutic potential of growth differentiation factors in the treatment of degenerative disc diseases. *JOR Spine* 2019; **2**: e1045 [PMID: 31463459 DOI: 10.1002/jsp2.1045]

26 **Hassan G**, Kasem I, Soukkarieh C, Aljamali M. A simple method to isolate and expand human umbilical cord derived mesenchymal stem cells: Using explant method and umbilical cord blood serum. *Int J Stem Cells* 2017; **10**: 184-192 [PMID: 28844128 DOI: 10.15283/ijsc17028]

27 **Perczel-Kovách K**, Hegedűs O, Földes A, Sangngoen T, Kálló K, Steward MC, Varga G, Nagy KS. STRO-1 positive cell expansion during Mosteogenic differentiation: A comparative study of three mesenchymal stem cell types of dental origin. *Arch Oral Biol* 2021; **122**: 104995 [PMID: 33278647 DOI: 10.1016/j.archoralbio.2020.104995]

28 **Lin G**, Liu G, Banie L, Wang G, Ning H, Lue TF, Lin CS. Tissue distribution of mesenchymal stem cell marker Stro-1. *Stem Cells Dev* 2011; **20**: 1747-1752 [PMID: 21208041 DOI: 10.1089/scd.2010.0564]

29 **Noort WA**, Kruisselbrink AB, in't Anker PS, Kruger M, van Bezooijen RL, de Paus RA, Heemskerk MH, Löwik CW, Falkenburg JH, Willemze R, Fibbe WE. Mesenchymal stem cells promote engraftment of human umbilical cord blood-derived CD34(+) cells in NOD/SCID mice. *Exp Hematol* 2002; **30**: 870-878 [PMID: 12160838 DOI: 10.1016/S0301-472X(02)00820-2]

30 **Ali SR**, Ahmad W, Naeem N, Salim A, Khan I. Small molecule 2'-deoxycytidine differentiates human umbilical cord-derived MSCs into cardiac progenitors in vitro and their in vivo xeno-transplantation improves cardiac function. *Mol Cell Biochem* 2020; **470**: 99-113 [PMID: 32415417 DOI: 10.1007/s11010-020-03750-6]

31 **Liu X**, Zhou L, Chen X, Liu T, Pan G, Cui W, Li M, Luo ZP, Pei M, Yang H, Gong Y, He F. Culturing on decellularized extracellular matrix enhances antioxidant properties of human umbilical cord-derived mesenchymal stem cells. *Mater Sci Eng C Mater Biol Appl* 2016; **61**: 437-448 [PMID: 26838870 DOI: 10.1016/j.msec.2015.12.090]

32 **Mo M**, Wang S, Zhou Y, Li H, Wu Y. Mesenchymal stem cell subpopulations: phenotype, property and therapeutic potential. *Cell Mol Life Sci* 2016; **73**: 3311-3321 [PMID: 27141940 DOI: 10.1007/s00018-016-2229-7]

33 **Wang ZH**, Li XL, He XJ, Wu BJ, Xu M, Chang HM, Zhang XH, Xing Z, Jing XH, Kong DM, Kou XH, Yang YY. Delivery of the Sox9 gene promotes chondrogenic differentiation of human umbilical cord blood-derived mesenchymal stem cells in an in vitro model. *Braz J Med Biol Res* 2014; **47**: 279-286 [PMID: 24652327 DOI: 10.1590/1414-431X20133539]

34 **McCoy EL**, Kawakami K, Ford HL, Coletta RD. Expression of Six1 homeobox gene during development of the mouse submandibular salivary gland. *Oral Dis* 2009; **15**: 407-413 [PMID: 19371398 DOI: 10.1111/j.1601-0825.2009.01560.x]

35 **Zhao Q**, Eberspaecher H, Lefebvre V, De Crombrugghe B. Parallel expression of Sox9 and Col2a1 in cells undergoing chondrogenesis. *Dev Dyn* 1997; **209**: 377-386 [PMID: 9264261 DOI: 10.1002/(SICI)1097-0177(199708)209:4<377::AID-AJA5>3.0.CO;2-F]

36 **Chimal-Monroy J**, Rodriguez-Leon J, Montero JA, Gañan Y, Macias D, Merino R, Hurle JM. Analysis of the molecular cascade responsible for mesodermal limb chondrogenesis: Sox genes and BMP signaling. *Dev Biol* 2003; **257**: 292-301 [PMID: 12729559 DOI: 10.1016/S0012-1606(03)00066-6]

37 **Goldring MB**, Tsuchimochi K, Ijiri K. The control of chondrogenesis. *J Cell Biochem* 2006; **97**: 33-44 [PMID: 16215986 DOI: 10.1002/jcb.20652]

38 **Hissnauer TN**, Baranowsky A, Pestka JM, Streichert T, Wiegandt K, Goepfert C, Beil FT, Albers J, Schulze J, Ueblacker P, Petersen JP, Schinke T, Meenen NM, Pörtner R, Amling M. Identification of molecular markers for articular cartilage. *Osteoarthritis Cartilage* 2010; **18**: 1630-1638 [PMID: 20950698 DOI: 10.1016/j.joca.2010.10.002]

39 **Sahu N**, Budhiraja G, Subramanian A. Preconditioning of mesenchymal stromal cells with low-intensity ultrasound: influence on chondrogenesis and directed SOX9 signaling pathways. *Stem Cell Res Ther* 2020; **11**: 6 [PMID: 31900222 DOI: 10.1186/s13287-019-1532-2]

40 **Zehentner BK**, Dony C, Burtscher H. The transcription factor Sox9 is involved in BMP-2 signaling. *J Bone Miner Res* 1999; **14**: 1734-1741 [PMID: 10491221 DOI: 10.1359/jbmr.1999.14.10.1734]

41 **Campbell DD**, Pei M. Surface markers for chondrogenic determination: a highlight of synovium-derived stem cells. *Cells* 2012; **1**: 1107-1120 [PMID: 24710545 DOI: 10.3390/cells1041107]

42 **Djouad F**, Delorme B, Maurice M, Bony C, Apparailly F, Louis-Plence P, Canovas F, Charbord P, Noël D, Jorgensen C. Microenvironmental changes during differentiation of mesenchymal stem cells towards chondrocytes. *Arthritis Res Ther* 2007; **9**: R33 [PMID: 17391539 DOI: 10.1186/ar2153]

43 **Sobajima S**, Kompel JF, Kim JS, Wallach CJ, Robertson DD, Vogt MT, Kang JD, Gilbertson LG. A slowly progressive and reproducible animal model of intervertebral disc degeneration characterized by MRI, X-ray, and histology. *Spine (Phila Pa 1976)* 2005; **30**: 15-24 [PMID: 15626975 DOI: 10.1097/01.brs.0000148048.15348.9b]

44 **Kushioka J**, Kaito T, Chijimatsu R, Okada R, Ishiguro H, Bal Z, Kodama J, Yano F, Saito T, Chung UI, Tanaka S, Yoshikawa H. The small compound, TD-198946, protects against intervertebral degeneration by enhancing glycosaminoglycan synthesis in nucleus pulposus cells. *Sci Rep* 2020; **10**: 14190 [PMID: 32843678 DOI: 10.1038/s41598-020-71193-6]

45 **Gruber HE**, Ingram J, Hanley EN Jr. An improved staining method for intervertebral disc tissue. *Biotech Histochem* 2002; **77**: 81-83 [PMID: 12083388 DOI: 10.1080/bih.77.2.81.83]

46 **Perez-Cruet M**, Beeravolu N, McKee C, Brougham J, Khan I, Bakshi S, Chaudhry GR. Potential of human nucleus pulposus-like cells derived from umbilical cord to treat degenerative disc disease. *Neurosurgery* 2019; **84**: 272-283 [PMID: 29490072 DOI: 10.1093/neuros/nyy012]

47 **Sive JI**, Baird P, Jeziorsk M, Watkins A, Hoyland JA, Freemont AJ. Expression of chondrocyte markers by cells of normal and degenerate intervertebral discs. *Mol Pathol* 2002; **55**: 91-97 [PMID: 11950957 DOI: 10.1136/mp.55.2.91]

48 **Meisel HJ**, Siodla V, Ganey T, Minkus Y, Hutton WC, Alasevic OJ. Clinical experience in cell-based therapeutics: disc chondrocyte transplantation A treatment for degenerated or damaged intervertebral disc. *Biomol Eng* 2007; **24**: 5-21 [PMID: 16963315 DOI: 10.1016/j.bioeng.2006.07.002]

49 **Longo UG**, Papapietro N, Petrillo S, Franceschetti E, Maffulli N, Denaro V. Mesenchymal stem cell for prevention and management of intervertebral disc degeneration. *Stem Cells Int* 2012; **2012**: 921053 [PMID: 22550520 DOI: 10.1155/2012/921053]

World Journal of Stem Cells

Submit a Manuscript: https://www.f6publishing.com

World J Stem Cells 2022 February 26; 14(2): 183-199

DOI: 10.4252/wjsc.v14.i2.183

ISSN 1948-0210 (online)

ORIGINAL ARTICLE

Basic Study

Extracellular vesicles from hypoxia-preconditioned mesenchymal stem cells alleviates myocardial injury by targeting thioredoxin-interacting protein-mediated hypoxia-inducible factor-1α pathway

Cheng-Yu Mao, Tian-Tian Zhang, Dong-Jiu Li, En Zhou, Yu-Qi Fan, Qing He, Chang-Qian Wang, Jun-Feng Zhang

Specialty type: Cell and tissue engineering

Provenance and peer review: Unsolicited article; Externally peer reviewed.

Peer-review model: Single blind

Peer-review report's scientific quality classification

Grade A (Excellent): A
Grade B (Very good): B, B
Grade C (Good): C, C
Grade D (Fair): 0
Grade E (Poor): 0

P-Reviewer: Abreu de Melo MI, Galderisi U, Kida YS, Prasetyo EP

Received: October 13, 2021
Peer-review started: October 13, 2021
First decision: November 8, 2021
Revised: November 29, 2021
Accepted: January 25, 2022
Article in press: January 25, 2022
Published online: February 26, 2022

Cheng-Yu Mao, Tian-Tian Zhang, Dong-Jiu Li, En Zhou, Yu-Qi Fan, Qing He, Chang-Qian Wang, Jun-Feng Zhang, Department of Cardiology, Shanghai Ninth People's Hospital affiliated to Shanghai Jiao Tong University School of Medicine, Shanghai 200010, China

Corresponding author: Jun-Feng Zhang, MD, PhD, Professor, Department of Cardiology, Shanghai Ninth People's Hospital affiliated to Shanghai Jiao Tong University School of Medicine, No. 280 Mohe Road, Baoshan District, Shanghai 200010, China.
junfengzhang9hos@163.com

Abstract

BACKGROUND

Extracellular vesicles (EVs) derived from hypoxia-preconditioned (HP) mesenchymal stem cells (MSCs) have better cardioprotective effects against myocardial infarction (MI) in the early stage than EVs isolated from normoxic (NC)-MSCs. However, the cardioprotective mechanisms of HP-EVs are not fully understood.

AIM

To explore the cardioprotective mechanism of EVs derived from HP MSCs.

METHODS

We evaluated the cardioprotective effects of HP-EVs or NC-EVs from mouse adipose-derived MSCs (ADSCs) following hypoxia *in vitro* or MI *in vivo*, in order to improve the survival of cardiomyocytes (CMs) and restore cardiac function. The degree of CM apoptosis in each group was assessed by the terminal deoxynucleotidyl transferase dUTP nick end-labeling and Annexin V/PI assays. MicroRNA (miRNA) sequencing was used to investigate the functional RNA diversity between HP-EVs and NC-EVs from mouse ADSCs. The molecular mechanism of EVs in mediating thioredoxin-interacting protein (TXNIP) was verified by the dual-luciferase reporter assay. Co-immunoprecipitation, western blotting, and immunofluorescence were performed to determine if TXNIP is involved in hypoxia-inducible factor-1 alpha (HIF-1α) ubiquitination and degradation *via* the chromosomal region maintenance-1 (CRM-1)-dependent nuclear transport pathway.

RESULTS

HP-EVs derived from MSCs reduced both infarct size (necrosis area) and apoptotic degree to a greater extent than NC-EVs from CMs subjected to hypoxia *in vitro* and mice with MI *in vivo*. Sequencing of EV-associated miRNAs showed the upregulation of 10 miRNAs predicted to bind TXNIP, an oxidative stress-associated protein. We showed miRNA224-5p, the most upregulated miRNA in HP-EVs, directly combined the 3′ untranslated region of TXNIP and demonstrated its critical protective role against hypoxia-mediated CM injury. Our results demonstrated that MI triggered TXNIP-mediated HIF-1α ubiquitination and degradation in the CRM-1-mediated nuclear transport pathway in CMs, which led to aggravated injury and hypoxia tolerance in CMs in the early stage of MI.

CONCLUSION

The anti-apoptotic effects of HP-EVs in alleviating MI and the hypoxic conditions of CMs until reperfusion therapy may partly result from EV miR-224-5p targeting TXNIP.

Key Words: Extracellular vesicles; Myocardial infarction; Mesenchymal stem cells; Hypoxia preconditioning; Thioredoxin-interacting protein; Hypoxia-inducible factor 1 alpha

Core Tip: Extracellular vesicles (EVs) from adipose-derived mesenchymal stem cells treated with hypoxia preconditioning improve tolerance toward myocardial infarction or hypoxic conditions and alleviate the degree of cardiomyocyte apoptosis until reperfusion therapy. The anti-apoptotic effects may result from EV miR-224-5p targeting thioredoxin-interacting protein (TXNIP) and subsequent TXNIP-mediated hypoxia-inducible factor-1 alpha ubiquitination and degradation *via* the chromosomal region maintenance-1-mediated nuclear transport pathway.

Citation: Mao CY, Zhang TT, Li DJ, Zhou E, Fan YQ, He Q, Wang CQ, Zhang JF. Extracellular vesicles from hypoxia-preconditioned mesenchymal stem cells alleviates myocardial injury by targeting thioredoxin-interacting protein-mediated hypoxia-inducible factor-1α pathway. *World J Stem Cells* 2022; 14(2): 183-199
URL: https://www.wjgnet.com/1948-0210/full/v14/i2/183.htm
DOI: https://dx.doi.org/10.4252/wjsc.v14.i2.183

INTRODUCTION

Myocardial infarction (MI) is an acute and fatal cardiovascular disease triggered by coronary occlusion, resulting ischemia-hypoxia of myocardial cells[1]. Despite significant progress in surgical treatment and medical therapy, MI remains remains a major cause of morbidity and mortality in clinical practice[2]. During the early period of MI, apoptosis is the predominant form of cardiomyocyte (CM) death[3]. However, if reperfusion therapy cannot be initiated in time to restore blood flow, initial apoptosis transitions into passive and irreversible necrosis[4]. Hence, patients with MI gain the greatest benefit from early intervention.

The molecular mechanisms underlying MI involve a double hit-related injury in CMs resulting from ischemia, hypoxia, and subsequent reoxygenation with reperfusion in infarcted tissue[5]. Sustained hypoxia and excessive mitochondrial reactive oxygen species (mROS) production are common triggers of myocardial apoptosis during early MI, which occur after the apoptosome activates caspase-3[6,7]. In addition, mROS and hypoxia-mediated upregulated thioredoxin-interacting protein (TXNIP)[8] interact with von Hippel–Lindau protein (pVHL) and hypoxia-inducible factor-1 alpha (HIF-1α) to promote the hypoxia-independent nuclear export and degradation of HIF-1α, hence weakening myocardial tolerance to hypoxia and eliciting anti-inflammatory responses[9]. The consequent activation of TXNIP and weakened tolerance to hypoxia both contribute to the larger number of CMs undergoing apoptosis and necrosis, which are difficult to reverse during the period from MI onset to reperfusion therapy[10]. Thus, due to CMs that are terminally differentiated and non-regenerative cells, the more CMs that die during the period before reperfusion, the worse the prognosis of MI[11]. Accordingly, despite some mechanisms remaining obscure, interference on TXNIP have been demonstrated to protect myocardial cells from hypoxic vulnerability, programmed death, and myocardial stunning caused by ischemia[12-14].

Mesenchymal stem cells (MSCs) are a heterogeneous population of multipotent stem cells, progenitors, and differentiated cells that are existed in most stromal tissues. MSCs possess immunoregulation effects and the function of remaining internal environment stabilization and cell repair. The

above-mentioned characteristics have become a cornerstone of the development of several potential therapeutic applications of MSCs, among which extracellular vesicles (EVs) derived from MSCs are the most promising[15,16]. EVs are cell-derived membranous particles, which contains membranous structures of 30-2000 nm in diameter, which are packaged and secreted by most types of cells, including MSCs, and microorganisms[17]. EVs mainly include exosomes and microvesicles which can regulate intracellular signal transduction by delivering proteins, mRNAs, and microRNAs (miRNAs) to targeting cells and tissues. EV carries homologous molecules from the mother cells and can adjust the biological functions of target cells, tissues, and organs, including differentiation, proliferation, migration, secretion, and death[18,19]. In turn, changes in the microenvironment and physiological state of EV-derived cells may influence the EV contents and their biological functions. Furthermore, a prevailing view is that the cellular origin of EVs significantly qualifies their biological function[20,21]. Accordingly, EVs derived from MSCs have potential in cardioprotection[22]. Thus, we determined if a preconditioned method would improve the cardioprotective effects of EVs derived from MSCs.

Because hypoxia preconditioning can enhance and strengthen the tolerance and adaptability of CMs to an anoxic environment, inflammation, and oxidative stress[23,24], the cardioprotective mechanism of EVs derived from hypoxia-preconditioned MSCs (HP-EVs) has not been fully elucidated in previous studies. We hypothesized that HP-EVs can protect CMs from ischemia and hypoxia much more effectively than EVs derived from normoxic MSCs (NC-EVs). For this purpose, EVs were extracted from mouse adipose-derived mesenchymal stem cells (ADSCs) which were pretreated with either normoxia or hypoxia preconditioning. Cardiac protection effects of HP and NC-EVs were measured *in vitro* and *in vivo*. Additionally, we explored the molecular, morphologic and phenotypic changes with regard to MI-triggered apoptosis in CMs and revealed the potential role for hypoxia-induced, EV-associated miRNAs in CM survival.

MATERIALS AND METHODS

MI and reperfusion mouse model

All animal care and procedures were approved by the Shanghai Ninth People's Hospital Institutional Ethics Committee (Shanghai, China). Animal experimental procedures were strictly performed and followed Directive 2010/63/EU. Eight-week-old male C57BL/6 mice were purchased from Shanghai Jessie Experimental Animal Co., Ltd. (Shanghai, China). Mice were fed standard mouse chow and water *ad libitum* under specific pathogen-free conditions (20-24 °C, 50%-60% humidity). All invasive procedures were performed under anesthesia. An anesthesia box with 2.5% isoflurane (RWD Life Science Co., Ltd., Shenzhen, China) was used to induce anesthesia for 3 min, and thereafter an animal anesthetic mask with 1.5%-2.0% isoflurane was administered in the anesthesia maintenance stage. Excess carbon dioxide inhalation was applied for euthanasia. A total of 80 healthy wild-type (WT) C57BL/6 male mice (20-24 g) were used for the experiments. The MI model was established as described by Gao *et al*[25]. Briefly, the left coronary artery (LCA) was ligated with a slipknot for 30, 60, 120, 240, and 480 min to establish a time-myocardial injury relationship. Then, the slipknot was released to achieve reperfusion therapy. Successful MI was confirmed based on dynamic electrocardiograph changes (ST-segment elevation). Sham-operated mice underwent the same procedure, with the exception that the left knot on the LCA was loosened.

Transthoracic echocardiography

Echocardiography was performed to assess (M mode) ejection fraction (EF) and fractional shortening (FS) in three sequential cardiac cycles on the third day after MI surgery using echocardiography (Vevo 770 High-Resolution Imaging System; Visualsonics Inc., Toronto, Canada).

Evaluation of area at risk and infarct size

At 12 h after loosening the knot on the LCA, the chest wall was re-opened under 1.5-2% isoflurane anesthesia to expose the heart. Then, the LCA was re-ligated and the aortic arch was clipped. Next, 1% Evans Blue [normal saline (NS) as the solvent] was retrogradely injected through the ascending aorta, and the aortic arch was clipped until the non-infarction area turned blue. Then, the heart was removed and harvested, washed in NS, and sliced horizontally (parallel to the short axis of the heart) below the level of ligation. Each piece was approximately 1 mm thick. All tissue pieces were immediately incubated in 1.5% 2,3,5-triphenyltetrazolium chloride (TTC) for 20 min at 37 °C [phosphate-buffered saline (PBS) as the solvent]. The infarct area and area at risk (AAR) zone were calculated by Image-Pro Plus 6.0 software. Infarct size (IS)/AAR × 100% and AAR/left ventricle (LV) area × 100% were assessed.

Isolation and culture of mouse ADSCs

ADSCs were isolated from the adipose tissue of C57BL/6 mice as previously described[26]. The characterization of ADSCs was performed by flow cytometry analyses of cluster of differentiation 34 (CD34), CD105, and CD106 (negative controls) and CD29, CD45, and CD90 (positive cell surface markers).

Isolation and culture of neonatal mouse CMs

Primary neonatal mouse CMs were extracted from approximately 150 1-day-old neonatal C57BL/6 mice as previously described[27]. Briefly, 75% ethanol solution was used to disinfect the neonatal mice for no more than 1 min. Then, chests were opened with the hearts quickly clipped, cut into pieces (approximate volume of 1 mm^3), and placed in PBS at 4 °C. The tissues were digested in 0.125% trypsin and 0.0075 g/mL collagenase IV diluted in PBS [without fetal bovine serum (FBS)] at 4 °C overnight. The supernatant was collected and centrifuged at 200 × *g* for 5 min. Then, the tissues and cells were resuspended and cultured in complete medium [Dulbecco's Modified Eagle Medium (DMEM)-high glucose containing 5% FBS at 37 °C, 5% CO_2] for 2 h to induce fibroblast attachment before CMs. The remaining supernatant (only containing CMs) was plated in new 2-cm dishes at a density of 1 × 10^6 cells/mL for a subsequent study. α-actinin staining was applied to identify the purity of the CMs. See Figure 1A for a flow chart of the isolation procedures for ADSCs and CMs.

In vitro CM hypoxia model

An *in vitro* model of mouse CM hypoxia was established by incubating cells in oxygen-free, low-glucose DMEM in a controlled atmosphere (5% CO_2, 95% N_2) for 2 h. Then, the incubation conditions were converted to normoxia FBS-free medium for 12 h. After treatment, the myocardial cells were collected and analyzed.

Hypoxic preconditioning of ADSCs

ADSCs were seeded in complete medium (DMEM/F12 with 10% EV-free FBS) for 24 h. Oxygen-free DMEM/F12 medium previously incubated overnight with 100% N_2 was prepared in advance. Hypoxic preconditioning was performed by exposing the cells to five cycles of hypoxia (60 min in oxygen-free DMEM/F12 medium and 5% CO_2, 95% N_2 cultured atmosphere) with intermittent reoxygenation (30 min in normal oxygen-containing DMEM/F12 medium and 5% CO_2, 75% N_2, 20% O_2 cultured atmosphere) in a hypoxic chamber (Forma-1025 Anaerobic System; Thermo Fisher Scientific, Waltham, MA, United States). After hypoxic preconditioning, ADSCs were cultured in serum-free DMEM/F12 medium in a normoxic environment (5% CO_2), and the supernatant was collected for EV extraction after 24 h.

Isolation and characterization of EVs

EVs were extracted from cultured ADSCs (approximately 10^7 *per* dish) in the absence or presence of exposure to hypoxic preconditioning by differential velocity centrifugation. Briefly, the cell culture supernatant was centrifuged at 2,000 × *g* for 30 min at 4 °C to remove cell debris. Then, the supernatant was collected and centrifuged at 100000 × *g* for 70 min to precipitate the EVs. The supernatant was discarded to remove contaminating proteins and EVs were re-suspended in PBS. Size distribution and concentration of the EVs were determined using the NanoSight NS300 Instrument (Malvern Instruments, Malvern, United Kingdom), and EV morphology was assessed by transmission electron microscopy (TEM). Expression of the EV surface markers [tumor susceptibility gene 101 (TSG101), CD63, CD81] was detected by western blotting.

EV injections

Eighty mice were randomly divided into the following four groups (n = 20 each): sham (no MI, control), MI, NC-EV (NC-EVs plus MI), and HP-EV (HP-EVs plus MI), which ensured a sample size of more than five mice *per* assay. In the NC-EV and HP-EV groups, EVs were administered at a dose of 1 μg/1 g body weight *via* injecting into the border zone of the infarcted heart at three sites immediately post-MI surgery.

Confirmation of EV uptake by CMs

EVs were labeled with PKH26 (Cat. MINI26; Sigma-Aldrich, St. Louis, MO, United States), and mouse CMs were labeled with phalloidin (Cat. A12379s; Thermo Fisher Scientific). Then, 500 μL EV solution was stained with 5 mL PKH26 and added to a culture of CMs, EVs, and cells followed by a 2-h incubation to allow endocytosis by mouse CMs. The CMs were washed three times with PBS and then fixed in 4% paraformaldehyde for 20 min, after which the nucleus was stained with Hoechst. An inverted microscope was used to detect the EVs phagocytized in the CMs.

Cell transfection

HEK 293T cells were transfected with miR-224-5p mimics and the TXNIP dual-luciferase plasmid (Ribobio, Shanghai, China). H9c2 CMs stably overexpressing TXNIP and TXNIP-L294A mutant were established by lentivirus (synthesis by ZoRin, Shanghai, China). ADSCs overexpressing miR-224 and miR224-negative control (NC) were infected with adeno-associated virus (AAV) containing the miR-224 or miR-224-NC sequence (RiboBio), and miR-224 was knocked out by CRISPR/Cas9 in ADSCs (RiboBio).

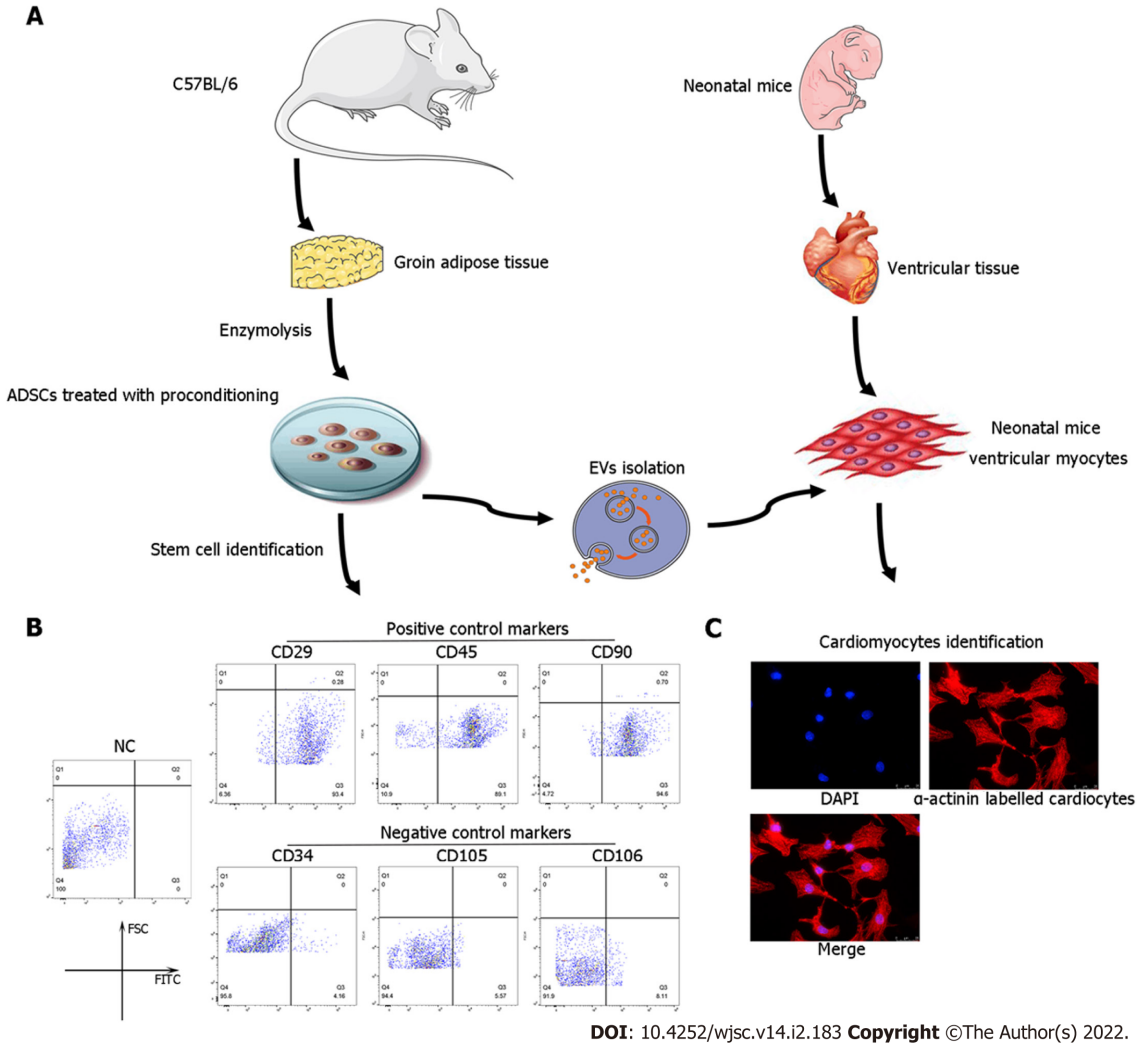

DOI: 10.4252/wjsc.v14.i2.183

Figure 1 Identification of adipose-derived mesenchymal stem cells and neonatal mouse cardiomyocytes. A: Flow chart of extracellular vesicles and neonatal mouse cardiomyocyte (CM) isolation; B: Characterization of adipose-derived mesenchymal stem cells (ADSCs) was performed by flow cytometry analyses of cluster of differentiation 34 (CD34), CD105, and CD106 (negative controls) and CD29, CD45, and CD90 (positive cell surface markers); C: Identification of neonatal mouse CMs, which were specifically stained with α-actinin. CM: Cardiomyocyte; ADSC: Adipose-derived mesenchymal stem cells; CD: Cluster of differentiation.

Dual luciferase reporter assay

First, miR-224-5p mimics and PGL3 Luciferase plasmids containing WT, NC, or mutated TXNIP 3′-untranslated region (3′-UTR) sequences were co-transfected in HEK 293T cells, which were cultured in 24-well plates and co-transfected at approximately 70% confluence. After 12 h, the cells were re-cultured in 96-well luciferase assay plates. The ratio of firefly to Renilla luciferase activity was detected after 36 h using the Dual-GLO™ Luciferase Assay System (Cat. E2920; Promega, Madison, WI, United States).

Quantitative polymerase chain reaction and western blotting

We used the RNAiso Plus extraction reagent (Cat. 9108; Takara, Dalian, China) to extract EV-associated RNA. Stem-loop primers (Ribobio Biotech) were used to generate the cDNA of miRNA. The cDNA was amplified by SYBR green-based quantitative polymerase chain reaction (qPCR). U6 small nuclear RNA was used as the internal control. Cardiac tissues and CM protein were extracted using radioimmunoprecipitation assay buffer. TSG101, CD63, CD81, TXNIP, HIF1, and ubiquitin antibodies were supplied by Abcam (Cambridge, MA, United States); α-tubulin was supplied by Cell Signaling Technology (Danvers, MA, United States).

Statistical analyses

SPSS 19.0 software was used for the data analyses (IBM Corp., Armonk, NY, United States). Whether the data fit the normal distribution was assessed by the Shapiro-Wilk test. Categorical variables were analyzed by the Pearson's chi-square test ($n \geq 5$) or Fisher's exact test ($n < 5$) with subsequent multiple comparisons using Bonferroni correction. One-way analysis of variance with subsequent post-hoc multiple comparisons test (Student-Newman-Keuls test) was applied for continuous variables. The

Kruskal–Wallis test was applied for nonparametric testing of multiple independent samples, and a Dunn-Bonferroni test used for post-hoc comparisons.

RESULTS

Characterization of ADSCs, ADSC-derived EVs, and mouse CMs

ADSCs isolated from mouse adipose tissue were identified by using cell surface markers of stem cells. The positive cell surface markers were CD29, CD45, and CD90 which demonstrated positive expression (> 95%) in flow cytometry assessment. Likewise, negative cell surface markers(CD34, CD105, and CD106) revealed low/negative expression (Figure 1B). Subsequently, neonatal mouse CMs were identified *via* α-actinin staining (Figure 1C). Sequential supercentrifugation was adapted to gain EVs from supernatant of ADSCs. TEM and the NanoSight Instrument were applied to verify the isolated EVs (Figure 2A and B). Results showed that the isolated EVs had a average diameter of 115 nm. Western blot assay revealed that EVs expressed three EV-associated markers: CD63, CD81, and TSG101 (Figure 2C). CMs' endocytosis of EVs was verified by PKH26-stained EVs detected *via* fluorescence microscopy (Figure 2D).

HP-EVs reduce myocardial injury in the early stage of MI and hypoxia

To access the temporal relationship of HP-EV cardioprotective effects *in vitro* and *in vivo*, MI models were established and LCAs were ligated for 0.5, 1, 2, 4, and 8 h followed by reperfusion for 12 h. Evans Blue/TTC staining was used to evaluate the area of viable myocardium in the HP-EV and MI groups *in vivo* (Figure 3A). The results demonstrated that, within the first 2 h, HP-EVs contributed to significant cardiomyocyte survival compared to the MI group, which peaked after 1 h of LCA ligation followed by 12 h of reperfusion (HP-EVs *vs* MI; $P = 0.0021$). Similarly, the Cell Counting Kit-8 assay was used to study the temporal relationship of HP-EV cardioprotective effects *in vitro* (Figure 3B). Neonatal mouse CMs were exposed to hypoxic conditions for 0.5, 1, 2, 4, and 8 h followed by 12 h of reoxygenation. CMs treated with HP-EVs showed significant cardioprotective effects against hypoxia compared to the control group, which peaked at 2 h (HP-EV *vs* hypoxia-CMs; $P = 0.0009$) and decreased with a prolonged period of hypoxia. Thus, 2-h hypoxia *in vitro* and 1-h MI *in vivo* were applied to subsequent experiments.

HP-EVs fail to alleviate myocardial injury in CMs subjected to a long period of hypoxia

We evaluated the cardioprotective effects of HP-EVs in improving heart function and alleviating the degree of CM apoptosis after a long period of hypoxia and ischemia (8 h of hypoxia for CMs and 8 h of LCA ligation in mice). The cardioprotective effects of HP-EVs did not reduce apoptosis nor improve heart function after a long period of hypoxia or ischemia ($P = 0.400$ and $P = 0.7136$ for CM apoptosis *in vitro*, Figure 4A and B; $P = 0.1519$ for myocardial apoptosis *in vivo*, Figure 4C; $P = 0.486$ for EF% and $P = 0.785$ for FS%, Figure 4D). These results indicated that the cardioprotective effects of HP-EVs might decrease with prolonged ischemia or hypoxia. Thus, in the case of late-stage apoptosis and irreversible necrosis induced by protracted and prolonged ischemia or hypoxia, ADSC-derived EVs (ADSC-EVs) contribute little to ameliorating myocardial injury, which is consistent with our conventional understanding that patients with MI gain the greatest benefit from early intervention.

ADSC-EVs reduce apoptosis in CMs subjected to hypoxia

To determine the anti-apoptotic effects of ADSC-EVs in preventing or attenuating MI-triggered apoptosis in CMs, apoptosis assays were performed by the Annexin V/PI, terminal deoxynucleotidyl transferase dUTP nick end-labeling (TUNEL), and caspase-3 activation assays in cultured neonatal mouse CMs subjected to hypoxia and were exposed to NC-EVs or HP-EVs prior to hypoxia. As is revealed in Figure 5A, pretreatment with NC-EVs decreased the apoptotic rate of CMs [$P = 0.0021$ compared to the hypoxia/reoxygenation (H/R) group]. However, the downregulation of apoptosis was significantly higher after exposure to HP-EVs ($P = 0.0080$ compared to NC-EVs). Over again, the cardioprotective effects were significantly greater in HP-EV-treated cells as determined by the TUNEL assay ($P = 0.0001$ compared to the H/R group; $P = 0.0291$ compared to NC-EVs) (Figure 5B). Meanwhile, as shown in Figure 5C, caspase-3 activation assays demonstrated a reduced trend in the enzymatic activity of caspase-3 after CM treatment with ADSC-EVs, with HP-EVs eliciting more significant anti-apoptotic effects ($P = 0.0001$ compared to the H/R group; $P = 0.0001$ compared to NC-EVs).

ADSC-EVs ameliorate myocardial damage in a mouse model of MI

To assess cardioprotective effects in alleviating MI-triggered myocardial injury of ADSC-EVs *in vivo*, *in situ* apoptosis was evaluated in infarct tissues by the TUNEL assay. Figure 6A demonstrates that the degree of *in situ* apoptosis was significantly improved in the NC-EV and HP-EV groups. Moreover, the HP-EV group had a greater ameliorative apoptotic rate than the NC-EV group. Cardiac IS and AAR were evaluated in ischemic myocardium injected with ADSC-EVs post-MI models establishment. As is

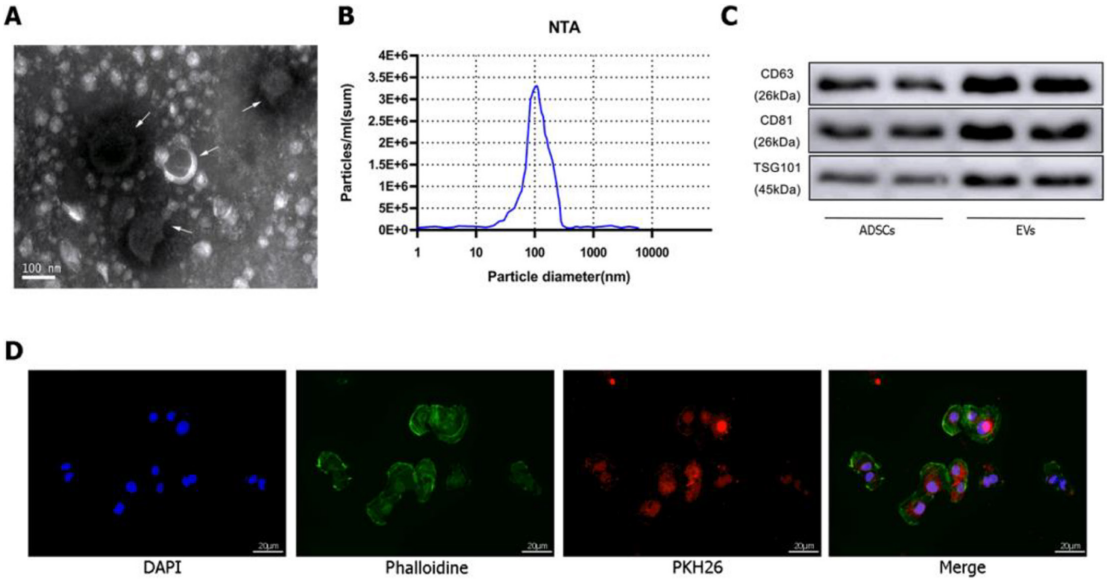

DOI: 10.4252/wjsc.v14.i2.183

Figure 2 Identification of extracellular vesicles. A: Transmission electron microscopy characterization of extracellular vesicles (EVs); B: Size distribution by intensity was detected using the NanoSight Instrument; C: EV biomarkers cluster of differentiation 63 (CD63), CD81, and tumor susceptibility gene 101 were identified by western blotting of adipose-derived mesenchymal stem cell (ADSC)-derived EVs and ADSCs; D: EV tracer assay was used to identify exosomes phagocytosed by cardiomyocytes. ADSC: Adipose-derived mesenchymal stem cell; EV: Extracellular vesicles.

revealed in Figure 6B, among the sham, MI, NC-EV, and HP-EVs groups, AAR/LV values were similar (LCA was re-ligated prior to Evans Blue staining to calculate the AAR/LV values). Significantly, the NC-EV and HP-EV groups showed markedly mitigated post-MI IS compared to the ischemia-reperfusion (IR) group. Once again, HP-EV group demonstrated a conspicuously mitigated IS region (NC-EV *vs* IR, $P = 0.0115$; HP-EV *vs* NC-EV, $P = 0.0213$).

ADSC-EVs improve cardiac function after MI reperfusion injury

Echocardiography on Day 3 post-MI revealed that EF and LV fractional shortening were markedly turned better of cardiac systolic function that treated with ADSC-EVs (Figure 6C), particularly HP-EVs (EF Day 3: NC-EVs *vs* IR, $P = 0.022$; HP-EVs *vs* NC-EVs, $P = 0.030$; FS Day 3: NC-EVs *vs* IR, $P = 0.031$; HP-EVs *vs* NC-EVs, $P = 0.017$).

Hypoxia preconditioning upregulates miR-224-5p, a potential TXNIP regulator, in ADSC-EVs

To discover the molecular mechanism of much more significant cardioprotective effects of HP-EVs against ischemia and hypoxia-induced CMs damage, sequencing analysis was applied to reveal nucleic acid molecular (miRNA) expression differences between NC-EVs and HP-EVs. The result of sequencing detected 88 miRNAs expression differences between HP-EVs and NC-EVs. Further analysis revealed 10 of them were potentially predicted to bind with TXNIP by the TargetScan and miRanda algorithms in the Encyclopedia of RNA Interactomes database (Figure 7A). The expression differences of these miRNAs were verified by quantitative polymerase chain reaction (Figure 7A). Then we chose miR-224-5p as candidate for further study for its most markedly upregulated expression among the 10 miRNAs in HP-EVs. In the follow-up verification work we used the dual-luciferase reporter assay to determine that miR-224-5p directly bind to TXNIP WT-3′-UTR region of its mRNA to inhibit translation process of TXNIP ($P = 0.0026$; Figure 7B).

ADSC-EV miR-224-5p ameliorates HIF-1α degradation and hypoxia-induced CM apoptosis by targeting TXNIP

To assess whether ADSC-EV miR-224-5p can attenuate the degradation of HIF-1α and hypoxia-induced apoptosis in CMs by inhibiting TXNIP, we established AAV-miR-224 ADSCs and ADSCs with miR-224 knocked out to obtain miR-224-5p overexpressing EVs and miR-224-5p knockout EVs, respectively. TXNIP, HIF1-αexpression level and apoptotic degree of CMs were evaluated on hypoxia-treated neonatal mouse CMs pre-processed with EVs derived from ADSCs, ADSCs overexpressing miR-224, and ADSCs with miR-224 knocked out by CRISPR/Cas9. As shown in Figure 7C, pre-treatment with EVs derived from ADSCs overexpressing miR-224 Led to the significant suppression of TXNIP expression relative to NC-ADSCs ($P = 0.0006$) and increase in HIF-1α expression ($P < 0.0001$). In EVs derived from ADSCs with miR-224 knocked-out, TXNIP expression was not inhibited ($P = 0.0018$) and HIF-1α expression was decreased ($P = 0.0002$) compared to the NC group. Furthermore, Annexin V/PI

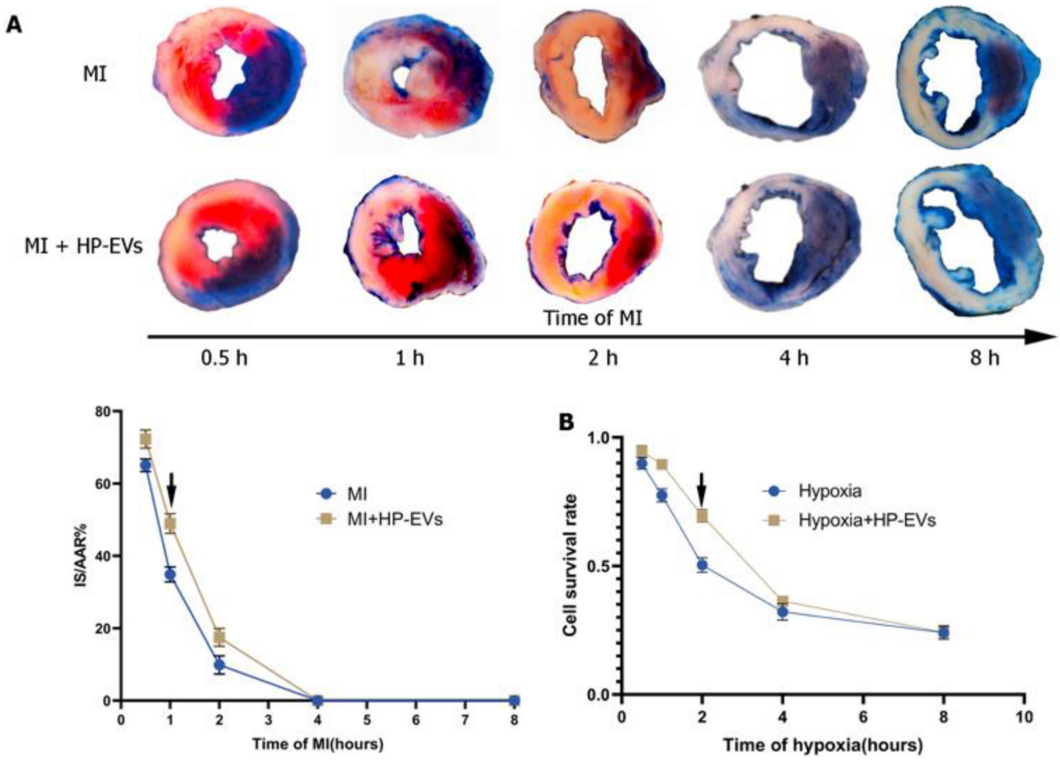

DOI: 10.4252/wjsc.v14.i2.183 **Copyright** ©The Author(s) 2022.

Figure 3 Evaluation of the temporal relationship of the cardioprotective effects of hypoxia-preconditioned extracellular vesicles. A: Temporal relationship of the cardioprotective effects of hypoxia-preconditioned extracellular vesicles (HP-EVs) *in vivo*. Myocardial infarction (MI) models were established with left coronary artery ligation for 0.5, 1, 2, 4, and 8 h followed by 12 h of reperfusion. Evans Blue/2,3,5-triphenyltetrazolium chloride staining was used to evaluate the area of viable myocardium in the HP-EV and MI groups (n = 5); B: Temporal relationship of the HP-EV cardioprotective effects *in vitro*. Hypoxia injury models were established for 0.5, 1, 2, 4, and 8 h of hypoxia followed by 12 h of reoxygenation. Cell Counting Kit-8 assay was used to evaluate the cell survival rate in the HP-EV and hypoxia groups (x axis was time of hypoxia, y axis was the value of absorbance of experimental/control group, which reflected the survival rate of cells in the experimental condition; n = 5). The arrows indicate the most significant difference, and the corresponding time points were adopted for subsequent research. MI: Myocardial infarction; HP-EV: Hypoxia-preconditioned extracellular vesicles.

staining indicated, as expected, a significant improvement in apoptosis in CMs treated with miR224-5p-overexpressing EVs compared to NC-EV-treated cells (P = 0.0002; Figure 7D). This effect was significantly reversed by miR-224-5p knockout EVs compared to the NC group (P = 0.0059).

TXNIP regulates the ubiquitination of HIF-1α in a chromosomal region maintenance-1-dependent manner

TXNIP binds to the β-domain of pVHL and promotes the degradation of HIF1α independently of hypoxia. A functional nuclear export signal (NES) in the chromosomal region maintenance-1 (CRM-1)-binding site (Leu294) of TXNIP is important for the formation of the TXNIP-pVHL-HIF-1α complex[9]. To further explore the mechanism by which TXNIP regulates HIF-1α degradation in CMs, TXNIP-overexpressing and TXNIP L294A mutant H9c2 cell lines were established (Cyagen Biosciences, Guangzhou, China). Our results demonstrated that the nuclear expression of HIF-1α was abolished in TXNIP-overexpressing cells in hypoxia. In TXNIP L294A mutant cells, the nuclear expression of HIF-1α was recovered. After treatment with leptomycin B, which specifically blocks CRM1-dependent nuclear export and is extensively used to investigate this process, TXNIP-induced HIF-1α degradation was inhibited (Figure 8A). Western blot analysis revealed that TXNIP induced the degradation of HIF-1α in H9c2 CMs in the presence and absence of hypoxia (Figure 8B). Moreover, the increased ubiquitination of HIF-1α induced by overexpressed TXNIP was detected (Figure 8C and D). However, this effect was not detected in TXNIP L294A mutant cells, which indicated that, as a functional NES binding site of CRM-1 in TXNIP, TXNIP-mediated ubiquitination and degradation of HIF-1α by the proteasome might be dependent on CRM-1-mediated nuclear transport and stabilization.

DISCUSSION

EVs are biocompatible, high-tissue penetrating, nano-sized secreted vesicles containing many types of biomolecules, including proteins, RNAs, DNAs, lipids, and metabolites. Their low immunogenicity and

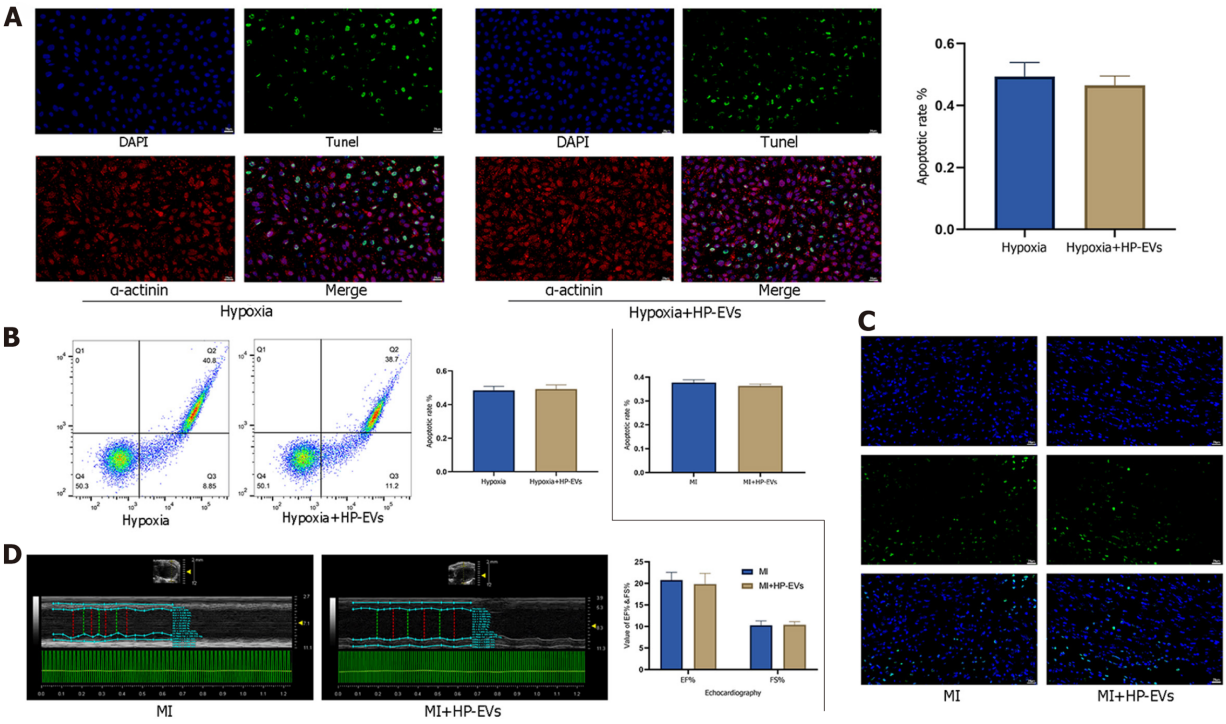

DOI: 10.4252/wjsc.v14.i2.183 **Copyright** ©The Author(s) 2022.

Figure 4 Cardioprotective effects of hypoxia-preconditioned extracellular vesicles after long periods of hypoxia and ischemia. A: Degree of *in situ* apoptosis of cardiomyocytes (CMs) in hypoxia and hypoxia-preconditioned extracellular vesicle (HP-EV) groups after a long period (8 h) of hypoxia followed by 12 h of reoxygenation, as determined by the terminal deoxynucleotidyl transferase dUTP nick end-labeling (TUNEL) assay (n = 5); B: Degree of CM apoptosis in the hypoxia and HP-EVs groups after a long period (8 h) of hypoxia followed by 12 h of reoxygenation, as determined by flow cytometry (n = 5); C: Degree of *in situ* apoptosis of CMs in the myocardial infarction (MI) and HP-EVs groups after a long period of MI [left coronary arteries (LCAs) were ligated for 8 h followed by 12 h of reperfusion], as determined by the TUNEL assay (n = 5); D: Echocardiography was used to examine the heart function of the MI and HP-EVs groups on Day 3 after a long period of MI (LCAs were ligated for 8 h followed by 12 h of reperfusion); ejection fraction and fractional shortening were detected (n = 5). MI: Myocardial infarction; HP-EV: Hypoxia-preconditioned extracellular vesicles.

ability to functionally modify recipient cells by transferring diverse bioactive constituents make them an excellent candidate for a next-generation drug delivery system[20,28,29]. Despite the tremendous achievements, clinical application of EVs remains challenging for the following reasons. There is no universally accepted gold standard for EVs extraction methods to meet clinical application, biosafety concerns regarding editing and modification of EVs, and the question of whether long-term clinical use of EVs could produce unacceptable side effects has not been resolved[30,31]. Thus, the goal of this study was to improve the therapeutic efficacy of MSC-derived EVs against MI-induced CM death by using a safe hypoxia preconditioning method *in vitro*, and to explore the mechanisms of the protective effects of EVs.

The idea of hypoxia preconditioning of ADSCs came from remote ischemic preconditioning (RIPC), which is a novel method where ischemia followed by reperfusion of one organ is believed to protect remote organs either due to release of biochemical messengers in the circulation or activation of nerve pathways, resulting in release of messengers that have a protective effect[32]. With regard to the underlying mechanism of RIPC in cardioprotection, whether such preconditioning efficacy may extended application *in vitro* to provide a promising treatment by using EVs generated by ADSCs exposure to hypoxia preconditioning[33]. For example, EVs generated by HP MSCs were adapted to improve traumatic spinal cord injury *via* its paracrine mechanisms and unfolded a myocardium preservation effect against ischemia-reperfusion injury[34,35]. Thus, we proposed to explore whether an *in vitro* RIPC process can change contents of EVs derived from ADSCs to strengthen its intrinsical cardioprotective potential. Our results revealed that HP-EVs elicited more significant inhibiting effect of MI-triggered CM death than NC-EVs. Notably, HP-EVs were changed its contained miRNA expression (88 miRNA) after ADSCs exposure to preconditioning, 10 of these upregulated miRNA are putative regulators of inflammasome activation based on the predicted binding affinity for TXNIP. We focused on the most upregulated miRNA (*i.e.* miR-224-5p) and verified both direct binding to TXNIP and a critical role for this interaction in the inhibition of MI-induced CM death.

Additionally, our results also objectively illustrated the fact that the timely opening of the infarction vessels and reducing the apoptosis of CMs during MI are equally crucial. Once delayed treatment occurs, CMs would change from a reversible injury state to necrosis, apoptotic necrosis, fibrous tissue replacement, and eventually to ventricular remodeling, which is often irreversible. Hence, for the

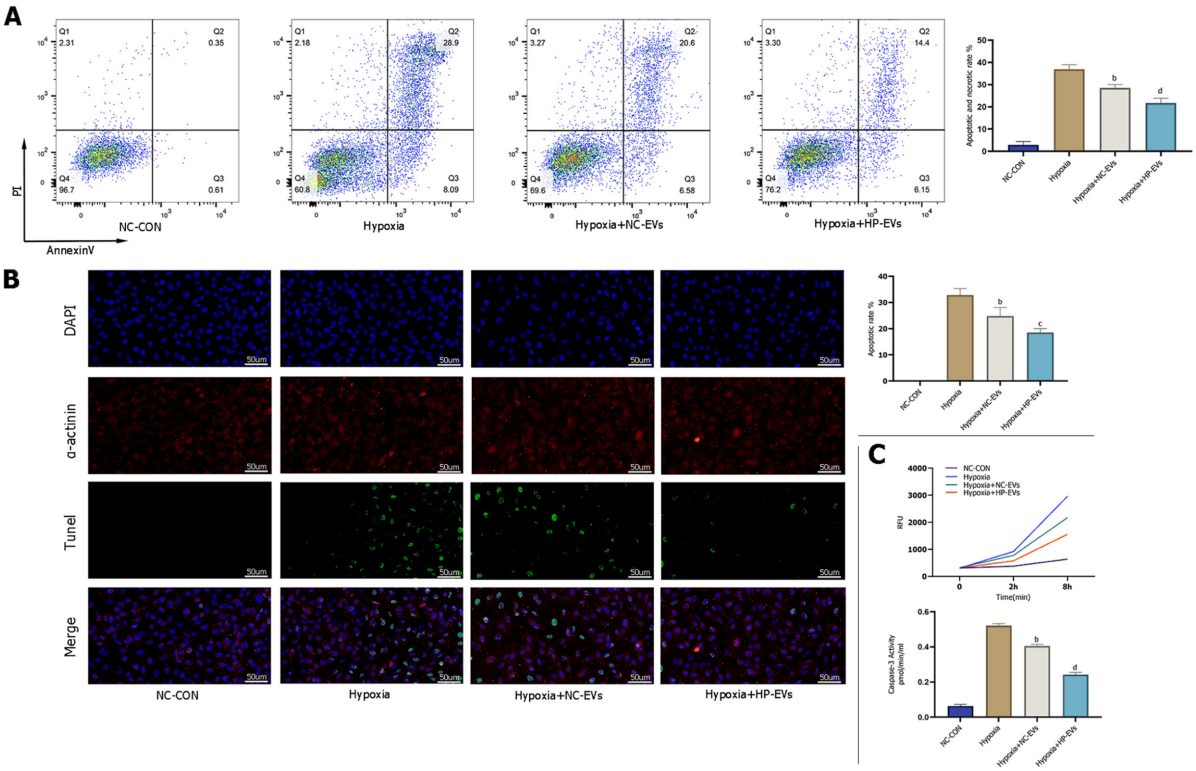

DOI: 10.4252/wjsc.v14.i2.183 **Copyright** ©The Author(s) 2022.

Figure 5 Hypoxia-preconditioned extracellular vesicles alleviated hypoxia/reoxygenation-induced apoptosis *in vitro*. A: Degree of cardiomyocyte (CM) apoptosis in control, hypoxia, normoxic extracellular vesicle (NC-EV), and hypoxia-preconditioned EV (HP-EV) groups after 2 h of hypoxia followed by 12 h of reoxygenation, as determined by the Annexin V/PI assay (n = 5); B: Degree of CM apoptosis in control, hypoxia, NC-EV, and HP-EV groups after 2 h of hypoxia followed by 12 h of reoxygenation, as determined by the terminal deoxynucleotidyl transferase dUTP nick end-labeling assay (n = 5); C: Caspase-3 activity of CMs in the control, hypoxia, NC-EV, and HP-EV groups after 2 h of hypoxia followed by 12 h of reoxygenation (n = 5). All data are expressed as the mean ± SD. $^{a}P < 0.05$, $^{b}P < 0.01$ compared with Hypoxia group; $^{c}P < 0.05$, $^{d}P < 0.01$ compared with Hypoxia + NC-EVs group. HP-EV: Hypoxia-preconditioned extracellular vesicles; NC-EV: Normoxic extracellular vesicle.

treatment of MI, on the one hand, we should emphasize timely reperfusion therapy; on the other hand, we should preserve more CMs without irreversible injury, even death, until the moment of artery recanalization to maintain overall heart function after reperfusion therapy by enhancing hypoxia tolerance. In this study, HP-EVs exhibited a significant cardioprotective effect against aggravated apoptosis in MI caused by hypoxia and ischemia. Mechanistically, the benefit of CMs was mainly derived from effective hypoxia tolerance induced by HP-EVs.

The hypoxia tolerance of CMs induced by HP-EVs revealed that the HIF-1 transcription factor partly contributed to this benefit. HIF-1, of which the active subunit 1α undergoes proteasomal oxygen-dependent degradation, has an essential cardioprotective role and is a key mediator of the adaptability of the myocardium to hypoxia[36]. Under aerobic conditions, hydroxylated HIF-1α is recognized by pVHL, which combines with HIF-1α in a ubiquitin ligase form to be exported into the cytoplasm, where HIF-1α is degraded. By contrast, hypoxia promotes the accumulation of unhydroxylated HIF-1α and translocation to the nucleus to initiate transcriptional activity[37]. The role of HIF-1 in ischemic cardiomyopathy is different from its role in mediating oxygen homeostasis, inflammation, autoimmunity, and tumor metastasis under hypoxic conditions[38]. In MI, hypoxia and slight mROS generation induced by the unstable membrane potential of mitochondria, which are two independent factors that increase TXNIP expression in CMs, expedite the export and degradation of HIF-1α through the pro-oxidative stress function of TXNIP[39,40]. Considering that CMs contain a large number of mitochondria, once ischemia and hypoxia occur, mitochondria dysfunction induces the high expression of TXNIP and high level of HIF-1α degradation, which decreases the tolerance of hypoxia of CMs, accelerating their death. Clinically, if the duration of the MI exceeds its 12 h-therapeutic time window or time from first medical contact to re-opening blocked blood vessels, which was defined as "90 min door-to-balloon time", CMs would enter an irreversible process of death, when even reperfusion therapy did not help[40,41]. It is assumed that reperfusion therapy can be performed in a fixed time period; thus, therapies that facilitate CM survival from onset of MI to reperfusion therapy (elevating the hypoxia tolerance of CMs in this fixed time period) are particularly significant. Moreover, when reperfusion/reoxygenation therapy is delayed or prolonged, enhancing the hypoxia tolerance of CMs may be an ideal choice in order to preserve more CMs that cannot regenerate rather than waiting for irreversible injury to occur before treatment. Thus, increasing hypoxia tolerance and timely reperfusion

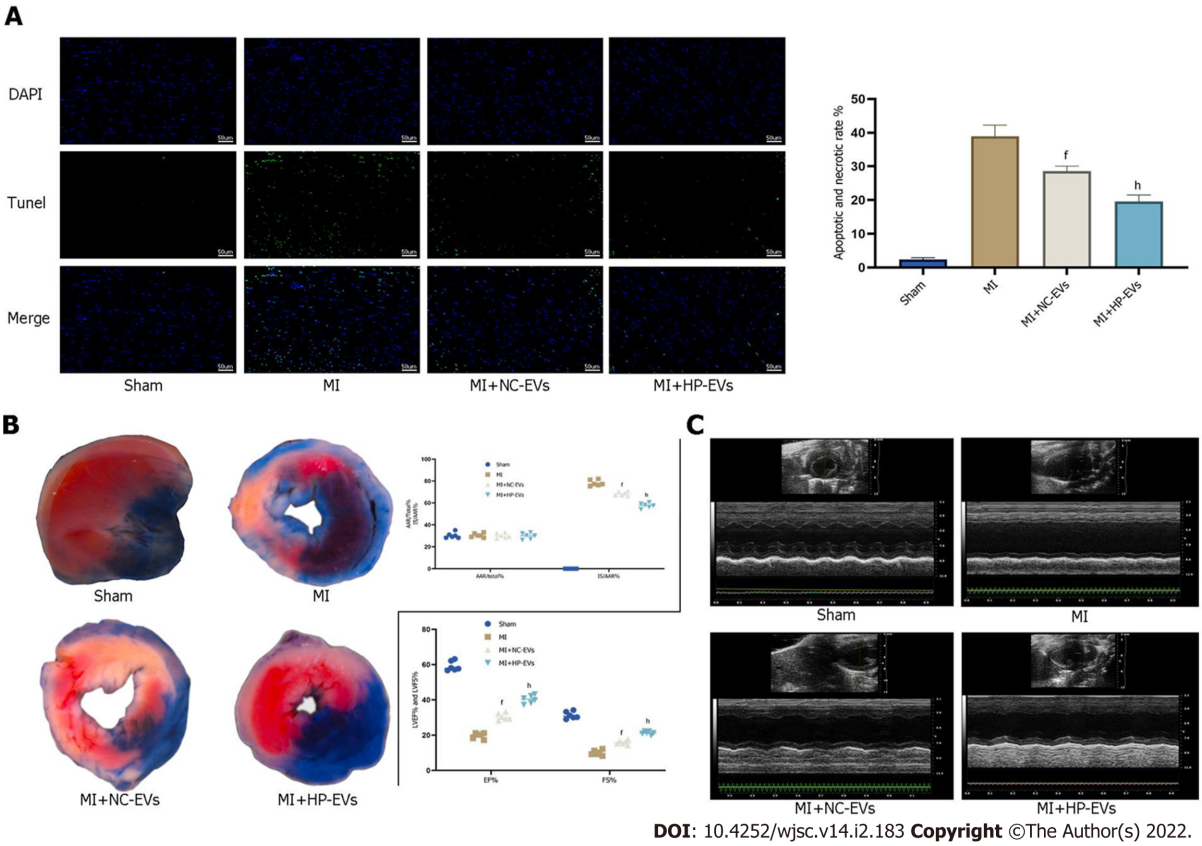

DOI: 10.4252/wjsc.v14.i2.183

Figure 6 Hypoxia-preconditioned extracellular vesicles alleviated hypoxia/reoxygenation-induced apoptosis *in vivo*. A: Degree of cardiomyocyte (CM) apoptosis in the control, sham, myocardial infarction (MI), normoxic extracellular vesicle (NC-EV), and hypoxia-preconditioned EV (HP-EV) groups after 2 h of left coronary artery (LCA) ligation followed by 12 h of reperfusion, as determined by the terminal deoxynucleotidyl transferase dUTP nick end-labeling assay (n = 5); B: HP-EV cardioprotective effects were assessed *in vivo*, and MI models were established with LCA ligation for 1 h followed by 12 h of reperfusion. Evans Blue/2,3,5-triphenyltetrazolium chloride staining was used to evaluate the area of viable myocardium in the sham, MI, NC-EV, and HP-EV groups (n = 5); C: Heart function of the sham, MI, NC-EV, and HP-EV groups was evaluated by echocardiography; ejection fraction and fractional shortening were detected (n = 6). All data are expressed as the mean ± SD. $^{e}P < 0.05$, $^{f}P < 0.01$ compared with MI group; $^{g}P < 0.05$, $^{h}P < 0.01$ compared with MI + NC-EVs group. MI: Myocardial infarction; HP-EV: Hypoxia-preconditioned extracellular vesicles; NC-EV: Normoxic extracellular vesicle.

therapy appear to be 'two-horse carriages' in preserving CMs in the early stage of MI.

As a core transcription factor antagonizing apoptosis and inflammation and promoting proliferation and hypoxia tolerance under hypoxia conditions, HIF-1α is key for controlling the expression of a myriad of genes involved in the hypoxic response; thus, its role in ischemic cardiomyopathy has received increasing attention[42]. In our previous study, we revealed that HP-EVs primarily target TXNIP to alleviate myocardial IR injury post-reperfusion therapy[43]. Theoretically and mechanistically, we demonstrated that TXNIP, which interacts with HIF-1α, involves the degradation of HIF1α through accelerating the nuclear export of ubiquitinated HIF-1α *via* the CRM-1 nuclear export pathway in hypoxic conditions. Thus, HIF-1α-induced tolerance to hypoxia is weakened under hypoxic conditions to exert severe ischemia or hypoxia injury in CMs, unlike its effect on tumor metabolism and angiogenesis under hypoxic conditions. HIF-1α has long been mainly considered an oxygen homeostasis regulator, probably because of its characteristic transcriptional activation[44,45]. However, recent studies have indicated that HIF-1α contributes to anti-apoptosis, regulation of energy metabolism, and collateral vessel generation[46,47]. Therefore, considering that HIF-1α has the potential to regulate hypoxia-related injury and our previous studies on the inhibitory effects of HP-EV on TXNIP, we confirmed that highly expressed TXNIP in hypoxic conditions triggers the degradation of HIF-1α. Furthermore, by targeting TXNIP, HP-EVs improve the prognosis of MI.

The limitation of this study was, due to the difficulty in effectively inhibiting the action of the myocardial proteasome, we did not assess HIF-1α ubiquitination *in vivo*. The interaction among pVHL, TXNIP, and HIF-1α as well as the mechanism of the CRM-1 nuclear export pathway under hypoxia/MI conditions remains to be further studied.

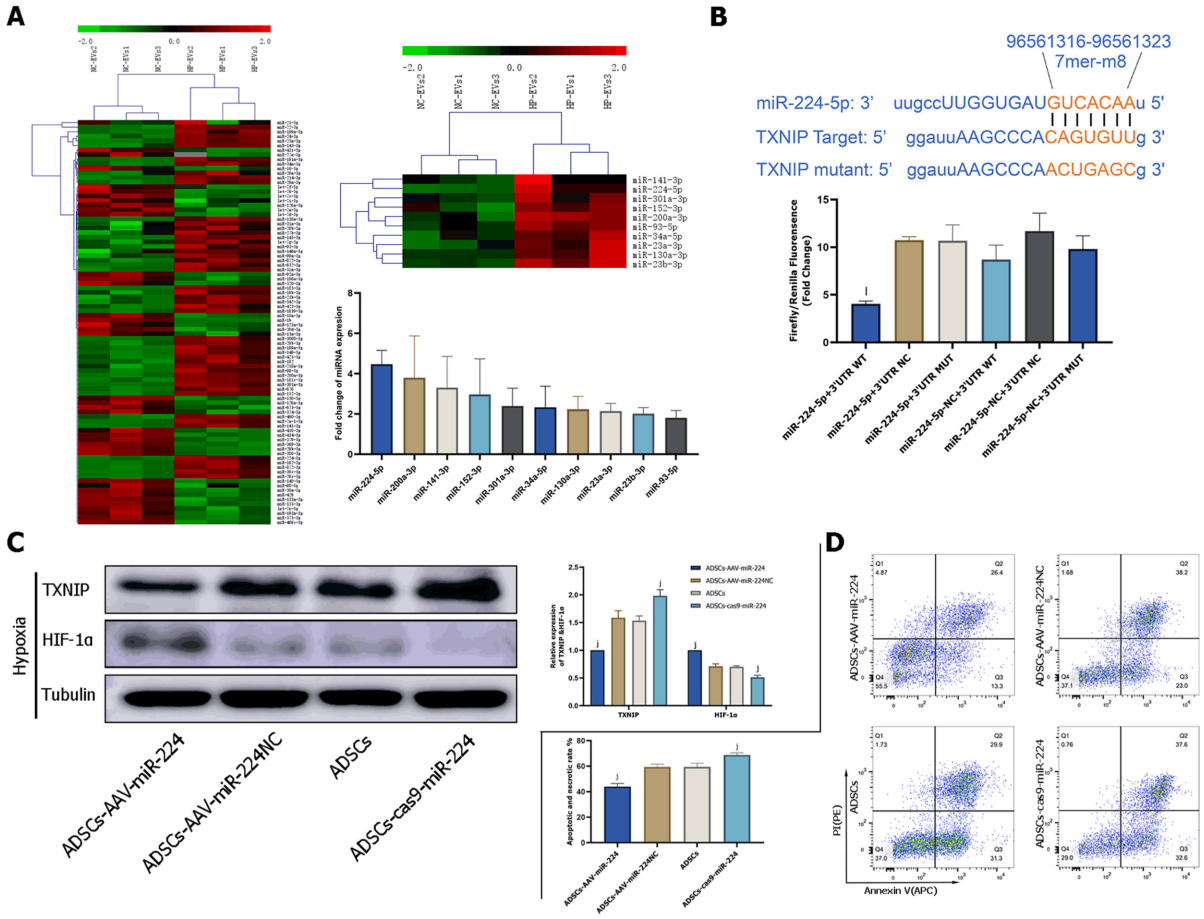

DOI: 10.4252/wjsc.v14.i2.183

Figure 7 Extracellular vesicle-associated miR-224-5p inhibits hypoxia-induced apoptosis in cardiomyocytes by downregulating thioredoxin-interacting protein. A: MicroRNA (miRNA) sequencing analysis in adipose-derived stem cell-extracellular vesicles (ADSC-EVs). A total of 88 miRNAs were upregulated in hypoxia preconditioned EVs (HP-EVs) compared to normoxic EVs (NC-EVs), of which 10 (shown in the heatmap) were predicted to associate with thioredoxin-interacting protein (TXNIP). Validation of differential EV-associated miRNA expression through quantitative PCR. U6 small nuclear RNA served as the internal reference; B: Dual luciferase reporter assay. HEK 293 T cells were co-transfected with miR-224-5p mimics and PGL3 Luciferase reporter plasmids containing wild-type (WT) or mutated TXNIP 3'-untranslated region (3'-UTR). mutated-TXNIP 3'-UTR served as the control. Dual luciferase reporter assay (All data are expressed as the mean ± SD , $^{k}P < 0.05$, $^{l}P < 0.01$, miR-224-5p + TXNIP WT 3'-UTR *vs* miR-224-negative + 3'-UTR-mutant groups; $n = 3$); C: Neonatal mouse CMs subjected to hypoxia were pre-treated with EVs derived from ADSCs (ADSCs group), ADSCs overexpressing miR-224 (ADSCs-AAV-miR-224 group), ADSCs overexpressing miR-224-NC (ADSCs-AAV-miR-224NC group) and ADSCs with miR-224 knocked-out (ADSCs-cas9-miR-224 group). Western blotting was used to detect the expression of hypoxia-inducible factor-1 alpha and TXNIP ($n = 5$); D: Neonatal mouse CMs subjected to hypoxia were pre-treated with EVs derived from ADSCs (ADSCs group), ADSCs overexpressing miR-224 (ADSCs-AAV-miR-224 group), ADSCs overexpressing miR-224-NC (ADSCs-AAV-miR-224NC group) and ADSCs with miR-224 knocked-out (ADSCs-cas9-miR-224 group). Annexin V/PI assay was used to assess the degree of apoptosis in four groups ($n = 5$). All data are expressed as the mean ± SD, $^{i}P < 0.05$, $^{i}P < 0.01$, compared with CMs subjected to hypoxia were pre-treated with EVs derived from ADSCs group(ADSCs group). HP-EV: Hypoxia-preconditioned extracellular vesicles; NC-EV: Normoxic extracellular vesicle; ADSC: Adipose-derived mesenchymal stem cell; WT: Wild-type.

CONCLUSION

In conclusion, our study demonstrated that EVs generated by ADSCs subjected to hypoxia preconditioning showed more significant cardioprotection against MI than EVs derived from normoxic ADSCs, partly due to the abundance of miRNAs targeting TXNIP in HP-EVs. TXNIP-aggravated ubiquitination of HIF-1α in CMs exposed to MI determines the tolerance of cells to hypoxia (Figure 9). Therefore, we propose that the downregulation of TXNIP by EV-associated miRNAs prevents the nuclear export and ubiquitination of HIF-1α, which protect CMs against early-stage ischemic injury by sustaining the transcriptional activity of HIF-1α. Our study provides novel insights into therapeutic approaches and the pathogenesis of MI and reveals that EVs derived from HP MSCs could help improve myocardial hypoxia tolerance when applied in the early stage of MI.

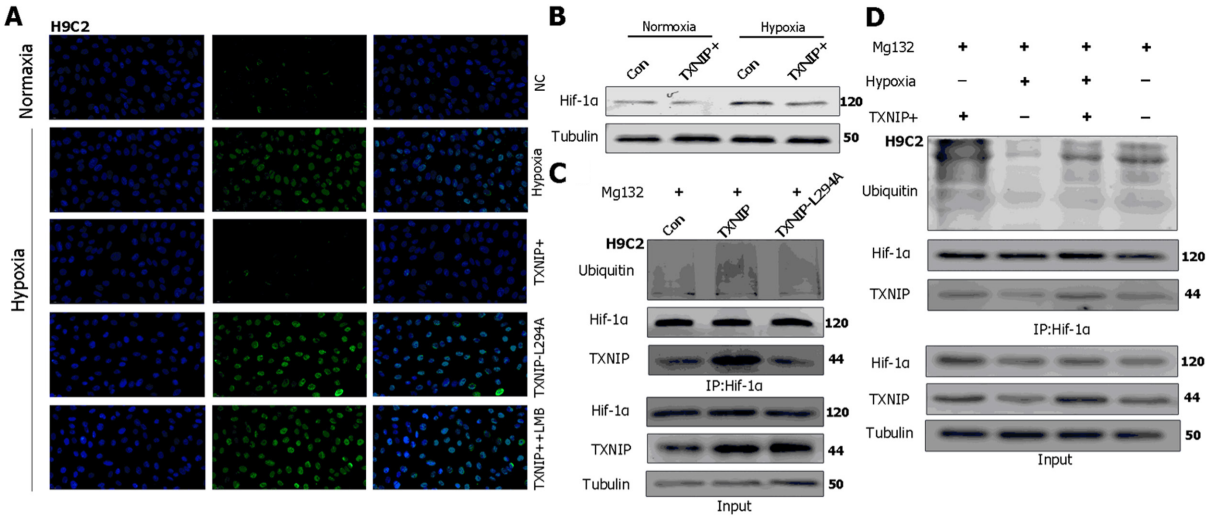

DOI: 10.4252/wjsc.v14.i2.183 **Copyright** ©The Author(s) 2022.

Figure 8 Thioredoxin-interacting protein promotes the ubiquitination of hypoxia-inducible factor-1 alpha through the chromosomal region maintenance-1 nuclear export pathway. A: H_9C_2 cardiomyocytes (CMs) overexpressing thioredoxin-interacting protein (TXNIP) or TXNIP-L294A mutant as indicated and leptomycin B were used to inhibit the chromosomal region maintenance 1 nuclear export pathway. The expression and cellular localization of hypoxia-inducible factor-1 alpha (HIF-1α) was analyzed by immunofluorescence staining; B: H_9C_2CMs were treated with hypoxia or normoxia and TXNIP was overexpressed as indicated. The expression of HIF-1α was analyzed by western blotting; C: H_9C_2 CMs were pretreated with MG132 for 2 h and TXNIP or TXNIP-L294A-mutant were overexpressed as indicated. The interaction of TXNIP and HIF-1α, and HIF-1α ubiquitination were assessed by immunoprecipitation with an anti-HIF-1α antibody; D: H_9C_2 CMs were pretreated with MG132 for 2 h. TXNIP was overexpressed and hypoxia treatment was applied as indicated. The interaction of TXNIP and HIF-1α, and HIF-1α ubiquitination were assessed by immunoprecipitation with an anti-HIF-1α antibody.

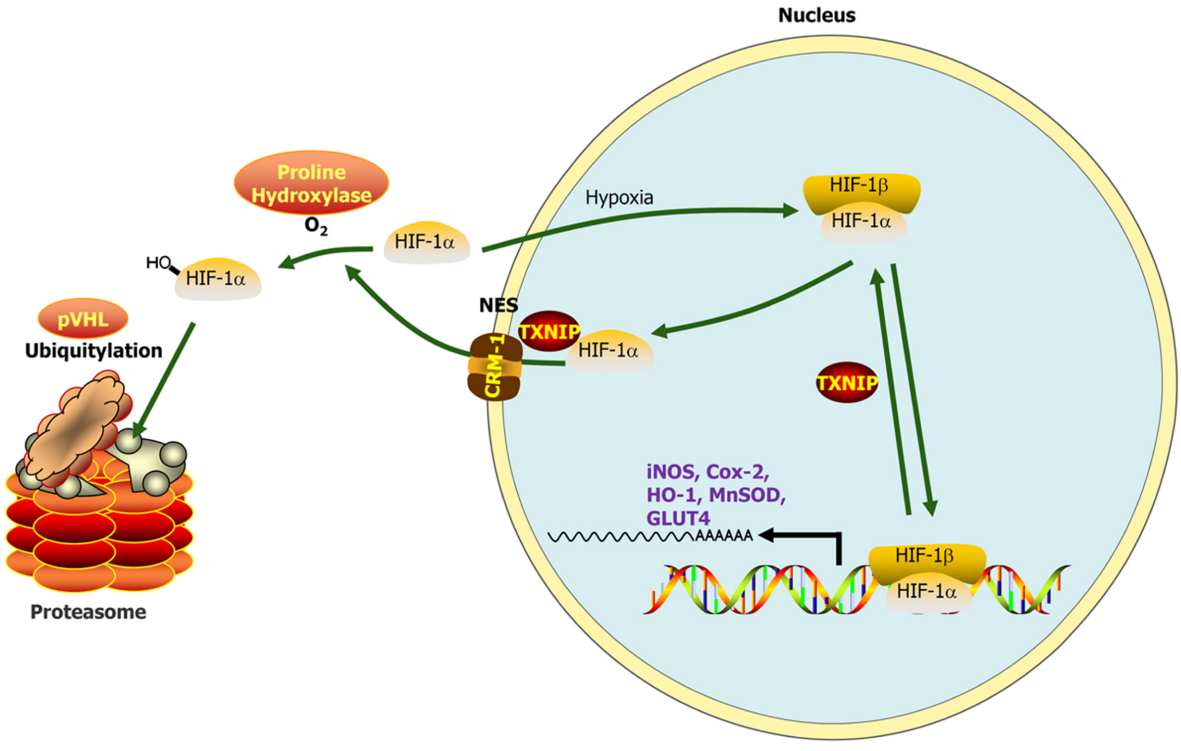

DOI: 10.4252/wjsc.v14.i2.183 **Copyright** ©The Author(s) 2022.

Figure 9 During myocardial infarction or hypoxia, hypoxia-inducible factor-1 alpha export is chromosomal region maintenance-1-dependent in the presence of thioredoxin-interacting protein, based on the association of thioredoxin-interacting protein with chromosomal region maintenance-1. Thioredoxin-interacting protein (TXNIP)-induced hypoxia-inducible factor-1 alpha (HIF-1α) nuclear export may be hypoxia-independent, which triggers ubiquitination and degradation by the proteasome in cardiomyocytes. As a transcription factor, the function of HIF-1 in promoting targeted gene transcription is abolished by hypoxia/myocardial infarction-triggered TXNIP activation. Our research aimed to clarify this process by hypoxia-preconditioned extracellular vesicles and the underlying mechanism.

ARTICLE HIGHLIGHTS

Research background

Previous studies have demonstrated that extracellular vesicles (EVs) derived from mesenchymal stem cells (MSCs) reveal the cardioprotective effects against myocardial infarction (MI). Hypoxia-preconditioned EVs (HP-EVs) derived from MSCs are thought to have better cardioprotective effects, and the underlying mechanisms have garnered increasing attention from scholars.

Research motivation

Although some scholars have focused on the effect of hypoxia preconditioning on MSCs, the underlying mechanisms remain unclear. Thus, this study focused on the mechanism underlying the cardioprotective effect of HP-EVs from MSCs.

Research objectives

We explored the cardioprotective mechanism of HP-EVs from MSCs.

Research methods

HP-EVs from mouse adipose-derived MSCs (ADSCs) were extracted, and their cardioprotective effect on improving the survival of cardiomyocytes (CMs) and ameliorating cardiac function were evaluated by Evans Blue/2,3,5-triphenyltetrazolium chloride staining and echocardiography. Mechanistically, microRNA (miRNA) sequencing was adopted to investigate the functional RNA diversity between HP-EVs or normoxic EVs (NC-EVs) from mouse ADSCs. Subsequently, the molecular mechanism of EVs in mediating thioredoxin-interacting protein (TXNIP) and TXNIP-mediated hypoxia-inducible factor-1 alpha (HIF-1α) ubiquitination were verified by the dual-luciferase reporter assay, immunoprecipitation, western blotting, and immunofluorescence.

Research results

HP-EVs reduced both infarct size (necrosis area) and the degree of apoptosis to a greater extent than NC-EVs in CMs subjected to hypoxia *in vitro* and mice suffering from MI *in vivo*. We showed that EV miRNA224-5p directly bound to the 3′-untranslated region of TXNIP and had a critical protective role against hypoxia-associated CM injury. Our results suggested that MI triggered TXNIP-mediated HIF-1α ubiquitination and degradation *via* the chromosomal region maintenance 1-dependent nuclear transport pathway in CMs, which led to aggravated injury and hypoxia tolerance in CMs in the early stage of MI.

Research conclusions

The anti-apoptotic effect of HP-EVs, which improves tolerance toward MI or hypoxic conditions and alleviates the degree of CM apoptosis until reperfusion therapy, may partly result from EV miR-224-5p targeting TXNIP.

Research perspectives

This study partly reveals the mechanism underlying the cardioprotective effect of HP-EVs and provides insights into potential therapies against MI.

FOOTNOTES

Author contributions: Mao CY, Zhang TT, Li DJ, and Zhou E contributed equally to this work, performed the experiments, and reviewed and edited the manuscript; Fan YQ and He Q wrote the paper; Zhang JF, and Wang CQ conceived of and funded the study; all authors read and approved the final manuscript.

Supported by National Natural Science Foundation of China, No. 81870264 and No. 81470546; the Shanghai Committee of Science and Technology, No. 18411950500; the Major Disease Joint Project of Shanghai Health System, No. 2014ZYJB0501; and Talent Cultivation Project of The Ninth People's Hospital Affiliated to Shanghai Jiao Tong University School of Medicine, No. JC202005.

Institutional review board statement: The study was reviewed and approved by the Institutional Review Board of Shanghai Ninth People's Hospital.

Institutional animal care and use committee statement: All animal procedures were approved by the Shanghai Ninth People's Hospital Institutional Ethics Committee and conducted in accordance with the guidelines of the Directive 2010/63/EU of the European Parliament.

Conflict-of-interest statement: The authors declare that they have no competing interests regarding this study.

Data sharing statement: The data that support the findings of this study are available from the corresponding author upon reasonable request.

ARRIVE guidelines statement: The authors have read the ARRIVE guidelines, and the manuscript was prepared and revised according to the ARRIVE guidelines.

Country/Territory of origin: China

ORCID number: Cheng-Yu Mao 0000-0001-9740-8835; Tian-Tian Zhang 0000-0001-8218-2757; Dong-Jiu Li 0000-0003-4372-6613; En Zhou 0000-0002-6073-8037; Yu-Qi Fan 0000-0002-0084-2895; Qing He 0000-0002-1078-350X; Chang-Qian Wang 0000-0002-7611-7761; Jun-Feng Zhang 0000-0001-9530-3263.

S-Editor: Fan JR
L-Editor: A
P-Editor: Zhang YL

REFERENCES

1 **Vogel B**, Claessen BE, Arnold SV, Chan D, Cohen DJ, Giannitsis E, Gibson CM, Goto S, Katus HA, Kerneis M, Kimura T, Kunadian V, Pinto DS, Shiomi H, Spertus JA, Steg PG, Mehran R. ST-segment elevation myocardial infarction. *Nat Rev Dis Primers* 2019; **5**: 39 [PMID: 31171787 DOI: 10.1038/s41572-019-0090-3]
2 **Hayes SN**, Tweet MS, Adlam D, Kim ESH, Gulati R, Price JE, Rose CH. Spontaneous Coronary Artery Dissection: JACC State-of-the-Art Review. *J Am Coll Cardiol* 2020; **76**: 961-984 [PMID: 32819471 DOI: 10.1016/j.jacc.2020.05.084]
3 **Frangogiannis NG**. Pathophysiology of Myocardial Infarction. *Compr Physiol* 2015; **5**: 1841-1875 [PMID: 26426469 DOI: 10.1002/cphy.c150006]
4 **James TN**. The variable morphological coexistence of apoptosis and necrosis in human myocardial infarction: significance for understanding its pathogenesis, clinical course, diagnosis and prognosis. *Coron Artery Dis* 1998; **9**: 291-307 [PMID: 9710689 DOI: 10.1097/00019501-199809050-00007]
5 **Nader ND**, Asgeri M, Davari-Farid S, Pourafkari L, Ahmadpour F, Porhomayon J, Javadzadeghan H, Negargar S, Knight PR 3rd. The Effect of Lipopolysaccharide on Ischemic-Reperfusion Injury of Heart: A Double Hit Model of Myocardial Ischemia and Endotoxemia. *J Cardiovasc Thorac Res* 2015; **7**: 81-86 [PMID: 26430494 DOI: 10.15171/jcvtr.2015.19]
6 **Sato T**, Machida T, Takahashi S, Iyama S, Sato Y, Kuribayashi K, Takada K, Oku T, Kawano Y, Okamoto T, Takimoto R, Matsunaga T, Takayama T, Takahashi M, Kato J, Niitsu Y. Fas-mediated apoptosome formation is dependent on reactive oxygen species derived from mitochondrial permeability transition in Jurkat cells. *J Immunol* 2004; **173**: 285-296 [PMID: 15210786 DOI: 10.4049/jimmunol.173.1.285]
7 **Burke AP**, Virmani R. Pathophysiology of acute myocardial infarction. *Med Clin North Am* 2007; **91**: 553-72; ix [PMID: 17640536 DOI: 10.1016/j.mcna.2007.03.005]
8 **Zhou R**, Tardivel A, Thorens B, Choi I, Tschopp J. Thioredoxin-interacting protein links oxidative stress to inflammasome activation. *Nat Immunol* 2010; **11**: 136-140 [PMID: 20023662 DOI: 10.1038/ni.1831]
9 **Shin D**, Jeon JH, Jeong M, Suh HW, Kim S, Kim HC, Moon OS, Kim YS, Chung JW, Yoon SR, Kim WH, Choi I. VDUP1 mediates nuclear export of HIF1alpha *via* CRM1-dependent pathway. *Biochim Biophys Acta* 2008; **1783**: 838-848 [PMID: 18062927 DOI: 10.1016/j.bbamcr.2007.10.012]
10 **Del Re DP**, Amgalan D, Linkermann A, Liu Q, Kitsis RN. Fundamental Mechanisms of Regulated Cell Death and Implications for Heart Disease. *Physiol Rev* 2019; **99**: 1765-1817 [PMID: 31364924 DOI: 10.1152/physrev.00022.2018]
11 **Fang X**, Wang H, Han D, Xie E, Yang X, Wei J, Gu S, Gao F, Zhu N, Yin X, Cheng Q, Zhang P, Dai W, Chen J, Yang F, Yang HT, Linkermann A, Gu W, Min J, Wang F. Ferroptosis as a target for protection against cardiomyopathy. *Proc Natl Acad Sci U S A* 2019; **116**: 2672-2680 [PMID: 30692261 DOI: 10.1073/pnas.1821022116]
12 **Li Y**, Miao LY, Xiao YL, Huang M, Yu M, Meng K, Cai HR. Hypoxia induced high expression of thioredoxin interacting protein (TXNIP) in non-small cell lung cancer and its prognostic effect. *Asian Pac J Cancer Prev* 2015; **16**: 2953-2958 [PMID: 25854388 DOI: 10.7314/apjcp.2015.16.7.2953]
13 **Zhou R**, Yazdi AS, Menu P, Tschopp J. A role for mitochondria in NLRP3 inflammasome activation. *Nature* 2011; **469**: 221-225 [PMID: 21124315 DOI: 10.1038/nature09663]
14 **Yang C**, Xia W, Liu X, Lin J, Wu A. Role of TXNIP/NLRP3 in sepsis-induced myocardial dysfunction. *Int J Mol Med* 2019; **44**: 417-426 [PMID: 31173172 DOI: 10.3892/ijmm.2019.4232]
15 **Galderisi U**, Peluso G, Di Bernardo G. Clinical Trials Based on Mesenchymal Stromal Cells are Exponentially Increasing: Where are We in Recent Years? *Stem Cell Rev Rep* 2021 [PMID: 34398443 DOI: 10.1007/s12015-021-10231-w]
16 **Mathew B**, Ravindran S, Liu X, Torres L, Chennakesavalu M, Huang CC, Feng L, Zelka R, Lopez J, Sharma M, Roth S. Mesenchymal stem cell-derived extracellular vesicles and retinal ischemia-reperfusion. *Biomaterials* 2019; **197**: 146-160 [PMID: 30654160 DOI: 10.1016/j.biomaterials.2019.01.016]

17 **Shao H**, Im H, Castro CM, Breakefield X, Weissleder R, Lee H. New Technologies for Analysis of Extracellular Vesicles. *Chem Rev* 2018; **118**: 1917-1950 [PMID: 29384376 DOI: 10.1021/acs.chemrev.7b00534]

18 **Terlecki-Zaniewicz L**, Lämmermann I, Latreille J, Bobbili MR, Pils V, Schosserer M, Weinmüllner R, Dellago H, Skalicky S, Pum D, Almaraz JCH, Scheideler M, Morizot F, Hackl M, Gruber F, Grillari J. Small extracellular vesicles and their miRNA cargo are anti-apoptotic members of the senescence-associated secretory phenotype. *Aging (Albany NY)* 2018; **10**: 1103-1132 [PMID: 29779019 DOI: 10.18632/aging.101452]

19 **Harrell CR**, Jovicic N, Djonov V, Arsenijevic N, Volarevic V. Mesenchymal Stem Cell-Derived Exosomes and Other Extracellular Vesicles as New Remedies in the Therapy of Inflammatory Diseases. *Cells* 2019; **8** [PMID: 31835680 DOI: 10.3390/cells8121605]

20 **van Niel G**, D'Angelo G, Raposo G. Shedding light on the cell biology of extracellular vesicles. *Nat Rev Mol Cell Biol* 2018; **19**: 213-228 [PMID: 29339798 DOI: 10.1038/nrm.2017.125]

21 **Mathieu M**, Martin-Jaular L, Lavieu G, Théry C. Specificities of secretion and uptake of exosomes and other extracellular vesicles for cell-to-cell communication. *Nat Cell Biol* 2019; **21**: 9-17 [PMID: 30602770 DOI: 10.1038/s41556-018-0250-9]

22 **Zhang N**, Song Y, Huang Z, Chen J, Tan H, Yang H, Fan M, Li Q, Wang Q, Gao J, Pang Z, Qian J, Ge J. Monocyte mimics improve mesenchymal stem cell-derived extracellular vesicle homing in a mouse MI/RI model. *Biomaterials* 2020; **255**: 120168 [PMID: 32562944 DOI: 10.1016/j.biomaterials.2020.120168]

23 **Broughton KM**, Sussman MA. Enhancement Strategies for Cardiac Regenerative Cell Therapy: Focus on Adult Stem Cells. *Circ Res* 2018; **123**: 177-187 [PMID: 29976686 DOI: 10.1161/CIRCRESAHA.118.311207]

24 **Lewinska A**, Adamczyk-Grochala J, Bloniarz D, Horeczy B, Zurek S, Kurowicki A, Woloszczuk-Gebicka B, Widenka K, Wnuk M. Remifentanil preconditioning protects against hypoxia-induced senescence and necroptosis in human cardiac myocytes *in vitro*. *Aging (Albany NY)* 2020; **12**: 13924-13938 [PMID: 32584786 DOI: 10.18632/aging.103604]

25 **Gao E**, Lei YH, Shang X, Huang ZM, Zuo L, Boucher M, Fan Q, Chuprun JK, Ma XL, Koch WJ. A novel and efficient model of coronary artery ligation and myocardial infarction in the mouse. *Circ Res* 2010; **107**: 1445-1453 [PMID: 20966393 DOI: 10.1161/CIRCRESAHA.110.223925]

26 **Yan W**, Lin C, Guo Y, Chen Y, Du Y, Lau WB, Xia Y, Zhang F, Su R, Gao E, Wang Y, Li C, Liu R, Ma XL, Tao L. N-Cadherin Overexpression Mobilizes the Protective Effects of Mesenchymal Stromal Cells Against Ischemic Heart Injury Through a β-Catenin-Dependent Manner. *Circ Res* 2020; **126**: 857-874 [PMID: 32079489 DOI: 10.1161/CIRCRESAHA.119.315806]

27 **Ehler E**, Moore-Morris T, Lange S. Isolation and culture of neonatal mouse cardiomyocytes. *J Vis Exp* 2013 [PMID: 24056408 DOI: 10.3791/50154]

28 **Sluijter JPG**, Davidson SM, Boulanger CM, Buzás EI, de Kleijn DPV, Engel FB, Giricz Z, Hausenloy DJ, Kishore R, Lecour S, Leor J, Madonna R, Perrino C, Prunier F, Sahoo S, Schiffelers RM, Schulz R, Van Laake LW, Ytrehus K, Ferdinandy P. Extracellular vesicles in diagnostics and therapy of the ischaemic heart: Position Paper from the Working Group on Cellular Biology of the Heart of the European Society of Cardiology. *Cardiovasc Res* 2018; **114**: 19-34 [PMID: 29106545 DOI: 10.1093/cvr/cvx211]

29 **Boulanger CM**, Loyer X, Rautou PE, Amabile N. Extracellular vesicles in coronary artery disease. *Nat Rev Cardiol* 2017; **14**: 259-272 [PMID: 28150804 DOI: 10.1038/nrcardio.2017.7]

30 **Lener T**, Gimona M, Aigner L, Börger V, Buzas E, Camussi G, Chaput N, Chatterjee D, Court FA, Del Portillo HA, O'Driscoll L, Fais S, Falcon-Perez JM, Felderhoff-Mueser U, Fraile L, Gho YS, Görgens A, Gupta RC, Hendrix A, Hermann DM, Hill AF, Hochberg F, Horn PA, de Kleijn D, Kordelas L, Kramer BW, Krämer-Albers EM, Laner-Plamberger S, Laitinen S, Leonardi T, Lorenowicz MJ, Lim SK, Lötvall J, Maguire CA, Marcilla A, Nazarenko I, Ochiya T, Patel T, Pedersen S, Pocsfalvi G, Pluchino S, Quesenberry P, Reischl IG, Rivera FJ, Sanzenbacher R, Schallmoser K, Slaper-Cortenbach I, Strunk D, Tonn T, Vader P, van Balkom BW, Wauben M, Andaloussi SE, Théry C, Rohde E, Giebel B. Applying extracellular vesicles based therapeutics in clinical trials - an ISEV position paper. *J Extracell Vesicles* 2015; **4**: 30087 [PMID: 26725829 DOI: 10.3402/jev.v4.30087]

31 **Elsharkasy OM**, Nordin JZ, Hagey DW, de Jong OG, Schiffelers RM, Andaloussi SE, Vader P. Extracellular vesicles as drug delivery systems: Why and how? *Adv Drug Deliv Rev* 2020; **159**: 332-343 [PMID: 32305351 DOI: 10.1016/j.addr.2020.04.004]

32 **Chen K**, Xu Z, Liu Y, Wang Z, Li Y, Xu X, Chen C, Xia T, Liao Q, Yao Y, Zeng C, He D, Yang Y, Tan T, Yi J, Zhou J, Zhu H, Ma J. Irisin protects mitochondria function during pulmonary ischemia/reperfusion injury. *Sci Transl Med* 2017; **9** [PMID: 29187642 DOI: 10.1126/scitranslmed.aao6298]

33 **Munshi AM**, Rigg E, Mehic J, Rosu-Myles M, Lavoie JRJC. Comparative study of hypoxic and normoxic preconditioned mesenchymal stem cell derived extracellular vesicles and their therapeutic implications. 2018; 20: S23 [PMID, [DOI: 10.1016/j.jcyt.2018.02.052]

34 **Liu W**, Rong Y, Wang J, Zhou Z, Ge X, Ji C, Jiang D, Gong F, Li L, Chen J, Zhao S, Kong F, Gu C, Fan J, Cai W. Exosome-shuttled miR-216a-5p from hypoxic preconditioned mesenchymal stem cells repair traumatic spinal cord injury by shifting microglial M1/M2 polarization. *J Neuroinflammation* 2020; **17**: 47 [PMID: 32019561 DOI: 10.1186/s12974-020-1726-7]

35 **Park H**, Park H, Mun D, Kang J, Kim H, Kim M, Cui S, Lee SH, Joung B. Extracellular Vesicles Derived from Hypoxic Human Mesenchymal Stem Cells Attenuate GSK3β Expression *via* miRNA-26a in an Ischemia-Reperfusion Injury Model. *Yonsei Med J* 2018; **59**: 736-745 [PMID: 29978610 DOI: 10.3349/ymj.2018.59.6.736]

36 **Eckle T**, Köhler D, Lehmann R, El Kasmi K, Eltzschig HK. Hypoxia-inducible factor-1 is central to cardioprotection: a new paradigm for ischemic preconditioning. *Circulation* 2008; **118**: 166-175 [PMID: 18591435 DOI: 10.1161/CIRCULATIONAHA.107.758516]

37 **Maxwell PH**, Wiesener MS, Chang GW, Clifford SC, Vaux EC, Cockman ME, Wykoff CC, Pugh CW, Maher ER, Ratcliffe PJ. The tumour suppressor protein VHL targets hypoxia-inducible factors for oxygen-dependent proteolysis. *Nature* 1999; **399**: 271-275 [PMID: 10353251 DOI: 10.1038/20459]

38 **Tekin D**, Dursun AD, Xi L. Hypoxia inducible factor 1 (HIF-1) and cardioprotection. *Acta Pharmacol Sin* 2010; **31**: 1085-1094 [PMID: 20711226 DOI: 10.1038/aps.2010.132]

39 **Kseibati MO**, Shehatou GSG, Sharawy MH, Eladl AE, Salem HA. Nicorandil ameliorates bleomycin-induced pulmonary fibrosis in rats through modulating eNOS, iNOS, TXNIP and HIF-1α levels. *Life Sci* 2020; **246**: 117423 [PMID: 32057902 DOI: 10.1016/j.lfs.2020.117423]

40 **Farrell MR**, Rogers LK, Liu Y, Welty SE, Tipple TE. Thioredoxin-interacting protein inhibits hypoxia-inducible factor transcriptional activity. *Free Radic Biol Med* 2010; **49**: 1361-1367 [PMID: 20692333 DOI: 10.1016/j.freeradbiomed.2010.07.016]

41 **O'Gara PT**, Kushner FG, Ascheim DD, Casey DE Jr, Chung MK, de Lemos JA, Ettinger SM, Fang JC, Fesmire FM, Franklin BA, Granger CB, Krumholz HM, Linderbaum JA, Morrow DA, Newby LK, Ornato JP, Ou N, Radford MJ, Tamis-Holland JE, Tommaso CL, Tracy CM, Woo YJ, Zhao DX, Anderson JL, Jacobs AK, Halperin JL, Albert NM, Brindis RG, Creager MA, DeMets D, Guyton RA, Hochman JS, Kovacs RJ, Ohman EM, Stevenson WG, Yancy CW; American College of Cardiology Foundation/American Heart Association Task Force on Practice Guidelines. 2013 ACCF/AHA guideline for the management of ST-elevation myocardial infarction: a report of the American College of Cardiology Foundation/American Heart Association Task Force on Practice Guidelines. *Circulation* 2013; **127**: e362-e425 [PMID: 23247304 DOI: 10.1161/CIR.0b013e3182742cf6]

42 **Kido M**, Du L, Sullivan CC, Li X, Deutsch R, Jamieson SW, Thistlethwaite PA. Hypoxia-inducible factor 1-alpha reduces infarction and attenuates progression of cardiac dysfunction after myocardial infarction in the mouse. *J Am Coll Cardiol* 2005; **46**: 2116-2124 [PMID: 16325051 DOI: 10.1016/j.jacc.2005.08.045]

43 **Mao C**, Li D, Zhou E, Gao E, Zhang T, Sun S, Gao L, Fan Y, Wang C. Extracellular vesicles from anoxia preconditioned mesenchymal stem cells alleviate myocardial ischemia/reperfusion injury. *Aging (Albany NY)* 2021; **13**: 6156-6170 [PMID: 33578393 DOI: 10.18632/aging.202611]

44 **Choudhry H**, Harris AL. Advances in Hypoxia-Inducible Factor Biology. *Cell Metab* 2018; **27**: 281-298 [PMID: 29129785 DOI: 10.1016/j.cmet.2017.10.005]

45 **Semenza GL**. Hypoxia-inducible factor 1 and cardiovascular disease. *Annu Rev Physiol* 2014; **76**: 39-56 [PMID: 23988176 DOI: 10.1146/annurev-physiol-021113-170322]

46 **Cheng SC**, Quintin J, Cramer RA, Shepardson KM, Saeed S, Kumar V, Giamarellos-Bourboulis EJ, Martens JH, Rao NA, Aghajanirefah A, Manjeri GR, Li Y, Ifrim DC, Arts RJ, van der Veer BM, Deen PM, Logie C, O'Neill LA, Willems P, van de Veerdonk FL, van der Meer JW, Ng A, Joosten LA, Wijmenga C, Stunnenberg HG, Xavier RJ, Netea MG. mTOR- and HIF-1α-mediated aerobic glycolysis as metabolic basis for trained immunity. *Science* 2014; **345**: 1250684 [PMID: 25258083 DOI: 10.1126/science.1250684]

47 **Creager MA**, Olin JW, Belch JJ, Moneta GL, Henry TD, Rajagopalan S, Annex BH, Hiatt WR. Effect of hypoxia-inducible factor-1alpha gene therapy on walking performance in patients with intermittent claudication. *Circulation* 2011; **124**: 1765-1773 [PMID: 21947297 DOI: 10.1161/CIRCULATIONAHA.110.009407]

World Journal of Stem Cells

Submit a Manuscript: https://www.f6publishing.com

World J Stem Cells 2022 February 26; 14(2): 200-213

DOI: 10.4252/wjsc.v14.i2.200

ISSN 1948-0210 (online)

SYSTEMATIC REVIEWS

Anti-fibrotic effect of adipose-derived stem cells on fibrotic scars

Sophie Vanderstichele, Jan Jeroen Vranckx

Specialty type: Transplantation

Provenance and peer review: Invited article; Externally peer reviewed.

Peer-review model: Single blind

Peer-review report's scientific quality classification

Grade A (Excellent): A
Grade B (Very good): B, B
Grade C (Good): 0
Grade D (Fair): 0
Grade E (Poor): 0

P-Reviewer: Casado-Diaz A, Mehanna RA, Salvadori M

Received: February 23, 2021
Peer-review started: February 23, 2021
First decision: April 20, 2021
Revised: May 1, 2021
Accepted: February 15, 2022
Article in press: February 15, 2022
Published online: February 26, 2022

Sophie Vanderstichele, Master in Medicine, KUL Leuven University, Leuven 3000, Belgium

Jan Jeroen Vranckx, Department of Plastic, Reconstructive Surgery, KU-Leuven University Hospitals, Leuven 3000, Belgium

Corresponding author: Jan Jeroen Vranckx, MD, PhD, Professor, Department of Plastic, Reconstructive and Aesthetic Surgery, KU-Leuven University Hospitals, Herestraat 49, Leuven 3000, Belgium. jan.vranckx@uzleuven.be

Abstract

BACKGROUND

Sustained injury, through radiotherapy, burns or surgical trauma, can result in fibrosis, displaying an excessive deposition of extracellular matrix (ECM), persisting inflammatory reaction, and reduced vascularization. The increasing recognition of fibrosis as a cause for disease and mortality, and increasing use of radiotherapy causing fibrosis, stresses the importance of a decent anti-fibrotic treatment.

AIM

To obtain an in-depth understanding of the complex mechanisms underlying fibrosis, and more specifically, the potential mechanisms-of-action of adipose-derived stomal cells (ADSCs) in realizing their anti-fibrotic effect.

METHODS

A systematic review of the literature using PubMed, Embase and Web of Science was performed by two independent reviewers.

RESULTS

The injection of fat grafts into fibrotic tissue, releases ADSC into the environment. ADSCs' capacity to directly differentiate into key cell types (*e.g.*, ECs, fibroblasts), as well as to secrete multiple paracrine factors (*e.g.*, hepatocyte growth factor, basis fibroblast growth factor, IL-10), allows them to alter different mechanisms underlying fibrosis in a combined approach. ADSCs favor ECM degradation by impacting the fibroblast-to-myofibroblast differentiation, favoring matrix metalloproteinases over tissue inhibitors of metalloproteinases, positively influencing collagen organization, and inhibiting the pro-fibrotic effects of transforming growth factor-β1. Furthermore, they impact elements of both the innate and adaptive immune response system, and stimulate angiogenesis on the site of injury (through secretion of pro-angiogenic cytokines like stromal cell-derived factor-1 and vascular endothelial growth factor).

CONCLUSION
This review shows that understanding the complex interactions of ECM accumulation, immune response and vascularization, is vital to fibrosis treatments' effectiveness like fat grafting. It details how ADSCs intelligently steer this complex system in an anti-fibrotic or pro-angiogenic direction, without falling into extreme dilation or stimulation of a single aspect. Detailing this combined approach, has brought fat grafting one step closer to unlocking its full potential as a non-anecdotal treatment for fibrosis.

Key Words: Fibrosis; Fat grafting; Adipose-derived stem cells; Angiogenesis; Anti-fibrotic effect; Immunomodulation

Core Tip: The goal of this review is to elucidate the potential mechanisms of action of fat grafting, and more specifically of adipose-derived stem cells (ADSCs), in hostile environment. Why can fat grafts turn the sclerotic environment after intense radiotherapy, burns or surgical trauma into a soft zone that can be further restored and reconstructed? In doing so, this review aims to complement existing literature by delivering an integrated approach to explain the positive effect of ADSCs on fibrosis, considering all 3 main fibrotic aspects, *i.e.*, extracellular matrix accumulation, innate and adaptive immune response and vascularization. It aims at acknowledging the complexity and reciprocal impact these aspects have, both from a clinical as well as a molecular point of view. While available literature so far only focused on a single one of these aspects, the question remains whether an integrated approach and explanation on these combined levels could improve the effectiveness and application areas of this treatment.

Citation: Vanderstichele S, Vranckx JJ. Anti-fibrotic effect of adipose-derived stem cells on fibrotic scars. *World J Stem Cells* 2022; 14(2): 200-213
URL: https://www.wjgnet.com/1948-0210/full/v14/i2/200.htm
DOI: https://dx.doi.org/10.4252/wjsc.v14.i2.200

INTRODUCTION

Fibrosis, or scarring, is a potential consequence of a dysregulated wound-healing process. Tissue injury triggers wound-healing, a complex dynamic process characterized by four distinct but overlapping phases, all limited in time: homeostasis, inflammation, proliferation and remodeling. Interference of the immune system, deposition of the extracellular matrix (ECM) and alteration of the vascularization are indispensable and, typically, reversible elements of the wound-healing. However, sustained injury results in reduced vascularization, persisting inflammatory reaction and excessive deposition of ECM, inducing fibrosis[1]. Radiotherapy-induced skin fibrosis (RISF), a late cutaneous side effect of external radiation, is an example of chronic tissue injury leading to fibrosis. RISF is often characterized by pain, limited range of motion, tissue contraction and aesthetic deformation. All result in a significant loss of quality of life for patients.

Fibrosis can affect nearly every tissue in the body leading to common diseases such as idiopathic pulmonary fibrosis, cirrhosis, renal fibrosis, myocardial fibrotic remodeling, fibrotic stricture as a common complication of Crohn's disease, and scar contractions after surgery, burns, trauma and radiotherapy. The increasing recognition of fibrosis as a cause for disease and mortality and the increasing use of radiotherapy, stresses the importance of a decent anti-fibrotic treatment[2].

In the early 20th century Hedrick, Zuk *et al*[3,4], reported the presence of adipose-derived stem cells (ADSCs), or adipose-derived stromal cells within adipose tissue obtained by lipoaspiration, the so-called stromal vascular fraction (SVF). Decades before, fat grafting was already used in reconstructive procedures as filler of defects, albeit without much confidence since this transfer of fat lobules occurred without intrinsic vascularization. Coleman *et al*[5] pioneered in making the fat graft aliquots soluble and performing the fat transfer as tiny liquid parcels of lipoaspirate, thus eliminating the need for vascularized transfer.

The discovery of ADSCs in 'ordinary' fat grafts was revolutionary in stem cell research, since it was assumed previously that stem cells resided mainly in embryonic tissues, placenta and bone marrow of the adult patient[3,4]. The option of obtaining large numbers of mesenchymal stem cells from lipoaspirates meant a significant paradigm change. Moreover, nowadays ADSCs can be reprogrammed [6,7]. Induced pluripotent stem cells, derived from skin or blood cells, that have been reprogrammed back into an embryonic-like pluripotent state, enable the development of an unlimited source of any

type of human cell required for therapeutic strategies[8,9].

Considering the fact that the SVF from fat grafts is easily accessible by lipo-aspiration, multipotent ADSCs emerged as attractive alternatives for soft tissue restoration and regeneration by adding cells, growth factors and active molecules to the microenvironment of the wound[10,11].

Plastic surgeons observed that fat grafting had a smoothening effect on scars and even on radiation-induced fibrosis. The application of fat grafting extended on various types of fibrosis such as Parry-Romberg syndrome, sclerodermia, dupuytren, hypertrophic scars *etc.*, A multitude of reports confirm these observations[12,13]. However, the mechanisms underlying these fibrosis-reducing effects of fat grafts remain unclear so far.

The goal of this review is to elucidate the potential mechanisms of action of fat grafting, and more specifically of ADSCs, in hostile environment. Why can fat grafts turn the sclerotic environment after intense radiotherapy, burns or surgical trauma into a soft zone that can be further restored and reconstructed? In doing so, this review aims to complement existing literature by delivering an integrated approach to explain the positive effect of ADSCs on fibrosis, considering all 3 main fibrotic aspects *i.e.*, ECM accumulation, innate and adaptive immune response and vascularization. It aims at acknowledging the complexity and reciprocal impact these aspects have, both from a clinical as well as a molecular point of view. While available literature so far only focused on a single one of these aspects, the question remains whether an integrated approach and explanation on these combined levels could improve the effectiveness and application areas of this treatment.

MATERIALS AND METHODS

A systematic review of the literature using PubMed, Embase and Web of Science was performed by two independent reviewers. Terms applied to the search included fat grafting, lipofilling, adipose tissue transplantation/transfer, adipose-derived stem cell, adipose-derived stromal cell, fibrosis, scar, keloid, radiation-induced skin fibrosis, myofibroblast, fibroblast, collagen, regenerative medicine, tissue engineering, immunomodulation, neovascularization and angiogenesis modulating agents. Inclusion criteria included animal studies, randomized controlled trials, case-control studies and reviews that were relevant for elucidating the anti-fibrotic effect of ADSCs, applied to multiple features of fibrosis (*e.g.*, dermal fibrosis after radiotherapy, hypertrophic scars, burns, sclerodermia) Exclusion criteria comprised of articles solely about clinical outcome measures, case reports, case series and literature focused on the technique of fat grafting. Language has been restricted to English. A structured summary of the review process is illustrated in Figure 1.

RESULTS

Mechanisms leading to fibrosis

Introduction and histology of fibrosis: Fibrosis is caused by a dysregulation of regular wound-healing (mostly through sustained injury), leading to an excessive deposition of ECM, persisting inflammatory reaction and reduced vascularization.

ECM is a non-cellular three-dimensional molecular network composed of proteins (*e.g.*, collagen, elastin, laminin, fibronectin) and ground substance (*e.g.*, glycosaminoglycans, such as hyaluronan and proteoglycans)[14-16]. The ECM regulates tissue development and homeostasis and constantly undergoes remodeling. Excessive accumulation of ECM components, such as collagens, fibronectin, proteoglycans, glycosaminoglycans and laminin are the typical characteristics of fibrosis regardless of the etiology[17]. Although all the beforementioned ECM components participate in the overall pathogenic process, collagen type I, collagen type III and fibronectin are the most dominating proteins found in fibrotic tissue[1,2]. Despite the fact that there is an increase in the amount of ECM, some ECM components (such as decorin) are less abundant in scars[13]. Besides the increase of ECM accumulation, fibrosis is also defined by a high amount of alfa-smooth muscle actin (α-SMA).

Microscopically, scar tissue (*e.g.*, after radiation) is characterized by flattening of the rete ridges, a thickened epidermis and dermis, and an irregular collagen organization (see Figure 2). Excessive proliferation of keratinocytes causes the epidermal thickening, while it is the excessive ECM that causes the thickened dermis. The abnormal collagen behavior displays itself in an increase in the number of collagens, altered fiber thickness, more cross-linking as well as a decreased degree of collagen organization[18].

Histological patterns do not only reflect the increased ECM deposition but also the enhanced inflammation and reduced vascularization, through decreased vessel density, microvascular obliteration and abnormal vascularization patterns[12].

ECM accumulation

The homeostasis of the ECM is a well-regulated process influenced by a variety of actors and is subject

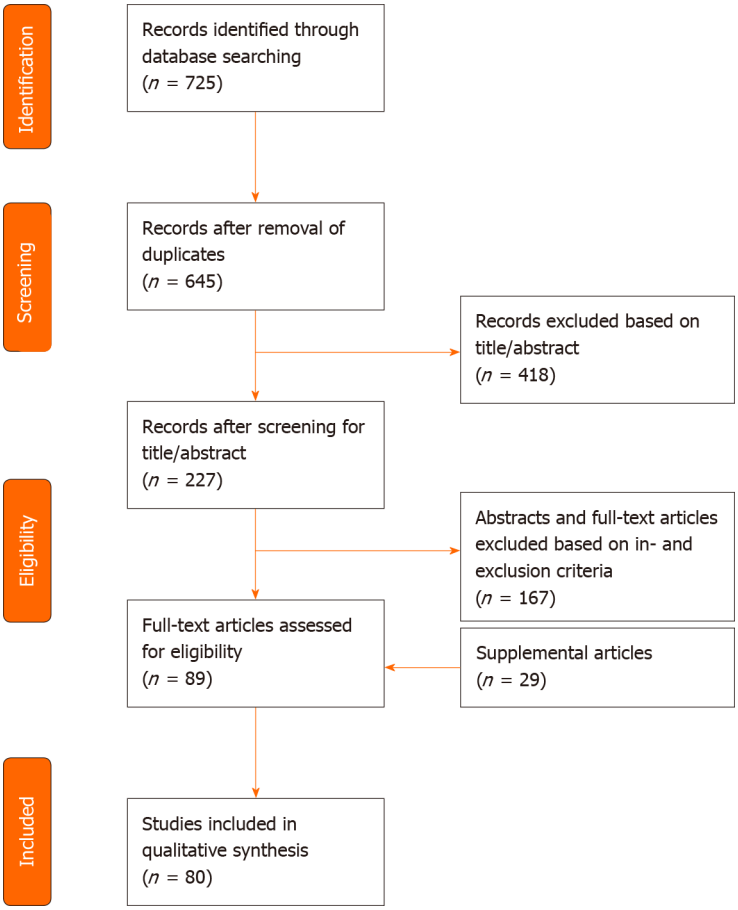

Figure 1 PRISMA flow diagram of search strategy and study selection.

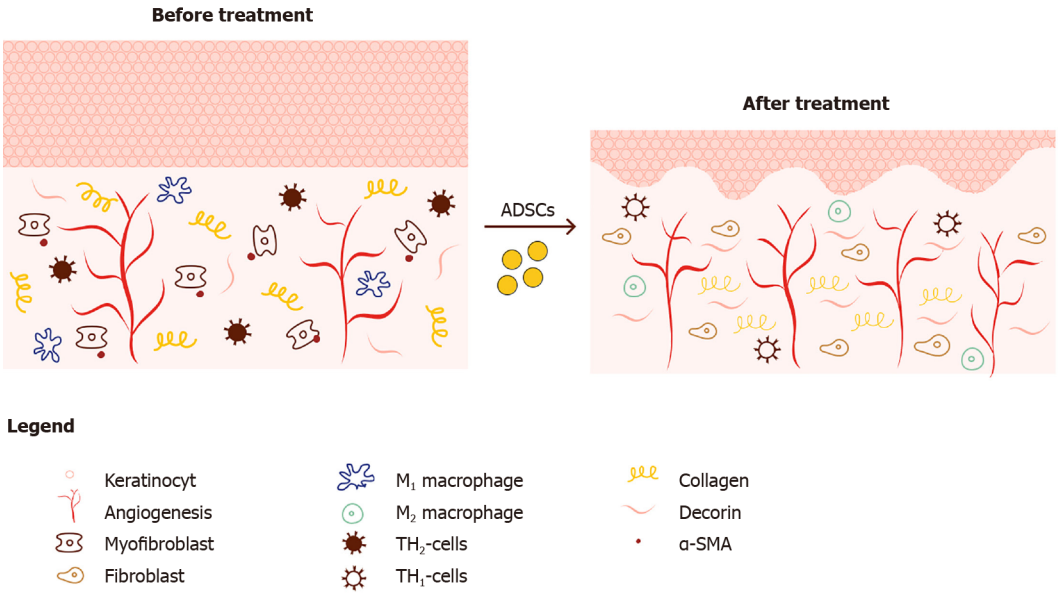

Figure 2 Schematic overview of histological changes in dermal scars before and after treatment with ADSC's.

to four major delicate balances. In fibrosis these balances are dysregulated, favoring deposition over degradation which results in overproduction of ECM.

Imbalance between fibroblasts and myofibroblasts: Fibroblasts play a crucial role in tissue homeostasis by regulating the ECM, which is constantly being synthesized, degraded and remodeled [19]. However, when fibroblasts can no longer coordinate this meticulous cross talk and interplay of cells and factors in an environment of chronic inflammation or repeated tissue damage, they transform

into professional repair cells *i.e.*, myofibroblasts. Myofibroblasts do not typically appear in healthy connective tissue[20]. Myofibroblasts produce large amounts of ECM and are capable of contraction, due to the expression of α-SMA[21]. Juhl *et al*[19] found that cytokines and growth factors such as interleukin 6 (IL-6), platelet-derived growth factor, and transforming growth factor-beta 1 (TGF-β1) facilitate a prolonged myofibroblast activation, which results in excessive ECM production manifested as fibrosis.

Imbalance between TIMPs and MMPs: Fibrotic tissue can be characterized by a decreased matrix metalloproteinase (MMP)/tissue inhibitors of metalloproteinases (TIMPs) ratio resulting in ECM accumulation. ECM degradation enzymes called MMPs, *vs* their opposing tissue inhibitors known as TIMPs also play a role in ECM remodeling. MMPs are endopeptidases, mainly produced by macrophages (12), and are categorized by their substrates and structure, into collagenases, gelatinases (MMP-2 and MMP-9), stromelysins, membrane-type-MMPs and others.

Zhao *et al*[2] show that fibrillar collagen, the pre-dominant structural protein in fibrotic tissue, is cleaved by MMP1, MMP8, MMP13, MMP14, MMP16, and MMP18, allowing other MMPs such as gelatinases (MMP2 and MMP9), to further degrade collagen (see Figure 3). Several mice studies confirm the relation of a certain MMP-deficiency or -stimulation with development of fibrosis or protection against fibrosis, respectively[12,22,23]. The opposite is applicable for TIMPs; TIMP upregulation has been associated with fibrosis[24]. This general classification however does not seem to be valid for all MMP and TIMP subtypes. The role of MMP-2 and MMP-9 is for example less clear, and MMP-9 has been associated with pro-fibrotic characteristics[25].

TGF-β1 and plasminogen activator inhibitor 1 (PAI1) are major regulators of the MMP and TIMP expression[26,27]. The persistent activation and/or production of PAI1, resulting in MMP inhibition, directly stimulates fibrosis (see Figure 3). TGF-β1 also decreases the MMP/TIMP ratio, as will be further detailed in 'Imbalance between multiple functions of TGF-b1 in regular vs hypertrophic scarring'. Fibroblasts derived from several fibrotic conditions such as keloid scars and scleroderma have demonstrated elevated levels of PAI1[27,28]. On the contrary, PAI1 deficiency protects mice from bleomycin induced lung fibrosis[27]. Taken together, upregulation of PAI1 substantially contributes to fibrosis. PAI1 is upregulated by TGF-β1, IL-1b, hypoxia and others. Ghosh *et al*[27] suggest that the increase of PAI1 Levels in fibroblasts from patients with scleroderma is linked to the activation of TGFβ 1/ SMAD axis.

Imbalance between organized and unorganized collagen fibers: Collagen organization can also influence the ECM balance through the extent in which they are cross-linked. Multiple fibrotic organ types show that crosslinking is disproportionately present and contribute to decreased ECM degradation and increased tissue stiffness[2]. Thus, fibrosis is characterized by favoring unorganized and cross-linked collagen, over normal collagen organization.

Imbalance between multiple functions of TGF-β1 in regular *vs* hypertrophic scarring: Continuous activation of TGF-β1/Smad axis has been reported to mediate the excessive production of ECM without appropriate remodeling. In a study by Juhl *et al*[19], TGF-β-treated human dermal fibroblasts showed an increase in collagen I, fibronectin gene and protein levels. They also observed a gene-upregulation of α-SMA, type III, IV and V collagen, fibronectin and TGF-β1 genes, while type VI collagen was downregulated. In experimental animal studies, constitutive activation of TGF-β1 signaling leads to organ fibrosis, while inhibition of TGF-β1 reduces fibrosis[29].

The pro-fibrotic feature of TGF-β1 is multifactorial. TGF-β1 signaling stimulates directly the ECM accumulation by increasing the synthesis of ECM components such as collagen, fibronectin, elastin, proteoglycans, fibrillin and laminin[2]. TGF-β1 also enhances ECM production indirectly by inhibiting MMPs and stimulating TIMPs[26]. TGF-β1 induces fibroblast-to-myofibroblast differentiation, which results in the secretion of additional ECM components and which facilitates tissue contraction[2]. The entire TGF-β1 pathway promotes collagen cross-linking and leads to increased rigidity and decreased ECM degradation. The main sources of TGF-β1 production are fibroblasts and activated immune cells such as macrophages. Both of these are reciprocally upregulated by the presence of TGF-β1 creating a positive 2nd order TGF-β1 production loop.

The TGF-β1/Smad axis is also critical in regular wound healing, exerting influence on both the inflammation and revascularization processes. TGF-β1 increases inflammation by drawing neutrophils and monocytes to the injury environment and stimulates the differentiation of monocytes into activated macrophages[30]. However, TGF-β1 may also induce anti-inflammatory effects[31,32]. This duality may be explained by its double origin (from macrophages or T-cells)[31] or by the distinctive temporal expression patterns during the sequential phases in wound repair[30].

Role of the innate and adaptive immune response in fibrosis

Aside from ECM accumulation, fibrosis is also driven by persistent low-grade inflammation, sustained by both the innate and adaptive immune response[31]. Multiple mechanisms lead to this increased or prolonged inflammation.

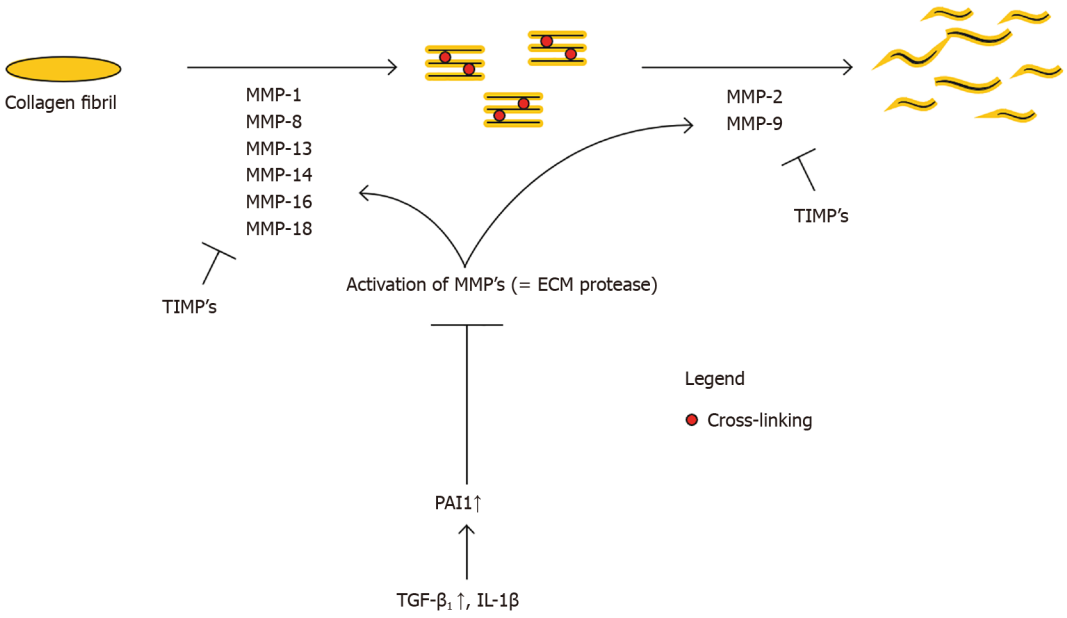

Figure 3 Collagen degradation. Collagen type 1 and type 3 are the predominant collagen types in fibrosis. ECM homeostasis requires a balance between collagen production and collagen degradation. MMPs manage the collagen degradation, while TIMPs inhibit MMPs, therefore inhibiting degradation. MMPs need activation, which is inhibited by PAI1. So, when TGF-β_1 increases, PAI1 renders more inhibition of MMPs activation, therefore inhibiting ECM turnover/ remodeling and increasing fibrosis. MMP: Matrix metalloproteinase; TIMP: Tissue inhibitor of metalloproteinase; TGF-β1: Transforming growth factor beta; IL-1β: Interleukin-1β; PAI1: Plasminogen activator inhibitor 1.

The first mechanism is governed by an increase of pro-inflammatory cytokines. Adipocytes, in a stress situation (*e.g.*, radiotherapy), synthesize pro-inflammatory proteins such as tumor necrosis factor-α (TNF-α), IL-6 and IL-8[33]. IL-6 also has pro-fibrotic features by persistent stimulation of fibroblasts, which may lead to the differentiation into myofibroblasts[19]. Furthermore, various innate inflammatory cells (*e.g.*, macrophages, neutrophils, mast cells and eosinophils) secrete a multitude of growth factors and cytokines, such as TNF-α, IL-1β. Studies by Miyazaki *et al*[34] and Kolb *et al*[35] found that mice who overexpress TNF-α or IL-1β in the lung, develop pulmonary fibrosis. In turn, TNF-α and IL-1β also increase expression of IL-6[31].

The second mechanism that leads to prolonged inflammation is *via* macrophages. Macrophages are vital in the wound healing process. However, redundant infiltration, overactivation, lack of differentiation and lack of clearance result in fibrotic tissue formation[18,36]. This pro-fibrotic activity manifests itself mostly in the early phases of the wound-healing process and results in the production of inflammatory mediators that can aggravate tissue injury, such as TNF-α, IL-1β, and a variety of toxic mediators, such as reactive oxygen and nitrogen species. Moreover, macrophages are known to produce the pro-fibrotic TGF-β1. Duffield *et al*[37] reported that early macrophage depletion effectively reduced the development of liver fibrosis in mice. Wynn *et al*[31] showed that limiting the pro-inflammatory activity of innate myeloid-lineage cells (incl. macrophages) may successfully treat fibrotic diseases. In later stages of the wound-healing process, a subset of macrophages convert into a suppressive phenotype and express multiple anti-inflammatory mediators (*e.g.*, IL-10, Arg1, Relm-α,…) that direct the resolution of the inflammatory response[38].

Furthermore, one can distinguish anti-inflammatory/pro tissue repair macrophages (M2) from pro-inflammatory/pro-fibrotic (M1) macrophages[39]. Thus, the balance between both types also plays a role in the pathogenesis of fibrosis. Multiple studies[40,41] observed that M2 macrophages suppress fibrosis and reduce inflammation by competing with T-helper 2 (TH2) cells and fibroblasts for l-arginine. This competition reduces the TH2 response and suppresses collagen synthesis by myofibroblasts[31]. Furthermore, literature[38] indicates that M2 cells are important inducers of regulatory T-cells, that have an anti-fibrotic effect.

It seems useful to target the inflammatory cascade and the innate immune response, to treat fibrotic disorders. However, the extent of fibrosis is not per se linked with the severity of inflammation, which suggests that other immunological mechanisms, such as the adaptive immune response, play an important role in the fibrotic process. Wynn[42] described how the TH1/TH2 paradigm seems to play a key role in sustaining the immune response. There are 3 types of T helper cells; TH1 CD4+ T cells, TH2 CD4+ T cells and regulatory T cells. This categorization is based on the cytokines each of these cells secrete.

TH1 cells are predominant in the initial response of the adaptive immune system to chronic injury. TH1 cells mainly secrete interferon-γ (IFN-γ) and IL-12, as well as associated pro-inflammatory cytokines. The TH1 responses are pro-inflammatory yet anti-fibrotic. They directly inhibit collagen

production by fibroblasts, stimulate ECM degradation by favoring MMPs over TIMP and inhibit TGF-b1 production[43]. Moreover, they indirectly inhibit fibrosis by reducing pro-fibrotic cytokine expression by TH2 cells (*e.g.*, IL-13)[44].

However, when the stimulus persists, TH2 cells and regulatory T cells collaborate to suppress the TH1 response to prevent the immune system from causing additional damage. In their response, TH2 cells mainly secrete IL-4, IL-5 and IL-13[44]. These factors stimulate fibrosis by enhancing collagen deposition through various mechanisms. On top of that, IL-13 specifically strengthens the pro-fibrotic TGF-β1-SMAD mechanism, while also independently stimulating collagen production by fibroblasts[45-48]. Therefore, despite TH2's facilitating function in wound healing, their response contributes to fibrosis. Specifically applied to post-irradiation fibrosis, Buttner *et al*[49] showed the increased concentrations of IL-4.

At last, the regulatory T-cells mainly secrete IL-10, which is anti-fibrotic by directly suppressing collagen synthesis by fibroblasts, and cooperates with TH1 cytokines to suppress collagen deposition [50-52].

Reduced vascularization

Radiation injury on the skin is characterized by microvascular obliteration and poor revascularization. The reduced vascularization results in diminished transport of oxygen, nutrients and essential factors of the immune system to the damage tissues. In the end, this may lead to the deterioration of the hypoxia, resulting in fibrosis.

DISCUSSION

Anti-fibrotic effect of ADSCs on scar tissue by fat grafting

Histological changes mediated by ADSCs on scar tissue: When injecting ADSCs into a fibrotic injury environment through fat grafting, multiple histological changes occur (see Figure 2). A restoration of the normal skin ridge pattern is observed. Several animal models[23,53] and *in vitro* models[12,54] show a decrease in ECM components' deposition such as collagen I, collagen III, fibronectin and elastin. The expression of α-SMA, SMAD-3 proteins and TGF-β1 seems to be decreased while the amount of decorin and MMP-1/TIMP-1 ratio is increased[12]. Furthermore, Zonari *et al*[55] and Zhang *et al*[53] show improved collagen fiber alignment, organization and less cross-linking. One can also distinguish a decrease in pro-inflammatory mediators/profibrotic factors (*e.g.*, IL-6, IL-8, connective tissue growth factor)[12]. Finally, an increase in vascularization and a normalization of the microvascular architecture is observed[13].

This histological overview is however not exhaustive. Multiple other factors and substances are impacted by the insertion of a fat graft, which will be further described through the impact they have on the key molecular balances of fibrosis.

Anti-fibrotic effect through ADSCs

The antifibrotic potential of ADSC can be exerted in a direct or indirect fashion.

ADSCs as multipotent progenitor cells: ADSCs are multipotent progenitor cells that have the intrinsic possibility to differentiate into various sorts of cells that play a role in the wound-healing process (*e.g.*, fibroblasts, keratinocytes, osteocytes, neural cells, endothelial cells, *etc*.). These ADSC cell products can in turn cause tissue regeneration and cell restoration[7]. ADSCs can also differentiate into mature adipocytes and serve as building blocks for a subcutaneous adipose layer that adds elasticity and pliability to the skin and volume required for thermoregulation. Adipogenesis is key for the effectiveness of ADSCs/fat grafts as it preserves the necessary fat tissue[33].

Paracrine: Moreover, ADSCs produce a myriad of trophic factors, which influence the formation and modulation of the ECM, and interact with the immune response and angiogenesis[7,13,30,32] (see Figure 4).

Interference with excessive ECM formation

Influence on fibroblast to myofibroblast differentiation: Studies show that gene expression of the pro-fibrotic marker α-SMA, produced specifically by myofibroblasts, is decreased upon administration of ADSCs[23,53,55,56]. Borovikova *et al*[30] describe multiple mechanisms: ADSCs inhibit the fibroblast-to-myofibroblast differentiation by secreting hepatocyte growth factor (HGF), IL-10 and p53. ADSCs also stimulate myofibroblast apoptosis by the secretion of basis fibroblast growth factor (bFGF) *via* the Rho/Rho kinase pathway and HGF *via* the FAK-extracellular signal-regulated kinase (ERK)-MMP signaling pathway. FGF is also reported to reverse the myofibroblast phenotype through its activation of ERK/MAP kinase pathway.

MMP *vs* TIMP balance: The administration of ADSCs by lipofilling has an antifibrotic effect by modulating MMP/TIMP ratio by various pathways (see Figure 5).

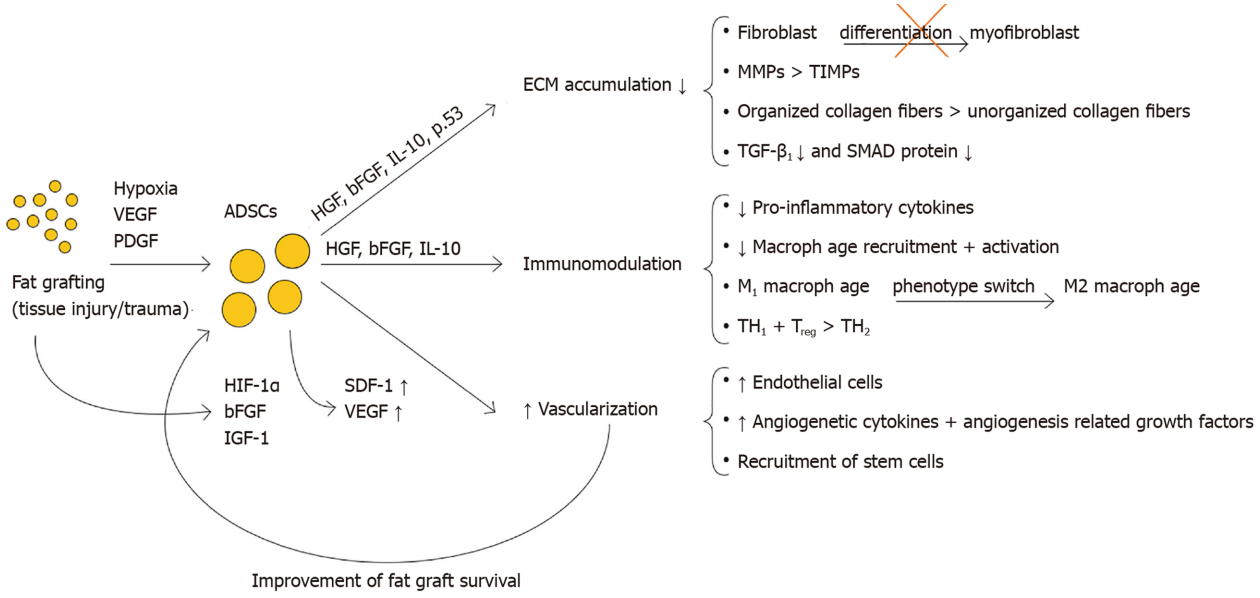

Figure 4 Main mechanisms of adipose-derived stromal cells antifibrotic action and their most important paracrine factors. VEGF: Vascular endothelial growth factor; PDGF: Platelet-derived growth factor; ADSCs: Adipose-derived stromal cells; HGF: Hepatocyte growth factor; bFGF: Basic fibroblast growth factor; IL-10: Interleukin-10; HIF-1β: Hypoxia-inducing factor-1β; IGF-1: Insulin-like growth factor-1; MMP: Matrix metalloproteinase; TIMP: Iissue inhibitor of metalloproteinase; TH1: T helper 1 cells; TH2: T helper 2 cells; Treg: Regulatory T cells.

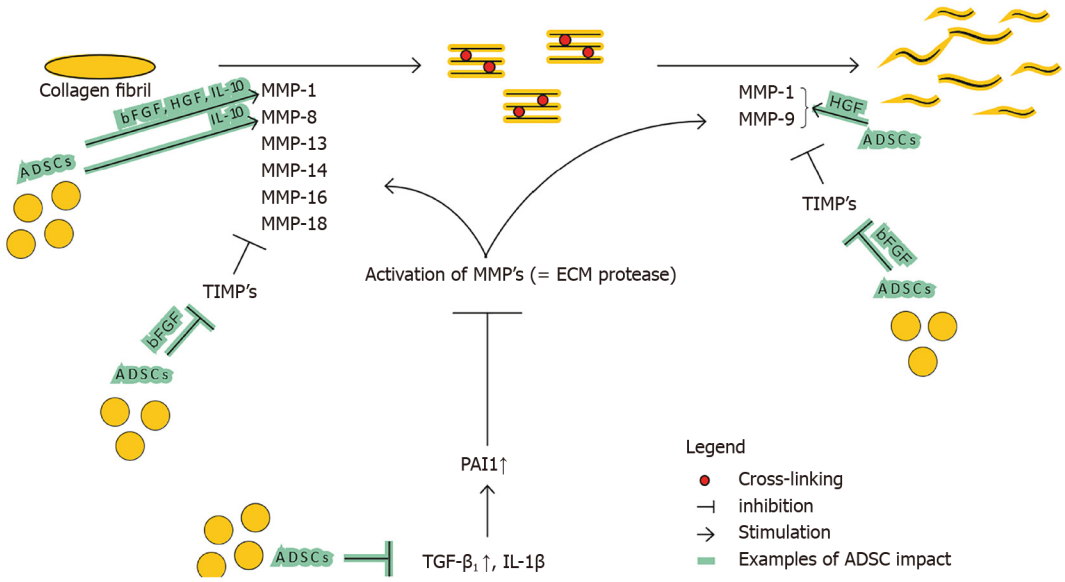

Figure 5 Impact of adipose-derived stromal cells on matrix metalloproteinase and tissue inhibitor of metalloproteinase balance. ADSCs: Adipose-derived stromal cells; MMP: Matrix metalloproteinase; TIMP: Tissue inhibitor of metalloproteinase; TGF-β1: Transforming growth factor beta; IL-1β: Interleukin-1β; PAI1: Plasminogen activator inhibitor 1; HGF: Hepatocyte growth factor; bFGF: Basic fibroblast growth factor; IL-10: Interleukin-10.

Deng *et al*[12] show that ADSCs enhance ECM degradation by increasing MMP-1/TIMP-1 ratio. On top of that, Spiekman *et al*[54] show that ADSCs promote the expression of MMP-1, MMP-2 and MMP-14. Presumably ADSCs enhance the ratio in favor of degradation by decreasing the major regulator of MMP and TIMP expression, TGF-β1. Decreased SMAD signaling also decreases the other crucial director, PAI1 which in turn results in MMP activation. Furthermore, ADSCs secrete HGF, which activates MMP-1, MMP-2 and MMP-9[57,58]. ADSCs also produce bFGF and IL-10 that influence the ratio significantly. IL-10 does this by increasing MMP-1 and MMP-8, and bFGF presumably by increasing MMP-1 and decreasing TIMP-1 expression[59-61]. bFGF also stimulates HGF production, strengthening the said HGF effect.

Finally, not all MMPs and TIMPs will necessarily have a singular effect (*e.g.*, increase of MMP-9 can in certain circumstances be pro-fibrotic *vs* the anti-fibrotic effect of other MMPs).

Improvement of collagen linking: Zonari *et al*[55] and Zhang *et al*[53] show improved collagen fiber alignment, organization and less cross-linking when ADSCs are inserted into the fibrotic injury environment. Given that cross-linking contributes to decreased ECM degradation[2], this decreased crosslinking has an anti-fibrotic effect.

TGF-b1/Smad axis: Section 'Imbalance between multiple functions of TGF-β1 in regular *vs* hypertrophic scarring' described the pro-fibrotic feature of the TGF-β1/Smad axis, through its multifactorial influence on the key mentioned balances leading to ECM accumulation, and thus fibrosis. Studies by Zonari *et al*[55], Uysal *et al*[56] and Spiekman *et al*[54], report that ADSCs decrease the presence of TGF-β1 as well as SMAD 2 and SMAD 3 proteins. An effect possibly contributing to this is given by Ejaz *et al*[62], who in their study describe a downregulation of TGF-β1 as a result of increased concentrations of HGF (also secreted by ADSCs). In turn, decreased TGF-β1 reduces ECM accumulation both through its direct as well as indirect effects (by reducing myofibroblast activation, favoring MMPs over TIMPs and decreasing collagen cross-linking), all mitigating fibrosis.

For completeness on ADSC impact, one can mention the impact of another member of the TGF-β cell group, *i.e.*, TGF-β3. Impacting the TGF-β1/TGF-β3 balance towards increasing TGF-β3, is linked to reduced scar formation in adult wound healing[30]. Multiple studies[23,55,63] have shown such an increase of TGF-β3 in fibrotic tissue after injection of ADSCs, resulting in decreased tissue stiffness.

Immunomodulation: The anti-fibrotic effect of ADSCs through their impact on elements of both the innate and adaptive immune response, has multiple facets.

ADSCs downregulate key pro-inflammatory cytokines. Carceller *et al*[64] indicates that, in an *in vivo* mouse model, ADSCs effectively suppress the inflammatory response through the downregulation of selected inflammatory mediators (*e.g.*, IL-1b, TNF-α, IL-6, leukotriene B4). A similar effect of ADSCs could be seen through their secretion of HGF, which is documented to lead to a decrease of pro-inflammatory cytokines (TNF-α, IL-12, monocyte chemoattractant protein 1, IFN-g) in a fibrosis model[30]. Also, ADSCs have the potency to modulate macrophage recruitment and activation, mostly by secreting bFGF, HGF and IL-10[30]. Kotani *et al*[32] show that ADSCs induce apoptosis of activated macrophages, and reduce infiltrations of macrophages, neutrophils and T lymphocytes. Therefore, through their immunomodulatory ability, ADSCs have an inhibitory effect on active macrophages. Moreover, Xie *et al*[65] showed that ADSCs promote a macrophage phenotype switch, favoring the anti-inflammatory M2 phenotype over the pro-inflammatory M1 in a mouse model.

Finally, ADSCs exhibit a suppressive effect on lymphocyte responses and induce a phenotypic conversion of T-cells. Kotani *et al*[32] describes, in the context of pulmonary fibrosis, that ADSCs inhibit the differentiation and proliferation of Th2-type mCD4+ T cells while promoting this for regulatory T cells. Given the pro-fibrotic effect of TH2-cells (see section 'Role of the innate and adaptive immune response in fibrosis'), this could suggest the phenotypic conversion of T cells as an important mechanism underlying the anti-inflammatory effect of ADSCs. Cho *et al*[66] in turn suggest that ADSCs have an inhibitory effect on inflammatory diseases either directly or by inducing T-Regulatory cells (through PGE2 and TGF-β1) and inhibiting TH2 cytokines.

Pro-angiogenic effect of fat grafting and ADSCs

Stimulating angiogenesis and revascularization has a positive effect on fibrosis. Rebuilding natural blood flow improves the delivery of supplemental oxygen and other key substances to the injury site. On top of that, angiogenesis allows for better survival of administered ADSC/fat grafts in general, enhancing beforementioned treatment effects. Evans *et al*[67] describe how ADSCs, like bone marrow-derived mesenchymal stem cells, have the capacity to differentiate into endothelial cells (ECs), that provide the required cellular building blocks for angiogenesis.

Additionally ADSCs secrete an array of pro-angiogenetic cytokines and growth factors such as HGF, vascular endothelial growth factor (VEGF), bFGF, G-CSF, GM-CSF, IL-7, M-CSF, stromal cell-derived factor-1 (SDF-1), *etc*.[33,68]. These factors may promote the angiogenic sprouting process based on endothelial cell migration, proliferation and tube formation[69].

In response to entering a hypoxic environment, ADSCs activate hypoxia-inducing factor-1α (HIF-1α), and release bFGF and insulin-like growth factor-1 (IGF-1), that in turn promote neovascularization by establishing high levels of VEGF at the graft site. This VEGF promotes EC proliferation and migration to the graft, as well as inhibits EC apoptosis[70]. Studies also show[71-73] that high quantities of VEGF found at the grafting site, promote monocyte differentiation into M2 type macrophages, reducing fibrosis. On the paracrine side, increasingly more literature details the importance of SDF-1 in angiogenesis. Murohara *et al*[68] states that SDF-1 Likely plays a key role in the ADSC-mediated angiogenesis. Other studies mention that SDF-1, like VEGF, improves revascularization and angiogenesis by recruiting stem cells such as endothelial progenitor cells and hematopoietic stem cells to the engrafted/ischemic site. It is reported that SDF-1/CXCR4 axis exerts one of the strongest chemotactic effects on BMSCs[74,75].

Macrophages play an important role in angiogenesis. Cai *et al*[76] reported that early macrophage infiltration in the graft environment appears to be key for angiogenesis and revascularization. However, when present for an extended period of time they can stimulate fibrosis. By initially releasing

angiogenetic cytokines (*e.g.*, VEGF, bFGF), macrophages stimulate vessel growth in a VEGF-dependent manner, while also generating recruitment signals for stem cells such as ECs. On top of that, M2 macrophages are a major source of SDF-1. Through all this, the macrophages role in angiogenesis is regulated in an important, though delicate and time-sensitive balance. ADSCs influences this balance, by stimulating a phenotype switch to M2 macrophages and by inhibiting a prolonged infiltration. Further research needs to clarify the impact of ADSCs on early macrophage infiltration, possibly through M-CSF.

Finally, it must be stated that in select cases of fibrosis (*e.g.*, liver fibrosis), angiogenesis can have a fibrosis stimulating effect[77]. This paradox indicates that the anti-fibrotic effect of ADSCs through angiogenetic stimulation, is case-dependent and remains particularly complex.

CONCLUSION

When injected into fibrotic tissue by using fat grafts, ADSCs exert anti-fibrotic and pro-angiogenic effects by impacting multiple distinctive mechanisms. Through their capacity to directly differentiate into key cell types that influence the wound healing process, as well as secrete multiple paracrine factors (*e.g.*, HGF, bFGF, IL-10), they carefully alter different mechanisms underlying fibrosis. ADSCs favor ECM degradation by modifying the fibroblast-to-myofibroblast differentiation, by favoring MMPs over TIMPs, by positively influencing collagen organization, and by inhibiting the pro-fibrotic effects of TGF-β1. In addition ADSCs influence both the innate and adaptive immune response system. The pro-angiogenic effect of ADSCs can be categorized into direct (direct differentiation into ECs) as well as indirect effects (secreting pro-angiogenic cytokines such as stromal cell-derived factor-1 and VEGF).

Increasingly more *in vitro* and *in vivo* studies tend to focus on the development of anti-fibrotic drugs on a single aspect of fibrosis, not considering the complex interactions nor the time dependency of these mechanisms. This review has shown that the understanding of the complex interaction between ECM accumulation, immune response and vascularization, is vital for the effectiveness of treatments against fibrosis, like fat grafting.

ADSCs have the ability to interact intensively *via* multiple mechanisms-of action. They intelligently steer multiple molecular balances in an anti-fibrotic or pro-angiogenic direction in a delicate manner. It is by these synergistic actions that ADSCs injected through fat grafts successfully soften fibrotic scars.

ARTICLE HIGHLIGHTS

Research background

The successful anti-fibrotic effect of clinical fat grafting has been described extensively in literature. However, the mechanisms leading to fibrosis and how adipose-derived stomal cells (ADSCs) can interact with these mechanisms to reduce fibrosis, are far from clarified today.

Research motivation

Fibrosis is increasingly recognized as an important cause for morbidity and mortality. Moreover, the increasing clinical use of radiotherapy results in an enhanced incidence of severe tissue damage by fibrosis. Therefore, an efficient anti-fibrotic treatment and a thorough understanding of its mechanism-of-action is mandatory.

Research objectives

The objective of this systematic review was to obtain an in-depth understanding of the complex mechanisms underlying fibrosis, and more specifically, the potential mechanisms-of-action of ADSCs in realizing their anti-fibrotic effect.

Research methods

This systematic review was conducted according to the PRISMA (Preferred Reporting Items for Systematic Reviews and Meta-Analyses) methodology. We clearly defined a set of objectives with pre-defined eligibility criteria. We performed a thorough and disciplined literature search to obtain all relevant studies that met the eligibility criteria.Each citation is associated with a set of Mesh terms that describe the content.

Research results

Systematic assessment of available literature was performed by two reviewers and one control to avoid bias. This process resulted in 80 references cited as reported in the PRISMA flow diagram. These references served as basic scientific platform to investigate the previously mentioned research objectives. Due to some contradictory findings in the molecular balances, we performed a supple-

mentary literature search trying to elucidate some of the more specific mechanisms-of-action. This review has shown that the understanding of the complex interaction between extracellular matrix (ECM) accumulation, immune response and vascularization, is vital for the effectiveness of treatments against fibrosis, like fat grafting.

Research conclusions

ADSCs have the ability to interact intensively with the healing environment *via* multiple mechanisms of action. Through their capacity to directly differentiate into key cell types that influence the wound healing process, as well as secrete multiple paracrine factors, ADSCs meticulously alter distinctive mechanisms underlying fibrosis. ADSCs stimulate ECM degradation by modifying the fibroblast-to-myofibroblast differentiation, by favoring matrix metalloproteinase over tissue inhibitors of metalloproteinases, by positively influencing collagen organization, and by inhibiting the pro-fibrotic effects of transforming growth factor-beta 1. In addition, ADSCs influence both the innate and adaptive immune response system. The pro-angiogenic effect of ADSCs exerted by direct differentiation into ECs, as well as by the secretion of pro-angiogenic cytokines such as stromal cell-derived factor-1 and vascular endothelial growth factor. ADSCs intelligently steer these molecular balances in a delicate manner. It is by these synergistic actions that ADSCs injected through fat grafts successfully soften fibrotic scars.

Research perspectives

This thorough systematic review describes the intensive and cross talk of ADSCs with surrounding cells and active molecules all having a significant effect on the outcome of fibrosis. This manuscript invites to further research to unravel the complex interactions of ADSCs and the seemingly contradictory effects depending on time and place of occurrence.

ACKNOWLEDGEMENTS

We would like to thank Prof. Opdenakker G, Professor of Microbiology and Immunology, Chairman BoD, Rega Institute, KU Leuven, for his expert opinion and guidance.

FOOTNOTES

Author contributions: The selection of articles was performed independently by both authors; Vanderstichele S conducted the systematic review, with Vranckx JJ providing scientific content and supervision; all authors have read and approved the final manuscript.

Conflict-of-interest statement: This article is not subject to any conflict of interest or financial disclosure.

PRISMA 2009 Checklist statement: The authors have read the PRISMA 2009 Checklist, and the manuscript was prepared and revised according to the PRISMA 2009 Checklist.

Country/Territory of origin: Belgium

ORCID number: Sophie Vanderstichele 0000-0001-7918-9376; Jan Jeroen Vranckx 0000-0002-0920-8620.

S-Editor: Wu YXJ
L-Editor: A
P-Editor: Li X

REFERENCES

1 **Milenkovic U**, Albersen M, Castiglione F. The mechanisms and potential of stem cell therapy for penile fibrosis. *Nat Rev Urol* 2019; **16**: 79-97 [PMID: 30367131 DOI: 10.1038/s41585-018-0109-7]
2 **Zhao X**, Kwan JYY, Yip K, Liu PP, Liu FF. Targeting metabolic dysregulation for fibrosis therapy. *Nat Rev Drug Discov* 2020; **19**: 57-75 [PMID: 31548636 DOI: 10.1038/s41573-019-0040-5]
3 **Zuk PA**, Zhu M, Mizuno H, Huang J, Futrell JW, Katz AJ, Benhaim P, Lorenz HP, Hedrick MH. Multilineage cells from

human adipose tissue: implications for cell-based therapies. *Tissue Eng* 2001; **7**: 211-228 [PMID: 11304456 DOI: 10.1089/107632701300062859]

4 **Zuk PA**, Zhu M, Ashjian P, De Ugarte DA, Huang JI, Mizuno H, Alfonso ZC, Fraser JK, Benhaim P, Hedrick MH. Human adipose tissue is a source of multipotent stem cells. *Mol Biol Cell* 2002; **13**: 4279-4295 [PMID: 12475952 DOI: 10.1091/mbc.e02-02-0105]

5 **Coleman SR**. Long-Term Survival of Fat Transplants: Controlled Demonstrations. *Aesthetic Plast Surg* 2020; **44**: 1268-1272 [PMID: 32766917 DOI: 10.1007/s00266-020-01847-3]

6 **Naderi N**, Combellack EJ, Griffin M, Sedaghati T, Javed M, Findlay MW, Wallace CG, Mosahebi A, Butler PE, Seifalian AM, Whitaker IS. The regenerative role of adipose-derived stem cells (ADSC) in plastic and reconstructive surgery. *Int Wound J* 2017; **14**: 112-124 [PMID: 26833722 DOI: 10.1111/iwj.12569]

7 **Shukla L**, Yuan Y, Shayan R, Greening DW, Karnezis T. Fat Therapeutics: The Clinical Capacity of Adipose-Derived Stem Cells and Exosomes for Human Disease and Tissue Regeneration. *Front Pharmacol* 2020; **11**: 158 [PMID: 32194404 DOI: 10.3389/fphar.2020.00158]

8 **Deinsberger J**, Reisinger D, Weber B. Global trends in clinical trials involving pluripotent stem cells: a systematic multi-database analysis. *NPJ Regen Med* 2020; **5**: 15 [PMID: 32983575 DOI: 10.1038/s41536-020-00100-4]

9 **Mora C**, Serzanti M, Consiglio A, Memo M, Dell'Era P. Clinical potentials of human pluripotent stem cells. *Cell Biol Toxicol* 2017; **33**: 351-360 [PMID: 28176010 DOI: 10.1007/s10565-017-9384-y]

10 **Opdenakker G**, Van Damme J, Vranckx JJ. Immunomodulation as Rescue for Chronic Atonic Skin Wounds. *Trends Immunol* 2018; **39**: 341-354 [PMID: 29500031 DOI: 10.1016/j.it.2018.01.010]

11 **Hendrickx B**, Verdonck K, Van den Berge S, Dickens S, Eriksson E, Vranckx JJ, Luttun A. Integration of blood outgrowth endothelial cells in dermal fibroblast sheets promotes full thickness wound healing. *Stem Cells* 2010; **28**: 1165-1177 [PMID: 20506500 DOI: 10.1002/stem.445]

12 **Deng J**, Shi Y, Gao Z, Zhang W, Wu X, Cao W, Liu W. Inhibition of Pathological Phenotype of Hypertrophic Scar Fibroblasts Via Coculture with Adipose-Derived Stem Cells. *Tissue Eng Part A* 2018; **24**: 382-393 [PMID: 28562226 DOI: 10.1089/ten.TEA.2016.0550]

13 **Spiekman M**, van Dongen JA, Willemsen JC, Hoppe DL, van der Lei B, Harmsen MC. The power of fat and its adipose-derived stromal cells: emerging concepts for fibrotic scar treatment. *J Tissue Eng Regen Med* 2017; **11**: 3220-3235 [PMID: 28156060 DOI: 10.1002/term.2213]

14 **Kendall RT**, Feghali-Bostwick CA. Fibroblasts in fibrosis: novel roles and mediators. *Front Pharmacol* 2014; **5**: 123 [PMID: 24904424 DOI: 10.3389/fphar.2014.00123]

15 **Theocharis AD**, Skandalis SS, Gialeli C, Karamanos NK. Extracellular matrix structure. *Adv Drug Deliv Rev* 2016; **97**: 4-27 [PMID: 26562801 DOI: 10.1016/j.addr.2015.11.001]

16 **Vermeulen P**, Dickens S, Degezelle K, Van den Berge S, Hendrickx B, Vranckx JJ. A plasma-based biomatrix mixed with endothelial progenitor cells and keratinocytes promotes matrix formation, angiogenesis, and reepithelialization in full-thickness wounds. *Tissue Eng Part A* 2009; **15**: 1533-1542 [PMID: 19086805 DOI: 10.1089/ten.tea.2008.0246]

17 **Vranckx JJ**, Yao F, Eriksson E. Gene transfer of growth factors for wound repair. The epidermis in wound healing. Boca Raton, FL USA: CRC Press, 2004: 265-283

18 **El Ayadi A**, Jay JW, Prasai A. Current Approaches Targeting the Wound Healing Phases to Attenuate Fibrosis and Scarring. *Int J Mol Sci* 2020; **21** [PMID: 32046094 DOI: 10.3390/ijms21031105]

19 **Juhl P**, Bondesen S, Hawkins CL, Karsdal MA, Bay-Jensen AC, Davies MJ, Siebuhr AS. Dermal fibroblasts have different extracellular matrix profiles induced by TGF-β, PDGF and IL-6 in a model for skin fibrosis. *Sci Rep* 2020; **10**: 17300 [PMID: 33057073 DOI: 10.1038/s41598-020-74179-6]

20 **Hinz B**, Lagares D. Evasion of apoptosis by myofibroblasts: a hallmark of fibrotic diseases. *Nat Rev Rheumatol* 2020; **16**: 11-31 [PMID: 31792399 DOI: 10.1038/s41584-019-0324-5]

21 **Stempien-Otero A**, Kim DH, Davis J. Molecular networks underlying myofibroblast fate and fibrosis. *J Mol Cell Cardiol* 2016; **97**: 153-161 [PMID: 27167848 DOI: 10.1016/j.yjmcc.2016.05.002]

22 **Holmbeck K**, Bianco P, Caterina J, Yamada S, Kromer M, Kuznetsov SA, Mankani M, Robey PG, Poole AR, Pidoux I, Ward JM, Birkedal-Hansen H. MT1-MMP-deficient mice develop dwarfism, osteopenia, arthritis, and connective tissue disease due to inadequate collagen turnover. *Cell* 1999; **99**: 81-92 [PMID: 10520996 DOI: 10.1016/s0092-8674(00)80064-1]

23 **Yun IS**, Jeon YR, Lee WJ, Lee JW, Rah DK, Tark KC, Lew DH. Effect of human adipose derived stem cells on scar formation and remodeling in a pig model: a pilot study. *Dermatol Surg* 2012; **38**: 1678-1688 [PMID: 22804839 DOI: 10.1111/j.1524-4725.2012.02495.x]

24 **Aoki M**, Miyake K, Ogawa R, Dohi T, Akaishi S, Hyakusoku H, Shimada T. siRNA knockdown of tissue inhibitor of metalloproteinase-1 in keloid fibroblasts leads to degradation of collagen type I. *J Invest Dermatol* 2014; **134**: 818-826 [PMID: 24042342 DOI: 10.1038/jid.2013.396]

25 **Lim DH**, Cho JY, Miller M, McElwain K, McElwain S, Broide DH. Reduced peribronchial fibrosis in allergen-challenged MMP-9-deficient mice. *Am J Physiol Lung Cell Mol Physiol* 2006; **291**: L265-L271 [PMID: 16825657 DOI: 10.1152/ajplung.00305.2005]

26 **Finnson KW**, McLean S, Di Guglielmo GM, Philip A. Dynamics of Transforming Growth Factor Beta Signaling in Wound Healing and Scarring. *Adv Wound Care (New Rochelle)* 2013; **2**: 195-214 [PMID: 24527343 DOI: 10.1089/wound.2013.0429]

27 **Ghosh AK**, Vaughan DE. PAI-1 in tissue fibrosis. *J Cell Physiol* 2012; **227**: 493-507 [PMID: 21465481 DOI: 10.1002/jcp.22783]

28 **Tuan TL**, Wu H, Huang EY, Chong SS, Laug W, Messadi D, Kelly P, Le A. Increased plasminogen activator inhibitor-1 in keloid fibroblasts may account for their elevated collagen accumulation in fibrin gel cultures. *Am J Pathol* 2003; **162**: 1579-1589 [PMID: 12707042 DOI: 10.1016/s0002-9440(10)64292-7]

29 **Derrett-Smith EC**, Denton CP, Sonnylal S. Animal models of scleroderma: lessons from transgenic and knockout mice. *Curr Opin Rheumatol* 2009; **21**: 630-635 [PMID: 19730378 DOI: 10.1097/BOR.0b013e32833130c1]

30 **Borovikova AA**, Ziegler ME, Banyard DA, Wirth GA, Paydar KZ, Evans GRD, Widgerow AD. Adipose-Derived Tissue in the Treatment of Dermal Fibrosis: Antifibrotic Effects of Adipose-Derived Stem Cells. *Ann Plast Surg* 2018; **80**: 297-307 [PMID: 29309331 DOI: 10.1097/SAP.0000000000001278]

31 **Wynn TA**, Ramalingam TR. Mechanisms of fibrosis: therapeutic translation for fibrotic disease. *Nat Med* 2012; **18**: 1028-1040 [PMID: 22772564 DOI: 10.1038/nm.2807]

32 **Kotani T**, Masutani R, Suzuka T, Oda K, Makino S, Ii M. Anti-inflammatory and anti-fibrotic effects of intravenous adipose-derived stem cell transplantation in a mouse model of bleomycin-induced interstitial pneumonia. *Sci Rep* 2017; **7**: 14608 [PMID: 29097816 DOI: 10.1038/s41598-017-15022-3]

33 **Doornaert M**, Colle J, De Maere E, Declercq H, Blondeel P. Autologous fat grafting: Latest insights. *Ann Med Surg (Lond)* 2019; **37**: 47-53 [PMID: 30622707 DOI: 10.1016/j.amsu.2018.10.016]

34 **Miyazaki Y**, Araki K, Vesin C, Garcia I, Kapanci Y, Whitsett JA, Piguet PF, Vassalli P. Expression of a tumor necrosis factor-alpha transgene in murine lung causes lymphocytic and fibrosing alveolitis. A mouse model of progressive pulmonary fibrosis. *J Clin Invest* 1995; **96**: 250-259 [PMID: 7542280 DOI: 10.1172/JCI118029]

35 **Kolb M**, Margetts PJ, Anthony DC, Pitossi F, Gauldie J. Transient expression of IL-1beta induces acute lung injury and chronic repair leading to pulmonary fibrosis. *J Clin Invest* 2001; **107**: 1529-1536 [PMID: 11413160 DOI: 10.1172/JCI12568]

36 **Cai J**, Li B, Liu K, Li G, Lu F. Macrophage infiltration regulates the adipose ECM reconstruction and the fibrosis process after fat grafting. *Biochem Biophys Res Commun* 2017; **490**: 560-566 [PMID: 28625922 DOI: 10.1016/j.bbrc.2017.06.078]

37 **Duffield JS**, Forbes SJ, Constandinou CM, Clay S, Partolina M, Vuthoori S, Wu S, Lang R, Iredale JP. Selective depletion of macrophages reveals distinct, opposing roles during liver injury and repair. *J Clin Invest* 2005; **115**: 56-65 [PMID: 15630444 DOI: 10.1172/JCI22675]

38 **Murray PJ**, Wynn TA. Protective and pathogenic functions of macrophage subsets. *Nat Rev Immunol* 2011; **11**: 723-737 [PMID: 21997792 DOI: 10.1038/nri3073]

39 **Perciani CT**, MacParland SA. Lifting the veil on macrophage diversity in tissue regeneration and fibrosis. *Sci Immunol* 2019; **4** [PMID: 31604845 DOI: 10.1126/sciimmunol.aaz0749]

40 **Herbert DR**, Hölscher C, Mohrs M, Arendse B, Schwegmann A, Radwanska M, Leeto M, Kirsch R, Hall P, Mossmann H, Claussen B, Förster I, Brombacher F. Alternative macrophage activation is essential for survival during schistosomiasis and downmodulates T helper 1 responses and immunopathology. *Immunity* 2004; **20**: 623-635 [PMID: 15142530 DOI: 10.1016/s1074-7613(04)00107-4]

41 **Pesce JT**, Ramalingam TR, Mentink-Kane MM, Wilson MS, El Kasmi KC, Smith AM, Thompson RW, Cheever AW, Murray PJ, Wynn TA. Arginase-1-expressing macrophages suppress Th2 cytokine-driven inflammation and fibrosis. *PLoS Pathog* 2009; **5**: e1000371 [PMID: 19360123 DOI: 10.1371/journal.ppat.1000371]

42 **Wynn TA**. Fibrotic disease and the T(H)1/T(H)2 paradigm. *Nat Rev Immunol* 2004; **4**: 583-594 [PMID: 15286725 DOI: 10.1038/nri1412]

43 **Marth T**, Strober W, Seder RA, Kelsall BL. Regulation of transforming growth factor-beta production by interleukin-12. *Eur J Immunol* 1997; **27**: 1213-1220 [PMID: 9174613 DOI: 10.1002/eji.1830270524]

44 **Wynn TA**, Cheever AW, Jankovic D, Poindexter RW, Caspar P, Lewis FA, Sher A. An IL-12-based vaccination method for preventing fibrosis induced by schistosome infection. *Nature* 1995; **376**: 594-596 [PMID: 7637808 DOI: 10.1038/376594a0]

45 **Lee CG**, Homer RJ, Zhu Z, Lanone S, Wang X, Koteliansky V, Shipley JM, Gotwals P, Noble P, Chen Q, Senior RM, Elias JA. Interleukin-13 induces tissue fibrosis by selectively stimulating and activating transforming growth factor beta(1). *J Exp Med* 2001; **194**: 809-821 [PMID: 11560996 DOI: 10.1084/jem.194.6.809]

46 **Ma LJ**, Yang H, Gaspert A, Carlesso G, Barty MM, Davidson JM, Sheppard D, Fogo AB. Transforming growth factor-beta-dependent and -independent pathways of induction of tubulointerstitial fibrosis in beta6(-/-) mice. *Am J Pathol* 2003; **163**: 1261-1273 [PMID: 14507636 DOI: 10.1016/s0002-9440(10)63486-4]

47 **Kaviratne M**, Hesse M, Leusink M, Cheever AW, Davies SJ, McKerrow JH, Wakefield LM, Letterio JJ, Wynn TA. IL-13 activates a mechanism of tissue fibrosis that is completely TGF-beta independent. *J Immunol* 2004; **173**: 4020-4029 [PMID: 15356151 DOI: 10.4049/jimmunol.173.6.4020]

48 **Ashcroft GS**, Yang X, Glick AB, Weinstein M, Letterio JL, Mizel DE, Anzano M, Greenwell-Wild T, Wahl SM, Deng C, Roberts AB. Mice lacking Smad3 show accelerated wound healing and an impaired local inflammatory response. *Nat Cell Biol* 1999; **1**: 260-266 [PMID: 10559937 DOI: 10.1038/12971]

49 **Büttner C**, Skupin A, Reimann T, Rieber EP, Unteregger G, Geyer P, Frank KH. Local production of interleukin-4 during radiation-induced pneumonitis and pulmonary fibrosis in rats: macrophages as a prominent source of interleukin-4. *Am J Respir Cell Mol Biol* 1997; **17**: 315-325 [PMID: 9308918 DOI: 10.1165/ajrcmb.17.3.2279]

50 **Hoffmann KF**, Cheever AW, Wynn TA. IL-10 and the dangers of immune polarization: excessive type 1 and type 2 cytokine responses induce distinct forms of lethal immunopathology in murine schistosomiasis. *J Immunol* 2000; **164**: 6406-6416 [PMID: 10843696 DOI: 10.4049/jimmunol.164.12.6406]

51 **Vaillant B**, Chiaramonte MG, Cheever AW, Soloway PD, Wynn TA. Regulation of hepatic fibrosis and extracellular matrix genes by the th response: new insight into the role of tissue inhibitors of matrix metalloproteinases. *J Immunol* 2001; **167**: 7017-7026 [PMID: 11739522 DOI: 10.4049/jimmunol.167.12.7017]

52 **Wangoo A**, Laban C, Cook HT, Glenville B, Shaw RJ. Interleukin-10- and corticosteroid-induced reduction in type I procollagen in a human ex vivo scar culture. *Int J Exp Pathol* 1997; **78**: 33-41 [PMID: 9166103 DOI: 10.1046/j.1365-2613.1997.d01-241.x]

53 **Zhang Q**, Liu LN, Yong Q, Deng JC, Cao WG. Intralesional injection of adipose-derived stem cells reduces hypertrophic scarring in a rabbit ear model. *Stem Cell Res Ther* 2015; **6**: 145 [PMID: 26282394 DOI: 10.1186/s13287-015-0133-y]

54 **Spiekman M**, Przybyt E, Plantinga JA, Gibbs S, van der Lei B, Harmsen MC. Adipose tissue-derived stromal cells inhibit TGF-β1-induced differentiation of human dermal fibroblasts and keloid scar-derived fibroblasts in a paracrine fashion. *Plast Reconstr Surg* 2014; **134**: 699-712 [PMID: 25357030 DOI: 10.1097/PRS.0000000000000504]

55 **Zonari A**, Martins TM, Paula AC, Boeloni JN, Novikoff S, Marques AP, Correlo VM, Reis RL, Goes AM.

Polyhydroxybutyrate-co-hydroxyvalerate structures loaded with adipose stem cells promote skin healing with reduced scarring. *Acta Biomater* 2015; **17**: 170-181 [PMID: 25662911 DOI: 10.1016/j.actbio.2015.01.043]

56 **Uysal CA**, Tobita M, Hyakusoku H, Mizuno H. The Effect of Bone-Marrow-Derived Stem Cells and Adipose-Derived Stem Cells on Wound Contraction and Epithelization. *Adv Wound Care (New Rochelle)* 2014; **3**: 405-413 [PMID: 24940554 DOI: 10.1089/wound.2014.0539]

57 **Iekushi K**, Taniyama Y, Azuma J, Sanada F, Kusunoki H, Yokoi T, Koibuchi N, Okayama K, Rakugi H, Morishita R. Hepatocyte growth factor attenuates renal fibrosis through TGF-β1 suppression by apoptosis of myofibroblasts. *J Hypertens* 2010; **28**: 2454-2461 [PMID: 20842048 DOI: 10.1097/HJH.0b013e32833e4149]

58 **Sherriff-Tadano R**, Ohta A, Morito F, Mitamura M, Haruta Y, Koarada S, Tada Y, Nagasawa K, Ozaki I. Antifibrotic effects of hepatocyte growth factor on scleroderma fibroblasts and analysis of its mechanism. *Mod Rheumatol* 2006; **16**: 364-371 [PMID: 17164998 DOI: 10.1007/s10165-006-0525-z]

59 **Eto H**, Suga H, Aoi N, Kato H, Doi K, Kuno S, Tabata Y, Yoshimura K. Therapeutic potential of fibroblast growth factor-2 for hypertrophic scars: upregulation of MMP-1 and HGF expression. *Lab Invest* 2012; **92**: 214-223 [PMID: 21946856 DOI: 10.1038/labinvest.2011.127]

60 **Shi HX**, Lin C, Lin BB, Wang ZG, Zhang HY, Wu FZ, Cheng Y, Xiang LJ, Guo DJ, Luo X, Zhang GY, Fu XB, Bellusci S, Li XK, Xiao J. The anti-scar effects of basic fibroblast growth factor on the wound repair in vitro and in vivo. *PLoS One* 2013; **8**: e59966 [PMID: 23565178 DOI: 10.1371/journal.pone.0059966]

61 **Shi JH**, Guan H, Shi S, Cai WX, Bai XZ, Hu XL, Fang XB, Liu JQ, Tao K, Zhu XX, Tang CW, Hu DH. Protection against TGF-β1-induced fibrosis effects of IL-10 on dermal fibroblasts and its potential therapeutics for the reduction of skin scarring. *Arch Dermatol Res* 2013; **305**: 341-352 [PMID: 23321694 DOI: 10.1007/s00403-013-1314-0]

62 **Ejaz A**, Epperly MW, Hou W, Greenberger JS, Rubin JP. Adipose-Derived Stem Cell Therapy Ameliorates Ionizing Irradiation Fibrosis *via* Hepatocyte Growth Factor-Mediated Transforming Growth Factor-β Downregulation and Recruitment of Bone Marrow Cells. *Stem Cells* 2019; **37**: 791-802 [PMID: 30861238 DOI: 10.1002/stem.3000]

63 **Borrelli MR**, Patel RA, Adem S, Diaz Deleon NM, Shen AH, Sokol J, Yen S, Chang EY, Nazerali R, Nguyen D, Momeni A, Wang KC, Longaker MT, Wan DC. The antifibrotic adipose-derived stromal cell: Grafted fat enriched with cd74+ adipose-derived stromal cells reduces chronic radiation-induced skin fibrosis. *Stem Cells Transl Med* 2020; **9**: 1401-1413 [PMID: 32563212 DOI: 10.1002/sctm.19-0317]

64 **Carceller MC**, Guillén MI, Ferrández ML, Alcaraz MJ. Paracrine in vivo inhibitory effects of adipose tissue-derived mesenchymal stromal cells in the early stages of the acute inflammatory response. *Cytotherapy* 2015; **17**: 1230-1239 [PMID: 26276006 DOI: 10.1016/j.jcyt.2015.06.001]

65 **Xie J**, Jones TJ, Feng D, Cook TG, Jester AA, Yi R, Jawed YT, Babbey C, March KL, Murphy MP. Human Adipose-Derived Stem Cells Suppress Elastase-Induced Murine Abdominal Aortic Inflammation and Aneurysm Expansion Through Paracrine Factors. *Cell Transplant* 2017; **26**: 173-189 [PMID: 27436185 DOI: 10.3727/096368916X692212]

66 **Cho KS**, Park MK, Mun SJ, Park HY, Yu HS, Roh HJ. Indoleamine 2,3-dioxygenase is not a pivotal regulator responsible for suppressing allergic airway inflammation through adipose-derived stem cells. *PLoS One* 2016; **11**: e0165661 [PMID: 27812173 DOI: 10.1371/journal.pone.0165661]

67 **Evans BGA**, Gronet EM, Saint-Cyr MH. How Fat Grafting Works. *Plast Reconstr Surg Glob Open* 2020; **8**: e2705 [PMID: 32802628 DOI: 10.1097/GOX.0000000000002705]

68 **Murohara T**, Shintani S, Kondo K. Autologous adipose-derived regenerative cells for therapeutic angiogenesis. *Curr Pharm Des* 2009; **15**: 2784-2790 [PMID: 19689349 DOI: 10.2174/138161209788923796]

69 **Patan S**. Vasculogenesis and angiogenesis. *Cancer Treat Res* 2004; **117**: 3-32 [PMID: 15015550 DOI: 10.1007/978-1-4419-8871-3_1]

70 **Dickens S**, Vermeulen P, Hendrickx B, Van den Berge S, Vranckx JJ. Regulable vascular endothelial growth factor165 overexpression by ex vivo expanded keratinocyte cultures promotes matrix formation, angiogenesis, and healing in porcine full-thickness wounds. *Tissue Eng Part A* 2008; **14**: 19-27 [PMID: 18333801 DOI: 10.1089/ten.a.2007.0060]

71 **Phipps KD**, Gebremeskel S, Gillis J, Hong P, Johnston B, Bezuhly M. Alternatively activated M2 macrophages improve autologous Fat Graft survival in a mouse model through induction of angiogenesis. *Plast Reconstr Surg* 2015; **135**: 140-149 [PMID: 25539302 DOI: 10.1097/PRS.0000000000000793]

72 **Dong Z**, Peng Z, Chang Q, Lu F. The survival condition and immunoregulatory function of adipose stromal vascular fraction (SVF) in the early stage of nonvascularized adipose transplantation. *PLoS One* 2013; **8**: e80364 [PMID: 24260375 DOI: 10.1371/journal.pone.0080364]

73 **Seaman SA**, Cao Y, Campbell CA, Peirce SM. Macrophage Recruitment and Polarization During Collateral Vessel Remodeling in Murine Adipose Tissue. *Microcirculation* 2016; **23**: 75-87 [PMID: 26638986 DOI: 10.1111/micc.12261]

74 **Hutchings G**, Janowicz K, Moncrieff L, Dompe C, Strauss E, Kocherova I, Nawrocki MJ, Kruszyna Ł, Wąsiatycz G, Antosik P, Shibli JA, Mozdziak P, Perek B, Krasiński Z, Kempisty B, Nowicki M. The Proliferation and Differentiation of Adipose-Derived Stem Cells in Neovascularization and Angiogenesis. *Int J Mol Sci* 2020; **21** [PMID: 32471255 DOI: 10.3390/ijms21113790]

75 **Xu FT**, Li HM, Yin QS, Liu DL, Nan H, Zhao PR, Liang SW. Human breast adipose-derived stem cells transfected with the stromal cell-derived factor-1 receptor CXCR4 exhibit enhanced viability in human autologous free fat grafts. *Cell Physiol Biochem* 2014; **34**: 2091-2104 [PMID: 25562157 DOI: 10.1159/000366404]

76 **Cai J**, Feng J, Liu K, Zhou S, Lu F. Early Macrophage Infiltration Improves Fat Graft Survival by Inducing Angiogenesis and Hematopoietic Stem Cell Recruitment. *Plast Reconstr Surg* 2018; **141**: 376-386 [PMID: 29036027 DOI: 10.1097/PRS.0000000000004028]

77 **Zadorozhna M**, Di Gioia S, Conese M, Mangieri D. Neovascularization is a key feature of liver fibrosis progression: anti-angiogenesis as an innovative way of liver fibrosis treatment. *Mol Biol Rep* 2020; **47**: 2279-2288 [PMID: 32040707 DOI: 10.1007/s11033-020-05290-0]

World Journal of Stem Cells

Submit a Manuscript: https://www.f6publishing.com

World J Stem Cells 2022 February 26; 14(2): 214-218

DOI: 10.4252/wjsc.v14.i2.214

ISSN 1948-0210 (online)

LETTER TO THE EDITOR

Physical energy-based ultrasound shifts M1 macrophage differentiation towards M2 state

Hao-Cheng Qin, Zhi-Wen Luo, Yu-Lian Zhu

Specialty type: Cell and tissue engineering

Provenance and peer review: Invited article; Externally peer reviewed.

Peer-review model: Single blind

Peer-review report's scientific quality classification

Grade A (Excellent): 0
Grade B (Very good): B, B
Grade C (Good): 0
Grade D (Fair): 0
Grade E (Poor): 0

P-Reviewer: Ankrah AO, Prasetyo EP

Received: November 5, 2021
Peer-review started: November 5, 2021
First decision: December 4, 2021
Revised: December 12, 2021
Accepted: February 16, 2022
Article in press: February 16, 2022
Published online: February 26, 2022

Hao-Cheng Qin, Yu-Lian Zhu, Department of Rehabilitation Medicine, Huashan Hospital, Fudan University, Shanghai 200040, China

Zhi-Wen Luo, Department of Sports Medicine, Huashan Hospital, Fudan University, Shanghai 200040, China

Corresponding author: Yu-Lian Zhu, MD, PhD, Chief Doctor, Doctor, Professor, Department of Rehabilitation Medicine, Huashan Hospital, Fudan University, No. 12 Wulumuqi Road, Shanghai 200040, China. zyljully@163.com

Abstract

Recently, we read with interest the article entitled "Unveiling the Morphogenetic Code: A New Path at the Intersection of Physical Energies and Chemical Signaling". In this paper, the investigation into the systematic and comprehensive bio-effects of physical energies prompted us to reflect on our research. We believe that ultrasound, which possesses a special physical energy, also has a certain positive regulatory effect on macrophages, and we have already obtained some preliminary research results that support our hypothesis.

Key Words: Ultrasound; Macrophages; Stem cells; Physical energies; Inflammation

Core Tip: Because physical energies can contribute to the recovery of tissue damage in multiple aspects, it is widely used in clinical practice. The unique insights of the article "Unveiling the Morphogenetic Code: A New Path at the Intersection of Physical Energies and Chemical Signaling" inspired the direction of our experiments concerning the impact of physical energies on stem cells. In the future, we will conduct experiments and analytical techniques to reveal the mechanism of the regulatory effects behind ultrasound.

Citation: Qin HC, Luo ZW, Zhu YL. Physical energy-based ultrasound shifts M1 macrophage differentiation towards M2 state. *World J Stem Cells* 2022; 14(2): 214-218
URL: https://www.wjgnet.com/1948-0210/full/v14/i2/214.htm
DOI: https://dx.doi.org/10.4252/wjsc.v14.i2.214

TO THE EDITOR

Recently, the article named "Unveiling the Morphogenetic Code: A New Path at the Intersection of Physical Energies and Chemical Signaling" contributed by the Editor-in-Chief Carlo Ventura[1] motivated us to reconsider the biological roles of physical energies. In that article, the authors provided a detailed summary of the developmental history of physical energy, especially bioelectricity, as well as its applications and prospects in stem cell research. We strongly support the proposition about the high efficacy of physical energy in tissue repair. An article recently released in "Science Translational Medicine" described how massage, which is also a physical stimulus, regulates muscle repair[2]. The systematic and accurate explanation of physical energies by the editor echoes our dedicated research, which is the effect of therapeutic ultrasound on macrophages.

As early as the 1920s, Wood and Loomis began to investigate ultrasound as a therapeutic intervention [3]. In recent years, one particular type of ultrasound, low-intensity pulsed ultrasound (LIPUS), has gained much attention. This is due to its non-thermal effects, such as acoustic cavitation and "cellular massage", which produce a range of biological effects[4]. Clinically, LIPUS can be used as a non-invasive adjunctive therapy for a variety of diseases, such as fractures, muscle injury, osteoarthritis, as well as nerve injury[4]. Besides, LIPUS has received considerable attention in the discipline of stem cell research. Salgarella *et al*[5] proved the bio-effect of ultrasound therapy on the proliferation and differentiation of C2C12 myoblasts *in vitro*, while the research of Wang *et al*[6] indicated that LIPUS promotes the production of mesenchymal stem cells (MSC) derived mainly from bone marrow differentiation. Both of these studies verified the positive bio-effects of this therapeutic technique. Tan *et al*[7] listed recent studies regarding the action of LIPUS on various neural stem cells and concluded that LIPUS can stimulate stem cells *in vitro*, promote stem cell proliferation, differentiation, and migration, and maintain stem cell activity. The findings of Wu *et al*[8] suggested that LIPUS regulates the Notch signalling pathway in the central nervous system, causing neural stem cell proliferation and differentiation. Additionally, LIPUS can also accelerate tissue repair[9] and promote the dissipation of inflammation[10], angiopoiesis[11], *etc.*

Our research focused on discovering how sound waves, a kind of physical energy, exert potential effects on macrophage polarisation, which is of great significance during the inflammation stage. To ensure accurate muscle regeneration, a balance between M1 and M2 activity (pro- and anti-inflammatory, respectively) shifting over time is required[12]. Previous studies have found that ultrasound may regulate macrophages in the spinal fusion model of male Sprague Dawley (SD) rats[13]. However, very few studies have explored the direct effect of ultrasound on macrophages *in vitro*. We induced macrophages into M1 macrophages using lipopolysaccharide to mimic the inflammatory microenvironment *in vivo*. Then, we collected and analysed the secretion composition and gene expression following ultrasound therapy. Details of the experiments are presented in Figure 1.

So far, we have already obtained some preliminary results. As Figure 2 indicates, after LIPUS treatment, the secretion of anti-inflammatory cytokine interleukin (IL)-10 significantly increased, while quantities of pro-inflammatory cytokines tumor necrosis factor-α and IL-6 fell substantially at genetic and secreted proteins levels. Besides, we determined that the phenotypes of the macrophages are polarised into M2 after ultrasound stimulation (Figure 3). According to the above experimental data, we can conclude that ultrasound facilitates the transition of macrophages from the M1 to M2 phenotype *in vitro*, which is consistent with da Silva Junior's discovery[14]. For subsequent research, we will further investigate the underlying mechanism of macrophage polarisation caused by LIPUS, and the potentially affected molecular pathways. Moreover, we will conduct both *in vivo* (skeletal muscle contusion model) [15] and *in vitro* experiments to verify the mechanism and ascertain how LIPUS exerts a series of downstream bio-effects.

Conclusion and perspective

Various studies have established that physical energies can modulate inflammation and further promote tissue repair. As a conventional form of physical energy, ultrasound has extensive application prospects due to its non-thermal mechanical effect. Accordingly, it warrants further investigation to elucidate its influence on cell signalling. We predict that subsequent research can be extended from the aspect of monotypic cell regulation to the integral tissue, by employing single-cell transcriptomic analysis and spatial transcriptomic analysis[16]. Thus, we will gain an increasingly comprehensive insight into the role of ultrasound in tissue repair.

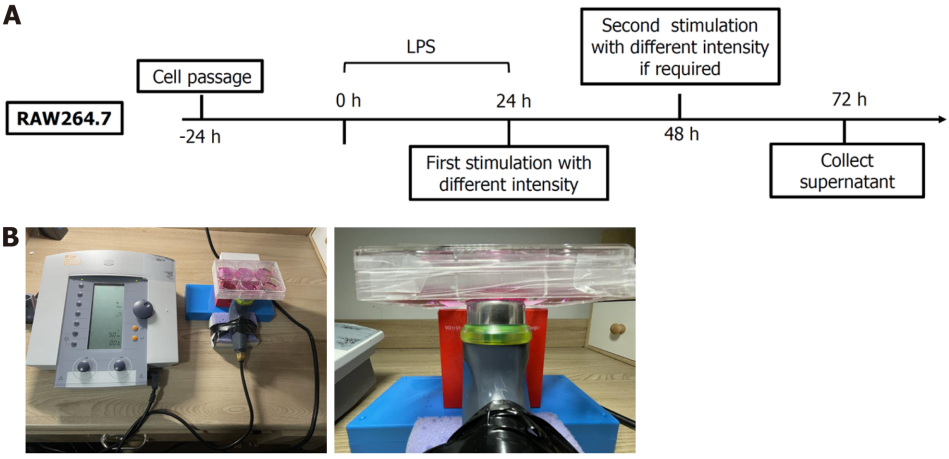

DOI: 10.4252/wjsc.v14.i2.214 **Copyright** ©The Author(s) 2022.

Figure 1 Experimental design for this study *in vitro* and the method of treating cells. A: At 24 h before lipopolysaccharide (LPS) was added to simulate the inflammatory environment, macrophages at the M1 stage were uniformly subcultured into the six-well plate. Then, The first ultrasound treatment was performed 24 h after the inflammatory environment was maintained. At 48 h, ultrasound was performed on the group requiring a second treatment. The supernatant of culture medium was separated after 24 d of culture (3 d after LPS was added); B: In order to easily adjust the ultrasonic probe to fit the culture holes on the bottom of the six-well plate, we fixed the ultrasonic probe on a sponge pad. Additionally, a box of the same height is used to support the six-hole plate to prevent it from tilting.

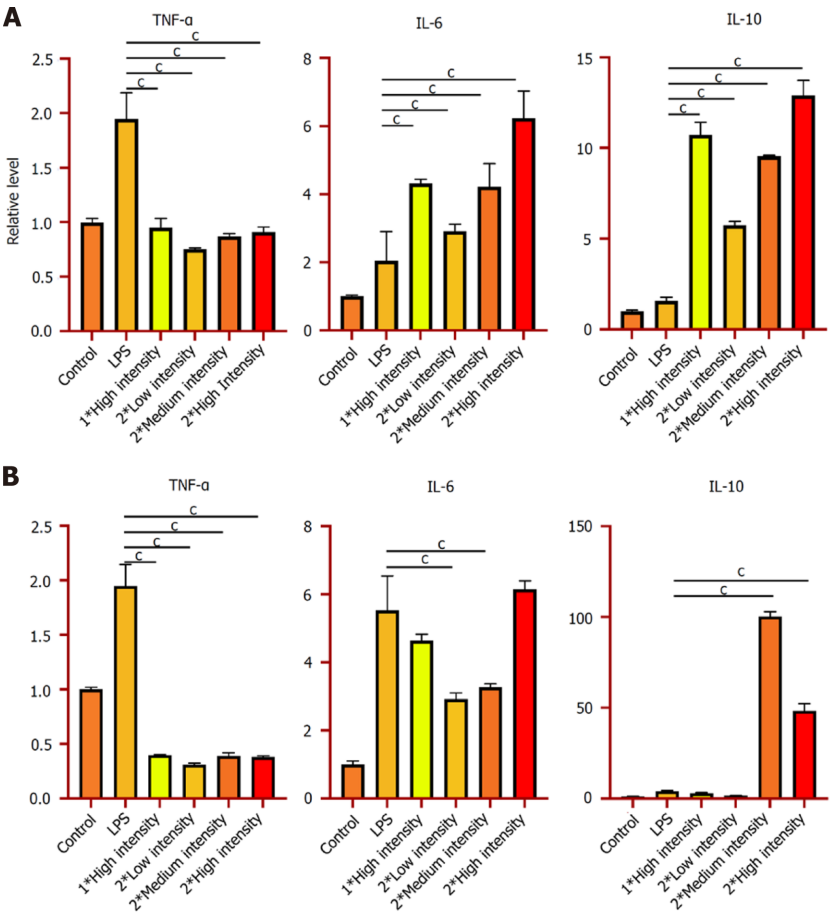

DOI: 10.4252/wjsc.v14.i2.214 **Copyright** ©The Author(s) 2022.

Figure 2 Low-Intensity pulsed ultrasound significantly increases the expression of anti-inflammatory cytokine and decreases the expression of pro-inflammatory cytokine. A: Real-time quantitative polymerase chain reaction (qPCR) was used to detect the gene expression of tumor necrosis factor (TNF)-α, interleukin (IL)-6, and IL-10 after being treated by low-intensity pulsed ultrasound (LIPUS); B: ELISA was used to analyze the protein expression of TNF-α, IL-6, and IL-10 after being treated with LIPUS. Data are expressed as the mean ± standard error of the mean. $^{a}P < 0.05$; $^{b}P < 0.01$; $^{c}P < 0.001$. Low intensity = 0.25 W/cm^2, medium intensity = 0.5 W/cm^2, and high intensity = 0.75 W/cm^2. TNF-α: Tumor necrosis factor-α; IL: Interleukin.

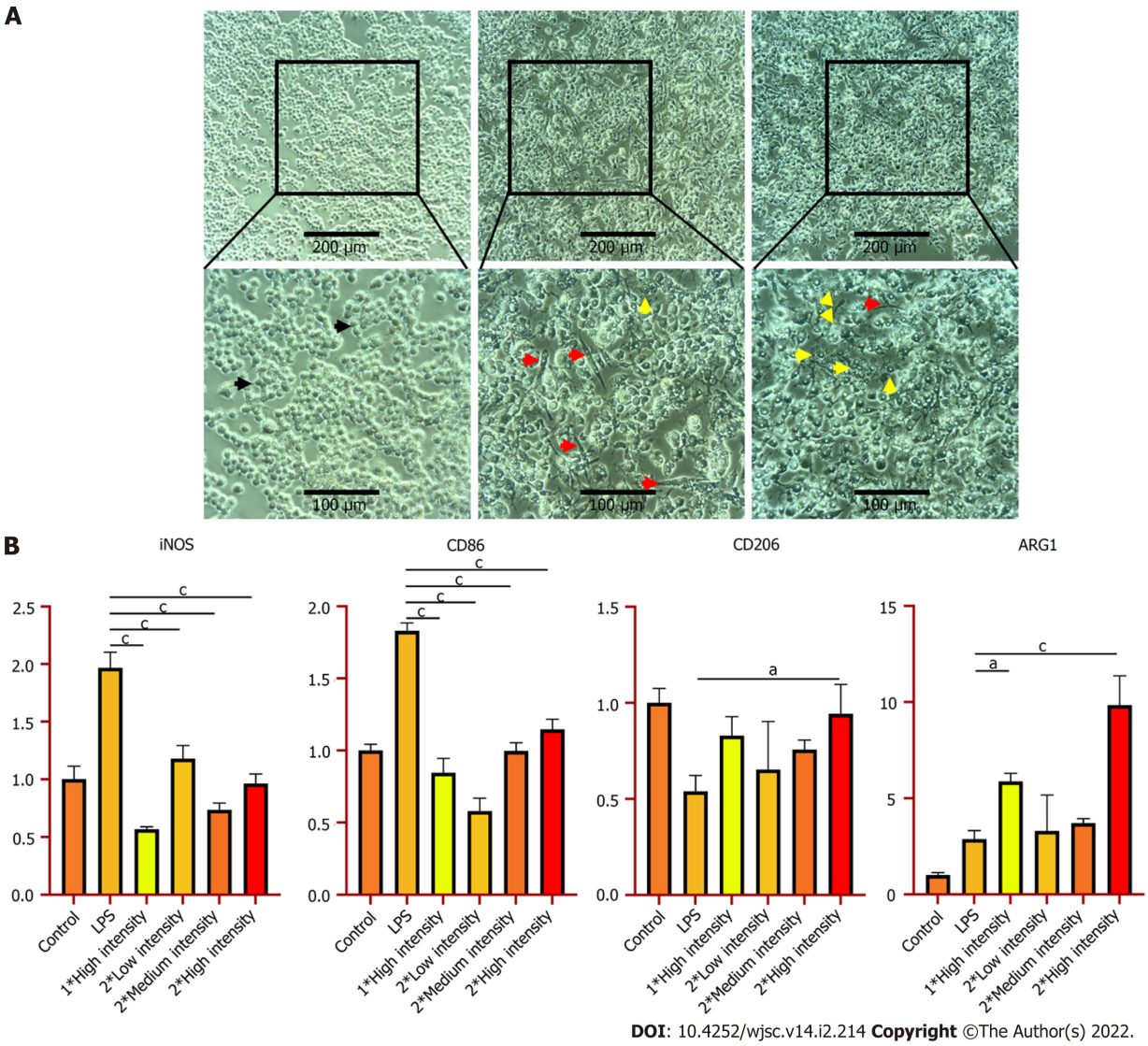

DOI: 10.4252/wjsc.v14.i2.214

Figure 3 Low-intensity pulsed ultrasound shifts M1 macrophages towards M2 state. A: The morphology of macrophages was observed by microscopy. Black, red, and yellow arrows represent M0, M1, and M2 macrophages, respectively; B: Quantitative polymerase chain reaction was used to detect the gene expression of cell phenotypes maker iNOS, CD86, CD206, and ARG1 after being treated by low-intensity pulsed ultrasound. Data are expressed as the mean ± standard error of the mean. $^{a}P < 0.05$; $^{b}P < 0.01$; $^{c}P < 0.001$. Low intensity = 0.25 W/cm^2, medium intensity = 0.5 W/cm^2, and high intensity = 0.75 W/cm^2.

FOOTNOTES

Author contributions: Qin HC and Luo ZW conducted the original search, wrote the first draft of the paper, and contributed to subsequent revisions of the manuscript; Zhu YL generated the original idea of this study and provided suggestions; Qin HC and Luo ZW made equal contributions to the work.

Conflict-of-interest statement: The authors declare no conflict of interest for this article.

Country/Territory of origin: China

ORCID number: Hao-Cheng Qin 0000-0003-2723-4299; Zhi-Wen Luo 0000-0002-0524-9951; Yu-Lian Zhu 0000-0001-5530-144X.

S-Editor: Fan JR
L-Editor: Wang TQ
P-Editor: Zhang YL

REFERENCES

1 **Tassinari R**, Cavallini C, Olivi E, Taglioli V, Zannini C, Ventura C. Unveiling the morphogenetic code: A new path at the intersection of physical energies and chemical signaling. *World J Stem Cells* 2021; **13**: 1382-1393 [PMID: 34786150 DOI: 10.4252/wjsc.v13.i10.1382]

2 **Seo BR**, Payne CJ, McNamara SL, Freedman BR, Kwee BJ, Nam S, de Lázaro I, Darnell M, Alvarez JT, Dellacherie MO, Vandenburgh HH, Walsh CJ, Mooney DJ. Skeletal muscle regeneration with robotic actuation-mediated clearance of neutrophils. *Sci Transl Med* 2021; **13**: eabe8868 [PMID: 34613813 DOI: 10.1126/scitranslmed.abe8868]

3 **Jiang X**, Savchenko O, Li Y, Qi S, Yang T, Zhang W, Chen J. A Review of Low-Intensity Pulsed Ultrasound for Therapeutic Applications. *IEEE Trans Biomed Eng* 2019; **66**: 2704-2718 [PMID: 30596564 DOI: 10.1109/TBME.2018.2889669]

4 **Lin G**, Reed-Maldonado AB, Lin M, Xin Z, Lue TF. Effects and Mechanisms of Low-Intensity Pulsed Ultrasound for Chronic Prostatitis and Chronic Pelvic Pain Syndrome. *Int J Mol Sci* 2016; **17** [PMID: 27376284 DOI: 10.3390/ijms17071057]

5 **Salgarella AR**, Cafarelli A, Ricotti L, Capineri L, Dario P, Menciassi A. Optimal Ultrasound Exposure Conditions for Maximizing C2C12 Muscle Cell Proliferation and Differentiation. *Ultrasound Med Biol* 2017; **43**: 1452-1465 [PMID: 28433437 DOI: 10.1016/j.ultrasmedbio.2017.03.003]

6 **Wang X**, Lin Q, Zhang T, Wang X, Cheng K, Gao M, Xia P, Li X. Low-intensity pulsed ultrasound promotes chondrogenesis of mesenchymal stem cells *via* regulation of autophagy. *Stem Cell Res Ther* 2019; **10**: 41 [PMID: 30670079 DOI: 10.1186/s13287-019-1142-z]

7 **Tan Y**, Guo Y, Reed-Maldonado AB, Li Z, Lin G, Xia SJ, Lue TF. Low-intensity pulsed ultrasound stimulates proliferation of stem/progenitor cells: what we need to know to translate basic science research into clinical applications. *Asian J Androl* 2021; **23**: 602-610 [PMID: 33818526 DOI: 10.4103/aja.aja_25_21]

8 **Wu Y**, Gao Q, Zhu S, Wu Q, Zhu R, Zhong H, Xing C, Qu H, Wang D, Li B, Ning G, Feng S. Low-intensity pulsed ultrasound regulates proliferation and differentiation of neural stem cells through notch signaling pathway. *Biochem Biophys Res Commun* 2020; **526**: 793-798 [PMID: 32268957 DOI: 10.1016/j.bbrc.2020.03.142]

9 **Yang B**, Li M, Lei H, Xu Y, Li H, Gao Z, Guan R, Xin Z. Low Intensity Pulsed Ultrasound Influences the Myogenic Differentiation of Muscle Satellite Cells in a Stress Urinary Incontinence Rat Model. *Urology* 2019; **123**: 297.e1-297.e8 [PMID: 30273612 DOI: 10.1016/j.urology.2018.09.020]

10 **Zheng C**, Wu SM, Lian H, Lin YZ, Zhuang R, Thapa S, Chen QZ, Chen YF, Lin JF. Low-intensity pulsed ultrasound attenuates cardiac inflammation of CVB3-induced viral myocarditis *via* regulation of caveolin-1 and MAPK pathways. *J Cell Mol Med* 2019; **23**: 1963-1975 [PMID: 30592150 DOI: 10.1111/jcmm.14098]

11 **Li J**, Guo W, Yu F, Liu L, Wang X, Li L, Fang B, Xia L. Low-intensity pulsed ultrasound promotes angiogenesis *via* the AKT pathway and DNA methylation in human umbilical vein endothelial cells. *Ultrasonics* 2022; **118**: 106561 [PMID: 34500338 DOI: 10.1016/j.ultras.2021.106561]

12 **De Santa F**, Vitiello L, Torcinaro A, Ferraro E. The Role of Metabolic Remodeling in Macrophage Polarization and Its Effect on Skeletal Muscle Regeneration. *Antioxid Redox Signal* 2019; **30**: 1553-1598 [PMID: 30070144 DOI: 10.1089/ars.2017.7420]

13 **Zhang ZC**, Yang YL, Li B, Hu XC, Xu S, Wang F, Li M, Zhou XY, Wei XZ. Low-intensity pulsed ultrasound promotes spinal fusion by regulating macrophage polarization. *Biomed Pharmacother* 2019; **120**: 109499 [PMID: 31707028 DOI: 10.1016/j.biopha.2019.109499]

14 **da Silva Junior EM**, Mesquita-Ferrari RA, França CM, Andreo L, Bussadori SK, Fernandes KPS. Modulating effect of low intensity pulsed ultrasound on the phenotype of inflammatory cells. *Biomed Pharmacother* 2017; **96**: 1147-1153 [PMID: 29191696 DOI: 10.1016/j.biopha.2017.11.108]

15 **Luo Z**, Lin J, Sun Y, Wang C, Chen J. Bone Marrow Stromal Cell-Derived Exosomes Promote Muscle Healing Following Contusion Through Macrophage Polarization. *Stem Cells Dev* 2021; **30**: 135-148 [PMID: 33323007 DOI: 10.1089/scd.2020.0167]

16 **van den Brink SC**, Alemany A, van Batenburg V, Moris N, Blotenburg M, Vivié J, Baillie-Johnson P, Nichols J, Sonnen KF, Martinez Arias A, van Oudenaarden A. Single-cell and spatial transcriptomics reveal somitogenesis in gastruloids. *Nature* 2020; **582**: 405-409 [PMID: 32076263 DOI: 10.1038/s41586-020-2024-3]

Published by **Baishideng Publishing Group Inc**
7041 Koll Center Parkway, Suite 160, Pleasanton, CA 94566, USA
Telephone: +1-925-3991568
E-mail: bpgoffice@wjgnet.com
Help Desk: https://www.f6publishing.com/helpdesk
https://www.wjgnet.com